Heterogenization on silica of metallocene catalysts for olefin polymerization

DOI:

[10.6100/IR594536](#)

Document status and date:
Published: 01/01/2005

Document Version:
Publisher's PDF, also known as Version of Record (includes final page, issue and volume numbers)

Please check the document version of this publication:

• A submitted manuscript is the version of the article upon submission and before peer-review. There can be important differences between the submitted version and the official published version of record. People interested in the research are advised to contact the author for the final version of the publication, or visit the DOI to the publisher's website.
• The final author version and the galley proof are versions of the publication after peer review.
• The final published version features the final layout of the paper including the volume, issue and page numbers.

[Link to publication](#)

Heterogenization on Silica of Metallocene Catalysts

for Olefin Polymerization

Madri Smit

Heterogenization on Silica of Metallocene Catalysts

for Olefin Polymerization

PROEFSCHRIFT

ter verkrijging van de graad van doctor aan de

Technische Universiteit Eindhoven, op gezag van de

Rector Magnificus, prof.dr.ir. C.J. van Duijn, voor een

commissie aangewezen door het College voor

Promoties in het openbaar te verdedigen

op donderdag 8 september 2005 om 16.00 uur

door

Madri Smit

geboren te Port Elizabeth, Zuid-Afrika

Dit proefschrift is goedgekeurd door de promotor:

prof.dr. C.E. Koning

Copromotor:

dr. J.C. Chadwick

Table of Contents

CHAPTER 1

Heterogenization of single-center catalysts

for α-olefin polymerization

SYNOPSIS: Polyolefins are commercially used in packing materials, foils, fibers, automotive and electrical applications. In the past, these materials were mainly synthesized via the polymerization of α-olefins in the presence of catalysts such as the Ziegler-Natta or Phillips catalyst systems. Recently, metallocenes immobilized on support materials have been introduced as successful polymerization catalysts in industry. Metallocene catalysts have the advantage of unique manipulation of polymer properties, thus making them ideal for the creation of new, application-oriented polymeric materials. These catalysts typically consist of a transition metal of Group IV and are encapsulated by ligands whose steric and electronic characteristics determine the properties of the catalyst. The activation of these systems for monomer incorporation is done via a so-called cocatalyst such as methylaluminoxane. The immobilization of these systems on support materials for ease of implementation in industrial setups, does, however, result in some complications.

The aim of this Chapter is to introduce the reader to vital concepts in olefin polymerization chemistry, focusing on the heterogenization of these systems on silica as support material. Additionally, the objectives of this research will be given.

1.1. SINGLE-SITE CATALYST SYSTEMS

1.1.1. Introduction

Ziegler-Natta catalyst systems, such as the combination of $TiCl_4$ and $Al(C_2H_5)_3$, generating $TiCl_3$, were first used in 1953-4 for the polymerization of α-olefins[1-4]. Ziegler and Natta shared the Nobel Prize in 1963 for this innovation. These systems produce linear polyethylene under relatively mild polymerization conditions, as well as isotactic polypropylene. The $TiCl_3$ catalysts developed and used in early manufacturing processes involving polymerization in hydrocarbon slurry have now been replaced by successive generations of high-activity $MgCl_2$-supported Ziegler-Natta catalysts, used in modern bulk and gas-phase processes for polypropylene and polyethylene production[5]. The suitability of $MgCl_2$ as support material for Ziegler-Natta catalysts is due to a number of factors[6-8], one of which is the similarity in ionic radius between Mg^{2+} and Ti^{4+}. These catalysts are complex systems, which contain a range of different active species and produce polymers having relatively broad molecular weight distributions and (in the case of polypropylene) relatively broad tacticity distributions.

The first homogeneous catalyst system (bis(cyclopentadienyl)titanium(IV)dichloride (titanocene)-alkylaluminum), producing uniform polymerization centers, was developed in 1957 by Natta[2] and Breslow[9]. However, due to poor catalyst activity such as 130 g PE/g Ti[10], short kinetic lifetimes resulting from rapid deactivation reactions[11,12], as well as lack of stereospecificity, these catalysts did not receive much attention.

Various attempts were made to improve catalyst activity, but Reichert and Meyer[13,14] were the first to accomplish this by the addition of small amounts of water to the $Cp_2TiEtCl/AlEtCl_2$ catalyst system. Sinn and Kaminsky[15] showed a major enhancement in activity to 500 000 g PE/g Ti in an ethylene polymerization system with Cp_2TiMe_2 as catalyst precursor, in combination with trimethylaluminum (TMA) or triethylaluminum (TEA) that had been reacted with half an equivalent of water. They found that the reaction of TMA with water resulted in the formation of an oligomeric product, $[-O-Al(CH_3)-]_n$, methylaluminoxane (MAO)[12].

INTERMEZZO 1: Metallocenes

Ferrocene (Figure 1-1) was the first metallocene and discovered by Fischer[16] and Wilkinson[17]. Ferrocene can be described as a positively charged metal ion, sandwiched between two cyclopentadienyl anions through π-bonding.
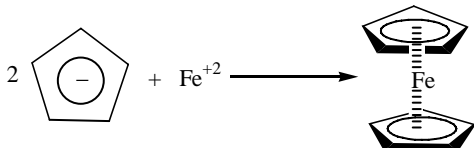
Scheme 1-1   Ferrocene, the first metallocene to be synthesized.

Figure 1-1   Zirconocene dichloride (inactive metallocene catalyst)

Shortly thereafter, Wilkinson discovered metallocenes in which higher charged metal ions such as zirconium (+4) would bond with two chlorine atoms to obtain a stable system (Figure 1-1). The cyclopentadienyl rings will form an angle with respect to each other to facilitate the large chlorine ligands.

These complexes typically consist of a Group IV metal that is encapsulated by two ligands. The active center is thus largely shielded against the influence of the immediate surroundings of the catalyst complex. The ligands can be either bridged or contain substituents and this gives further control over the characteristics of the resulting polymers in an olefin polymerization setup in the presence of a suitable cocatalyst.

This marked the beginning of an era portraying rapid growth in polyolefin knowledge. High activity zirconocene/MAO systems are able to polymerize a wide variety of monomers, producing polymers with narrow molecular weight distributions (MWDs) and, through further manipulation of the catalyst structure, polymers with desired tacticity. However, decay type kinetics with ethylene copolymers, high Al:Zr ratios required to obtain high activities and stable kinetic profiles, the high cost of MAO, the inability of the catalysts to adapt to industrial slurry and gas phase setups, as well as poor polymer morphology prove to be the challenges with these MAO/metallocene catalyst systems.

Generally, it was proposed that an unsaturated cation-like metal center ($[Cp_2Mt^+R]$, Figure 1-2) acts as the active species for olefin polymerization[18]. Isolation of the active catalyst species was for the first time possible with non-aluminum systems based on

boranes[19]. These compounds prove to act as cocatalysts for olefin polymerization in the presence of metallocenes. They are also easier to isolate and characterize than the MAO/metallocene systems and thus represent a possible alternative. These cocatalysts are, however, sensitive to poisons in the polymerization system and an additional alkylaluminum is required as scavenger. Figure 1-2 illustrates the activated catalyst species that form after reaction of bis(cyclopentadienyl)zirconium dimethyl as precursor with MAO and a borate cocatalyst system, respectively.
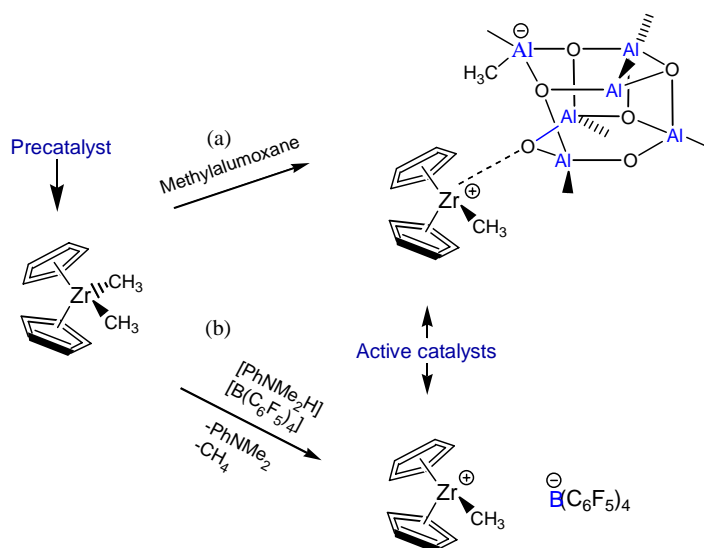
Figure 1-2:   Activation of a metallocene precatalyst with cocatalysts
                      such as (a) methylaluminoxane and (b) a borate

Polyolefins are produced by multiple insertions of olefin monomers into a metal-carbon bond. Olefin insertion occurs by the *cis*-opening of the double bond (both new bonds are on the same side of the inserting olefin) and with chain migratory insertion (it is the alkyl group on the metal that migrates to the olefin with a net exchange of two available coordination positions on the metal center).

Propylene polymerization generally takes place via primary (1,2) insertion. The monomer enantionface inserted preferentially is the one which, in the transition state, places its substituent anti to the first C-C bond of the growing polymer chain (minimizes non-bonded interactions). The active metal center bearing the growing alkyl chain must have an available coordination site for the incoming monomer. Insertion occurs via chain

migration to the closest carbon of the olefin double bond, which undergoes *cis*-opening, with the formation of the new metal-carbon and carbon-carbon bonds. The new C-C bond is then on the site previously occupied by the co-ordinated monomer molecule. This is illustrated in Scheme 1-2.
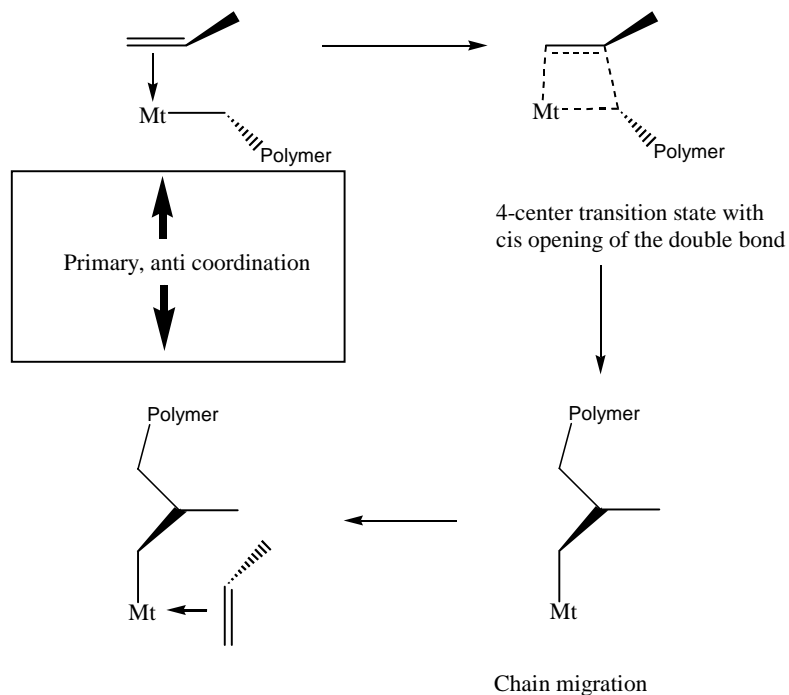
Scheme 1-2   Schematic representation of coordination and insertion during olefin polymerisation with transition metals. (Mt = metal atom)[20]

The next landmark in polyolefin chemistry was the discovery of *ansa* metallocenes by Brintzinger *et al* in 1982[21]. These are metallocenes that consist of ligands that are bridged and are also referred to as C_2 symmetric metallocenes. They allow for the controlled synthesis of polymers with predetermined tacticity. In 1984 Ewen[22], at Exxon, demonstrated that appropriate titanocenes could synthesize partially isotactic poly(propylene). A year later, highly isotactic material was obtained with analogous zirconocenes by Kaminsky *et al*[23]. These innovations were followed by the synthesis of a C_s symmetric zirconocene ([Me$_2$C(Flu)(Cp)]ZrCl$_2$) by Ewen *et al*[24] that allowed for the production of high quantities of syndiotactic polypropylene. It is beyond the scope of this introduction to cover the details of the massive growth in metallocene chemistry in the

last two decades, but Figure 1-3 provides a glimpse of the possibilities in metallocene manipulation and the effect on polymer microstructure.

Symmetry	Example	Polymer (ie Poly(propylene))
C_{2v} Achiral		Atactic
C_2 Chiral	racemic form	Isotactic
C_s Achiral	mesomeric form	Atactic
C_s Prochiral		Syndiotactic
C_1 Chiral		Hemi-isotactic
		Isotactic
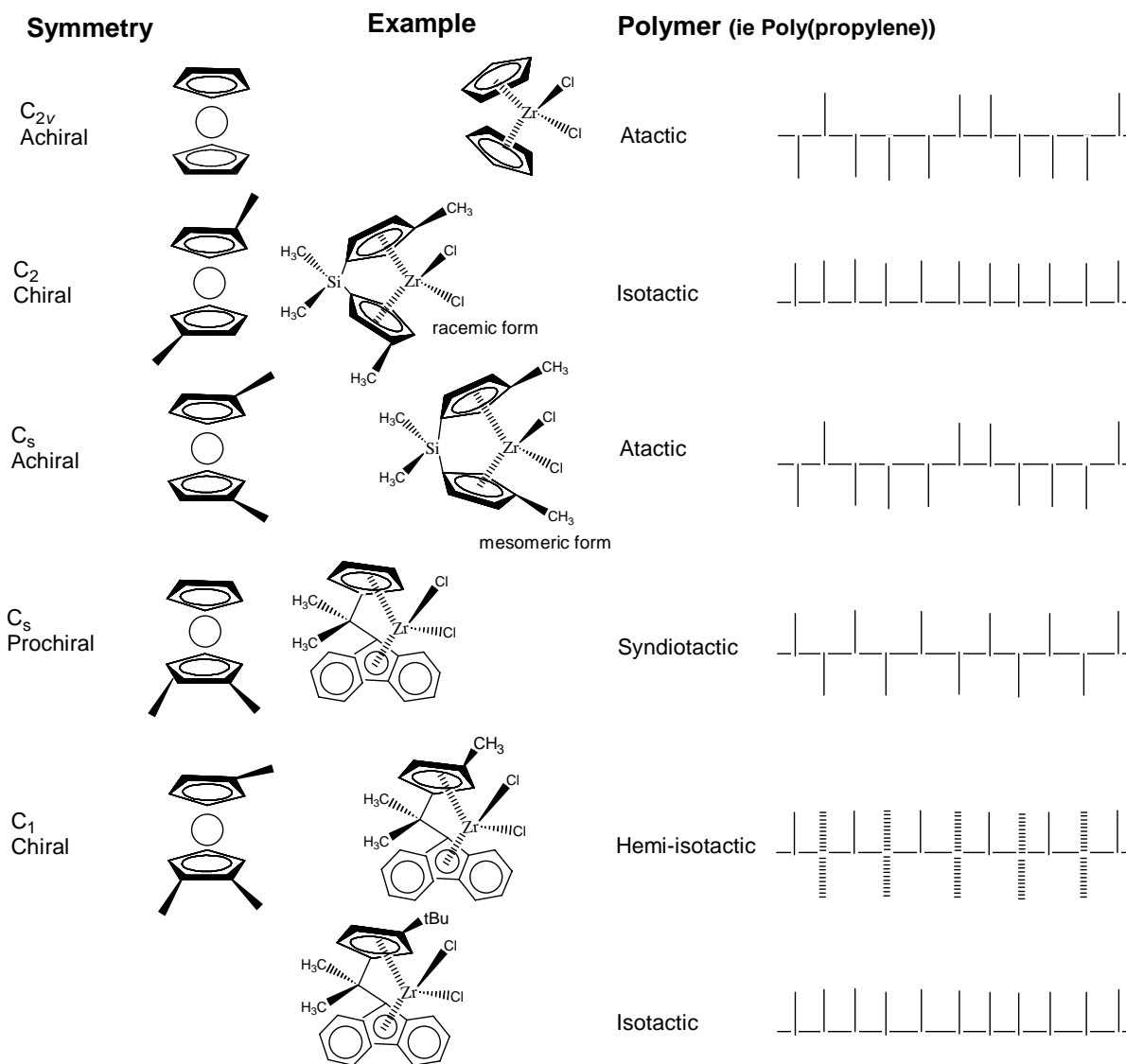
Figure 1-3   Steric control as a function of metallocene symmetry (Ewen's Symmetry Rules)[20].

INTERMEZZO 2: Single-Center or Single-Site catalysts[20]

Metallocenes are often referred to as single-site or single-center catalysts. It is therefore important to be able to distinguish between site and center. A metallocene-type active center has a minimum of two sites (the two tetrahedral positions previously occupied by the two chlorine atoms of the metallocene precatalyst) on which chain growth can initiate. The characteristics of the active sites are dependent on the metal, the ligands and the structure of the metal-bonded chain end. The number of possible active sites can thus be increased by the last inserted monomer unit. Different sites can thus be different in regioselectivity, enantioface selectivity and reactivity. Thus, the active center changes during a single chain growth, but statistically behaves the same from one polymer chain to another. Such species are therefore referred to as single-center catalysts.

Another noteworthy addition to the coordination catalyst family is the half-sandwiched metallocenes. The constrained geometry catalyst $[Me_2Si(C_5Me_4)(N\text{-}t\text{-}Bu)]TiCl_2$ polymerizes ethylene and 1-octene to produce C_6-branched polyethylene chains[25-27]. Additionally, it also re-incorporates polymer chains with unsaturated chain ends.

The challenge in metallocene chemistry lays in the adaptation of these systems for implementation in industrial gas phase and slurry processes. Immobilization of the MAO-activated catalyst systems on support materials, of which silica and other materials are widely being investigated, seems to be a plausible solution[28-32]. BASF produced the first heterogenized metallocene-based polyolefin (Luflexen (very low density polyethylene)) brands in 1995[33]. This technology was soon employed by various other companies in their gas and slurry phase polymerization setups. Exxon (Exact), Mitsui Petrochemicals (Evolve) and a BASF/SHELL joint venture (Elenac, now part of Basell) developed LLDPE, while MDPE is produced by Borealis under the name of Borecen[34]. Isotactic polypropylene is produced by Basell (Metocene[35]) and by Exxon Mobil (Achieve[34]).

Although employed in industry, a better understanding of elementary reactions and control, as well as identification of all factors influencing the behavior of the heterogenized single-center catalyst systems, is required before widespread optimal industrial use is possible.

1.1.2. Supported Catalysts for Olefin Polymerization

Polyolefins are industrially produced via four techniques: 1) radical initiated polymerization; 2) homogeneous polymerization; 3) slurry phase polymerization and 4) gas phase polymerization[36,37]. Coordination catalysts are ideal for the last two polymerization setups with the main requirement being that these metallocene systems should be immobilized on a solid support material. Quite a number of good reviews are available on this topic[29,30,32].

Support materials often employed are $MgCl_2$[38-40], Al_2O_3[38,39,41] and SiO_2[28]. SiO_2 is a support material that has extensively been used in industry (with the chromium (Phillips) and the constrained geometry catalyst) for the production of polyolefins. The preparation of this material is also a well-defined art and the high functionality (playing an important role in the successful immobilization of species) of the silica surface makes this material very popular amongst researchers. Support materials provide not only a way to introduce the catalyst into the reactor, but also serve as a template for the growing polymer[42,43] (see Intermezzo 3). Undesired or uncontrolled polymer growth results in reactor *fouling*. The latter refers to an unstable reaction operation and/or uncontrolled deposition of polymer on the walls and other parts of the reactor.

Crucial variables in the heterogenization of metallocenes for olefin polymerization are the nature of the support (as mentioned above) and the immobilization method. Literature can be divided into three main methodologies for the immobilization of metallocenes on support materials, as summarized in the work of Ribeiro *et al.*[28] and given later in this dissertation.

Considering published literature on the effect of heterogenization on polymerization activity and polymer properties, it is apparent that a significant decrease in catalyst activity is generally observed. This led various researchers (Soga and Kaminaka[38,44], Ciardelli *et al.*[45], Kaminsky and Renner[46], Sacchi *et al.*[47], Kaminaka and Soga[41,48]) to take a closer look at the nature of the active centers after immobilization on support materials. Unfortunately, only a few techniques exist that can provide insight into the interaction between the support and adsorbate on a molecular level. Some of the earliest work on

this was carried out by Marks *et al.,*[49-51] using integrated chemical and spectroscopic techniques which suggested a relationship between the surface/adsorbate microstructure and observed catalyst activity

---

INTERMEZZO 3: Particle Growth

The two most accepted models for particle growth in heterogeneous catalysis, are the multigrain (MGM)[52] and the polymer flow (PFM)[53] models. On contact of the catalyst particle (surface and ideally also inside the pores) with fresh monomer, polymer chains would start to grow. At a certain time, the support fragments and micrograins move apart, although the original particle shape will stay intact. The individual fragments will each serve as nucleus for further polymer growth. Ideally, the polymer particle will be an exact replica of the original catalyst particle. The necessity of fragmentation and the consequences due to a lack thereof will be discussed later in this dissertation (Chapters 3 and 5). The choice of support material and the immobilization method are two critical variables.

Figure 1-4 An illustration of polymer growth on a solid catalyst/support particle[30]

One of the advantages of heterogenization of MAO/metallocene systems is that less MAO is employed (50-400 equivalents to 1 equivalent of catalyst), thus eliminating one of the major drawbacks of these systems. Industrially, polyethylenes are produced with typical molecular weights (MWs) of 200000–300000 g/mol, while the molecular weight distributions (MWDs) are application dependent and can vary from narrow to broad.

Heterogeneous metallocene systems[46,47,54] produce polymers with broad MWDs. The broadening could result from interactions between the metallocene and the support, leading to active centers differing in electronic and steric characteristics. Isotactic polypropylene (PP) produced by Ziegler-Natta catalysts has a Tm $\geq$ 165 °C, a triad [*mm*] content of 95% and a crystallinity of 70 %. Homogeneous metallocenes often give low and broad melting temperatures[55], where the lower melting temperature observed is probably due to lower isotacticity and imperfect regiospecificity (where propylene is not inserted purely in a 1,2 fashion). Additionally, homogeneous systems[47,56] produce PP with narrow MWDs, whereas Ziegler-Natta PPs show MWDs of 5-8. Various types of polymers, including ethylene/cycloolefin copolymers, which are inaccessible using Ziegler-Natta catalysis, can be produced with metallocene systems. Metallocenes are known for their capability to produce random copolymers with narrow MWDs, as well as narrow chemical composition distributions (CCDs)[57-63]. The relative magnitude of the copolymerization activity ratios is determined by the coordination-gap aperture in the metallocene/cocatalyst complex. Chien and He[58] showed that it is possible to obtain the same activity and copolymerization reactivity ratios for the heterogenized *racemic* ethylene-bridged bis(indenyl) zirconium dichloride (*rac*-Et(Ind)$_2$ZrCl$_2$) as for the homogeneous analogue.

1.2. OBJECTIVES AND OUTLINE OF THIS STUDY

The major objective of this study was to obtain a better understanding of heterogenized single-center catalyst systems. This was attempted by addressing key issues regarding the immobilization of single-center catalyst systems on silica.

1. Extensive characterization of the support material, often neglected, as well as simple characterization techniques for these materials will be discussed in Chapter 2;

2. The method of immobilization is a crucial variable in heterogeneous metallocene catalysis, as it influences particle fragmentation and thus polymer particle growth directly. Additionally, it also affects catalyst behavior and thus control over the resulting polymer properties. This will be addressed in Chapter 3;

3. Various aspects regarding methylaluminoxane are still a mystery to the scientific community. Considering the complexity of a heterogeneous metallocene system, it is only logical that the role of MAO in these systems will warrant some attention (Chapter 4);

4. Good particle morphology is essential to avoid reactor *fouling* and the formation of fines in the reactor setup that can be detrimental to the continuous operation of a polyolefin plant. Polymer growth at various stages of the polymerization will be studied in ethylene homo- and copolymerization by means of SEM imaging in order to define the effect of the comonomer on polymerization activity and support fragmentation during polymerization. Attention is also paid to the effects of catalyst immobilization on copolymer composition distribution (Chapter 5);

5. The results in Chapter 5 reveal that the catalyst productivity in ethylene homopolymerization and the composition distribution of ethylene/1-hexene copolymers are both influenced by monomer mass transport effects. In Chapter 6, it is shown that these effects can be alleviated by pre-polymerization with either propylene or ethylene/1-hexene, prior to ethylene homo- and copolymerization;

6. The studied MAO/silica systems are compared to an alternative support material and cocatalyst to establish the relevance of this work (Chapter 7);

Finally, a Technological Assessment will be made, discussing possible industrial and technological applications and/or consequences of the results described in this thesis.

1.3. REFERENCES

1. Ziegler, K. *Angew. Chem.* **1955**, *67*, 541.

2. Natta, G. *J. Am. Chem. Soc.* **1957**, *79*, 2975.

3. Wilke, G. *Angew. Chem., Int. Ed. Engl.* **2003**, *42*, 5000.

4. Corradini, P. *J. Polym. Sci., Part A: Polym. Chem.* **2004**, *42*, 391.

5. Moore, E.P. *Polypropylene Handbook. Polymerization, Characterization, Properties, Processing, Applications*; Hanser Publishers: Munich, **1996**.

6. Quirk, R.P. *Transition Metal Catalyzed Polymerizations: Alkenes and Dienes*; Harwood Academic Publications: New York, **1983**.

7. Van der Ven, S. *Propylene and other Polyolefins. Preparation and Characterization*; Elsevier: Amsterdam, **1990**.

8. Kashiwa, N. *J. Polym. Sci., Part A: Polym. Chem.* **2004**, *42*, 1.

9. Breslow, D.S.; Newburg, N.R. *J. Am. Chem. Soc.* **1957**, *79*, 5072.

10. Cihlar, J.; Mejlik, J.; Hamrik, O.; Hudea, P.; Majer, J. *Makromol. Chem.* **1980**, *181*, 2549.

11. Kaminsky, W.; Sinn, H. *Adv. Organomet. Chem.* **1980**, *18*, 99.

12. Reichert, K.H. in *Transition Metal Catalyzed Polymerizations: Alkene and Dienes*; Harwood Academic Publications: Ed. Quirk, R.P.: New York, **1981**.

13. Meyer, K.R.; Technical University München: München, **1970**.

14. Reichert, K.H.; Meyer, K.R. *Angew. Chem.* **1973**, *169*, 163.

15. Sinn, H.; Kaminsky, W. *Adv. Organomet. Chem.* **1980**, *18*, 99.

16. Fischer, E.O. *Angew. Chem.* **1962**, *22*, 620.

17. Wilkinson, G.; Birmingham, I.M. *J. Am. Chem. Soc.* **1954**, *76*, 4281.

18. Dyachkovskii, F.S.; Shilov, A.K.; Shilov, A.Y. *J. Polym. Sci., Part-C* **1967**, *109*, 2333.

19. Jordan, R.F. *Adv. Organomet. Chem.* **1991**, *32*, 325.

20. Resconi, L.; Cavallo, L.; Fait, A.; Piemontesi, F. *Chem. Rev.* **2000**, *100*, 1253.

21. Wild, F.R.W.P.; Zsolnai, L.; Huttner, G.; Brintzinger, H.H. *J. Organomet. Chem.* **1982**, *232*, 233.

22. Ewen, J.A. *J. Am. Chem. Soc.* **1984**, *106*, 6355.

23. Kaminsky, W.; Külper, K.; Brintzinger, H.H.; Wild, F.R.W.P. *Angew. Chem. Int. Ed.* **1985**, *24*, 507.

24. Ewen, J.A.; Jones, R.L.; Razavi, A.; Ferrara, J.P. *J. Am. Chem. Soc.* **1988**, *110*, 6255.

25. Brintzinger, H.H.; Fischer, D.; Mulhaupt, R.; Rieger, B.; Waymouth, R.M. *Angew. Chem., Int. Ed. Engl.* **1995**, *34*, 1143.

26. Manhanthappa, M.K.; Cole, A.P.; Waymouth, R.M. *Organometallics* **2004**, *23*, 836.

27. Eberle, T.; Spaniol, P.T.; Okuda, J. *Eur. J. Inorg. Chem.* **1998**, 237.

28. Ribeiro, M.; Deffieux, A.; Portela, M. *Ind. Chem. Eng. Res.* **1997**, *36*, 1224.

29. Hlatky, G.G. *Coord. Chem. Rev.* **1999**, *181*, 243.

30. Carnahan, E.; Jacobsen, G. *Catal. Tech.* **2000**, *4*, 74.

31. Chien, J.C.W. *Top. Catal.* **2000**, *7*, 23.

32. Kristen, M. *Top. Catal*. **2000**, *7*, 89.

33. Lux, M. *Proceedings of Metallocenes Europe '98 Conference*, Brussels, **1995**.

34. Kristen, M. *Top. Catal.* **1999**, *7*, 89.

35. *European Chemical News* **1997**, 1637.

36. Karol, F.J. *Macromol. Symp.* **1995**, *89*, 563.

37. Hogan, J.P.; Norwood, D.D.; Ayres, C.A. *J. Appl. Polym. Sci., Appl. Polym. Symp.* **1981**, *36*, 49.

38. Soga, K.; Kaminaka, M. *Makromol. Chem.* **1993**, *194*, 1745.

39. Soga, K.; Uozomi, T.; Saito, M.; Shiono, T. *Macromol. Chem. Phys.* **1994**, *195*, 1503.

40. Sarma, S.S.; Satyanarayana, G.; Sivaram, S. *Polym. Sci.* **1994**, *1*, 315.

41. Kaminaka, M.; Soga, K. *Polymer* **1992**, *33*, 1105.

42. Hermann, H.-F.; Böhm, L.L. *Polym. Commun.* **1991**, *32*, 58.

43. Nowlin, T.E.; Mink, R.I.; Lo, F.Y.; Kumar, T. *J. Polym. Sci., Part A: Polym. Chem.* **1991**, *29*, 1167.

44. Soga, K.; Kaminaka, M. *Makromol. Chem. Rapid. Commun.* **1992**, *13*, 221.

45. Ciardelli, F.; Altomare, A.; Arribas, G.; Conti, G.; Masi, F.; Menconi, F. In *Catalyst design for Tailor-made Polyolefins*; Soga, K.; Terano, M., Eds.; Elsevier: Kanazawa, **1994**, p 257.

46. Kaminsky, W.; Renner, F. *Makromol. Chem. Rapid. Commun.* **1993**, *14*, 239.

47. Sacchi, M.C.; Zucchi, D.; Tritto, I.; Locatelli, P. *Macromol. Rapid Commun.* **1995**, *16*, 581.

48. Kaminaka, M.; Soga, K. *Macromol. Rapid Commun.* **1991**, *12*, 367.

49. He, M.-Y.; Xiong, G.; Toscano, P.J.; Burwell, R.L.J.; Marks, T.J. *J. Am. Chem. Soc.* **1985**, *107*, 641.

50. Hedden, D.; Marks, T.J. *J. Am. Chem. Soc.* **1988**, *110*, 1647.

51. Finch, W.C.; Gillespie, R.D.; Hedden, D.; Marks, T.J. *J. Am. Chem. Soc.* **1990**, *112*, 622.

52. Nagel, E.J.; Kirillov, V.A.; Ray, W.H. *Ind. Chem. Prod. Res. Dev.* **1980**, *19*, 372.

53. Schmeal, W.R.; Street, J.R. *AIChe. J.* **1971**, *17*, 1188.

54. Chen, Y.-X.; Rausch, M.D.; Chien, J.C.W. *J. Polym. Sci., Part A: Polym. Chem.* **1995**, *33*, 2093.

55. Huang, J.; Rempel, G.L. *Prog. Polym. Sci.* **1995**, *20*, 459.

56. Fink, G.; Steinmetz, B.; Zechlin, J.; Przybyla, C.; Tesche, B. *Chem. Rev.* **2000**, *100*, 1377.

57. Zambelli, A.; Longo, P.; Ammendola, P.; Grassi, A. *Chim. Ital.* **1986**, *116*, 731.

58. Chien, J.; He, D. *J. Polym. Sci: Polym. Chem.* **1991**, *29*, 1585.

59. Zambelli, A.; Grassi, A.; Galimberti, M.; Mazzocchi, R.; Piemontesi, F. *Macromol. Chem., Rapid Commun.* **1991**, *12*, 523.

60. Herfert, N.; Fink, G. *Prep. Mat. Sci. Eng.* **1992**, *67*, 31.

61. Chien, J.; Nozaki, T. *J. Polym. Sci., Polym. Chem. Ed.* **1993**, *31*, 227.

62. Rossi, A.; Zhang, J.; Odian, G. *Macromolecules* **1996**, *29*, 2331.

63. Arnold, M.; Henschke, O.; Knorr, J. *Macromol. Chem. Phys.* **1996**, *197*, 363.

CHAPTER 2

Characteristics of Silica as Support Material

SYNOPSIS: Characterization of heterogeneous catalyst systems is extremely difficult and it is thus important to know as much about the individual components as possible. Silica is widely employed in industry (Phillips catalysts), as well as in academic institutions[1] as a support material for catalysts employed in olefin polymerization systems. Siliceous materials facilitate participation in adsorption and catalysis by their characteristic porosity and surface geometry. Silica's are typically regarded as polymers of silicic acid, consisting of SiO_4 tetrahedra. The surface chemistry of these materials is controlled by the nature, distribution and accessibility of free and bound silanols.

The aim of this chapter is to introduce the key characteristics of silica as a support material, as well as the primary analysis techniques and thus, create a basis of knowledge for the rest of this work.

Keywords: silica; chemical modification; silanols

2.1. INTRODUCTION

Transition metal catalysts are prone to react with polar compounds in their vicinity, resulting in the deactivation of these systems. It is therefore important to know the amount of available hydroxyl groups on the silica surface and their reactivity towards these catalyst systems. This information is vital in order to fully understand immobilization chemistry and its effect on catalyst activity.

Silicon atoms on the surface of amorphous silica are by definition not in exact regular geometrical arrangement. The hydroxyl groups are thus not spaced equidistantly from each other and therefore display different behavior during adsorption and chemical modification. Kislev's[2] work on surface hydroxyl groups resulted in a large interest in this field. Surface silanols are now divided into two main classes: free silanols (isolated silanols) and bound silanols (vicinal and geminal silanol groups). Additionally, internal or intraglobular silanols have also been investigated and defined as those silanols that are inaccessible to water[3]. The type and the number of surface functional groups can additionally be controlled via dehydroxylation that entails the condensation of hydroxyl groups to form siloxane bonds.

We have chosen MS-3040 and Sylopol 948 spherical silica materials for this work. In this section, the characteristics of these systems will be given in terms of nitrogen adsorption data (BET), infrared spectroscopy (IR), chemical modification (elemental analysis) and scanning electron microscopy (SEM).

2.2. EXPERIMENTAL

2.2.1. Materials

All reactions were carried out under argon atmosphere. Silica support materials, MS-3040 (PQ Corporation) and Sylopol 948 (Grace AG), were kindly donated by their respective suppliers. n-Heptane (Biosolve) was distilled over potassium before use, while 1,1,1,3,3,3-hexamethyldisilazane (HMDS) was placed on lithium aluminum hydride and degassed after obtaining it from Sigma-Aldrich.

2.2.2. Support Synthesis

2.2.2.1.   *Calcination*

The various silica materials were calcined, respectively, in a calibrated oven at 250 °C and 600 °C under a N_2/O_2 (3:1) flow. The silica was heated at 15°C/minute until the desired temperature was reached and then held isothermally for three hours, after which the sample was left to cool to ambient temperature.

2.2.2.2.   *Chemical modification for determination of available hydroxyl groups*

The free silanol groups on the surface of the silica materials were determined via modification with hexamethyldisilazane (HMDS). 200 mg of silica (independent of type and calcination temperature) was slurried in 3 mL of n-heptane. HMDS (1 mL) was then added under agitation and the temperature of the oil bath was raised to 50 °C. The slurry was left for 4 hours, after which it was removed from the oil bath and left for 15 minutes to cool down. It was then transferred to a shaker for four hours. The slurry was once again placed in a 50 °C oil bath for 1 hour after which it was removed and left overnight under argon atmosphere. The next day, the slurry was dried under evacuation (22 mbar) to obtain a free-flowing powder.

2.2.3. Characterization techniques

Nitrogen adsorption measurements were carried out on an ASAP 2010 Multigas system (Micrometrics instruments corp.) at –195.86 ºC. Samples were placed under vacuum at 125 ºC for at least 3 hours before analysis. (All samples displayed the same weight before and after sample preparation and analysis.) Adsorption data were used to determine the surface areas using the Brunauer Emmet Teller method, while the pore volumes and pore diameters were determined with the Barett Joyner Halenda (BJH) method for mesoporous materials.   Inductively coupled plasma atomic emission spectroscopy (ICP-AES analysis), for the determination of the elemental composition of the support materials, was carried out by the Kolbe Microanalytisches Laboratorium (in Mülheim an der Ruhr, Germany). Support morphology was studied on a Philips environmental scanning electron microscope (XL-30 ESEM-FEG), equipped with an

energy dispersive X-ray spectrometer (EDX) for local and area distribution analyses of elements. Secondary electron (SE) imaging of the sample surfaces was performed in high vacuum mode using an acceleration voltage of 1 KV. No additional coating of the sample surface was required, as the effect of charging was minimized by the choice of analysis conditions. Infrared spectra of the individual support particles were obtained using a Biorad UMA 500 Infrared microscope coupled with a Biorad FTS 6000 FT-IR spectrometer. The particles were measured in a Linkam THMS600 hot stage, fitted with ZnSe windows, in a nitrogen atmosphere. The spectra were recorded with a resolution of 2 cm^{-1}, co-adding 100 scans.

2.3. RESULTS AND DISCUSSION

2.3.1. Nitrogen Adsorption Characteristics

Brunauer Emmet Teller (BET) surface measurements were performed after heating the sample for a predetermined time under vacuum. A good sample typically renders the same mass before and after a measurement. In BET analysis, the surface area (m^2/g), pore size distribution (pore volume (Fv(r$_p$)) and the pore area (F$_A$(r$_p$)) distributions) can be determined via the adsorption/desorption behavior of gaseous nitrogen on a particular sample, under various temperature and pressure conditions. Figure 2-1 illustrates a typical isotherm in which a multilayer of adsorbate is formed with increasing relative gas pressure.
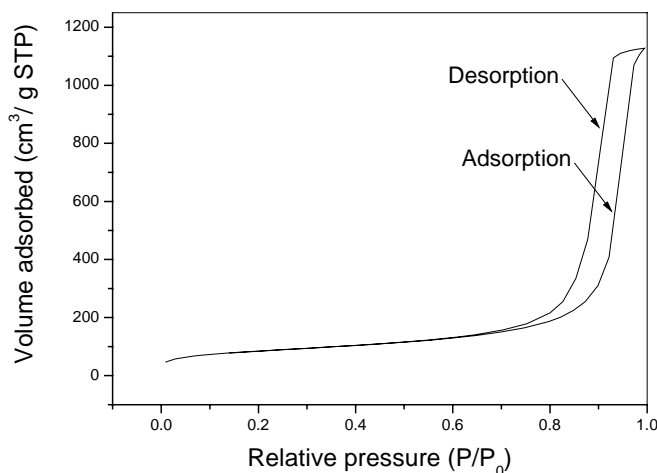
Figure 2-1 A typical isotherm observed for a mesoporous material (e.g. Sylopol 948 calcined at 600 °C).

The silica's utilized in this study belong to the IUPAC classification *mesoporous* (pore diameter of 2-50 nm) materials.

Capillary condensation (dependent on mean pore diameter) results in a further increase in adsorbed gas and is normally observed above p/p_0 of 0.4. The plateau around p/p_0 of 1 indicates that all the mesopores are filled with the liquid adsorbate. The adsorption-desorption curve shows a distinct hysteresis loop in that the amount adsorbed is always greater than the amount desorbed. This can be explained via capillary condensation during the adsorption run with an increase in adsorbate, followed by retardation in the desorption run. This is characteristic for all mesoporous materials. The surface area (determined from the BET equation) of the silica sample is important, as the amount of functional groups is normally expressed per nanometer square (nm^2) and gives a microscopical image of the surface. In this study, however, it is important to relate the number of moles of hydroxyl groups on the surface to the number of moles of the chemical compound required for the modification of the silica surface. Data regarding the surface hydroxyl groups will thus be given in mmol OH-groups/g of silica (see Section 2.3.4.).

Insight into the availability of the reactive surface silanols and the sorption characteristics of the material is given by the pore size distribution and pore volume data (calculated from the BJH (Barett, Joyner and Halenda) equation). This is especially interesting to compare before and after chemical modification, to determine whether the particular reagent reacts with the available hydroxyl groups inside the pores. In combination with other methods (e.g. infrared spectroscopy (IR) and energy dispersive x-ray (EDX) analysis) conclusions can be drawn regarding the effectiveness with reference to the particular reagent, the immobilization method or the type of silica employed (see Chapter 3).

The given support materials were calcined at different temperatures (see Section 2.2.2.1.) followed by subsequent nitrogen adsorption analysis. It is clear (Table 2-1) that significant differences in surface area (130-150 m^2/g), surface area of pores (115-139 m^2/g), pore volume (1 cm^3/g), pore diameter (4-34 nm), as well as particle size ranges, are observed between the two different types of silica materials.

Table 2-1   Surface characteristics of silica support materials, as determined by nitrogen adsorption.

Type	Supplier	T_{cal}[a] (ºC)	Surface area (m^2/g)	Surface area of pores (m^2/g)	Pore volume (cm^3/g)	Pore diameter (nm)
MS-3040	PQ	250	434	407	2.7	265
		600	454	429	2.6	245
Sylopol 948	Grace	250	304	292	1.7	231
		600	304	290	1.7	241

[a]Calcination temperature

It should also be noted that there is not much difference between the same silica calcined at two different temperatures. Condensation of the hydroxyl groups through calcination does, however, influence the surface area of the pores (only in the case of MS-3040) and the pore diameters.

2.3.2. Particle Morphology

SEM imaging provides a visualization of particle morphology and particle size distribution. In Figure 2-2 (a and b), one can see a clear difference in the particle size distribution between the two silica materials. MS-3040 particle sizes range between 60-170 μm, while 40-100 μm is observed for Sylopol 948. These broad particle size distributions should be kept in mind when polymer particle morphology is investigated with EDX/SEM imaging in the rest of this dissertation. Additionally, it should also be noted that the MS-3040 particles appear to be much more spherical than those observed for Sylopol 948. As discussed in Chapter 1, particle growth proceeds via particle fragmentation and ideally the polymer particle will be an exact replica of the catalyst/support particle.
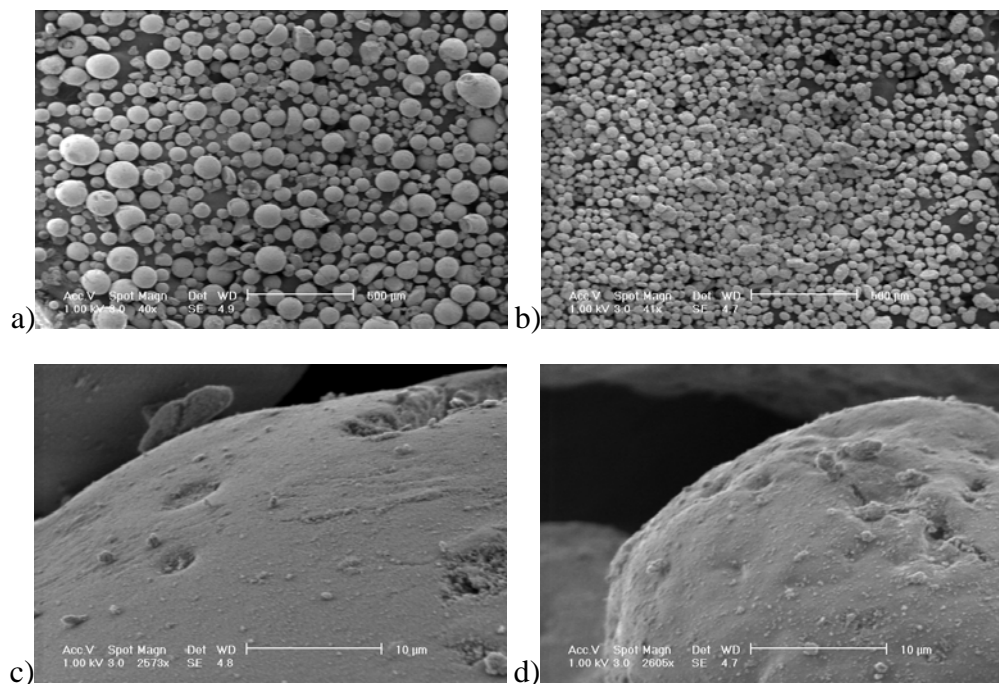
Figure 2-2 SEM imaging of MS-3040 ((a) and (c)) and Sylopol 948 ((b) and (d)), calcined at 250 °C, at magnifications of $\pm$ 40 and $\pm$ 2600, respectively.

2.3.3. Type of Functional Groups on silica surface

Various methods for the analysis of the available surface hydroxyl groups on silica can be obtained from literature, of which thermo gravimetric analysis[4-6], chemical methods such as titration[4,7-9] and spectroscopic methods such as infrared spectroscopy[8,10] have shown to be the most common. Scheme 2-1 depicts the three possible surface hydroxyl groups ((1) geminal, (2) vicinal and (3) isolated) that could be present on silica and tuned under various controlled temperatures.
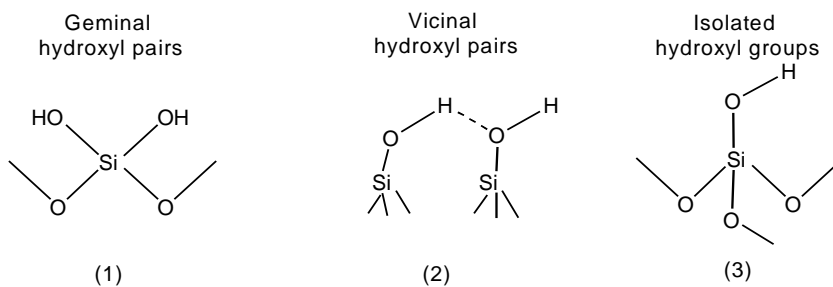
Scheme 2-1 Possible functional groups present on silica surfaces[11].

The latter is often referred to as the process of calcination. The amount and type of surface functional groups can also be controlled via chemical dehydration.

In Figure 2-3 the infrared spectrum of Sylopol 948 measured in air, is depicted. Bands centered at 1971 cm^{-1}, 1867 cm^{-1} and 1632 cm^{-1} represent overtones and combinations of intense Si-O fundamental modes. The two peaks marked with a star (*) should be of equal intensity in the absence of water (see Figure 2-4 of the calcined silica analogues). The broadening observed between 3500 cm^{-1} - 2600 cm^{-1} also supports the presence of water. This makes it difficult to identify the individual types of hydroxyl groups present.
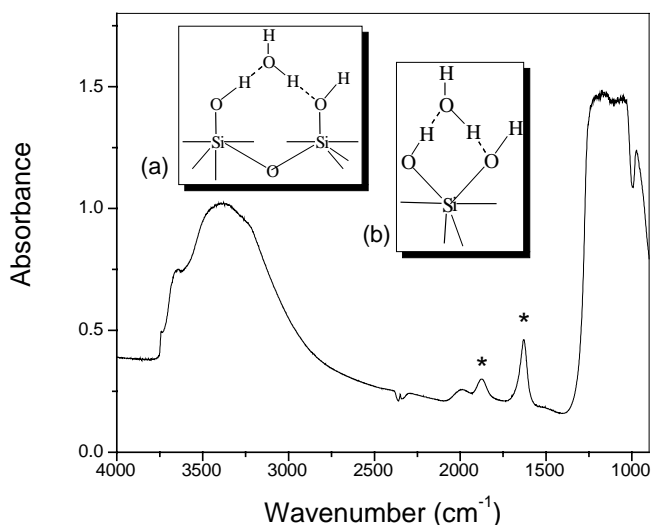
Figure 2-3   An infrared spectrum, accompanied by a schematic representation of the interaction between water and surface hydroxyl groups ((a) isolated and (b) geminal) of Sylopol 948 analyzed in air.

A possible illustration of the interaction of water with a) isolated (usually identified at 3746 cm^{-1}), as well as b) geminal (usually identified at 3742 cm^{-1}) hydroxyl groups on the silica surface in air is also given in Figure 2-3. (Geminal hydroxyl groups are, however, very difficult to identify in IR spectroscopy, as the peak observed at 3746 cm^{-1} for isolated silanols could easily overshadow the peak at 3742 cm^{-1}.)

Typically, one expects to observe vicinal (3520 cm^{-1}) and isolated (3746 cm^{-1}) hydroxyl groups on the surface of the 250 °C calcined silica's and mainly isolated silanols

on the 600 °C calcined silica materials. The influence of these modifications can be seen in Figure 2-4.
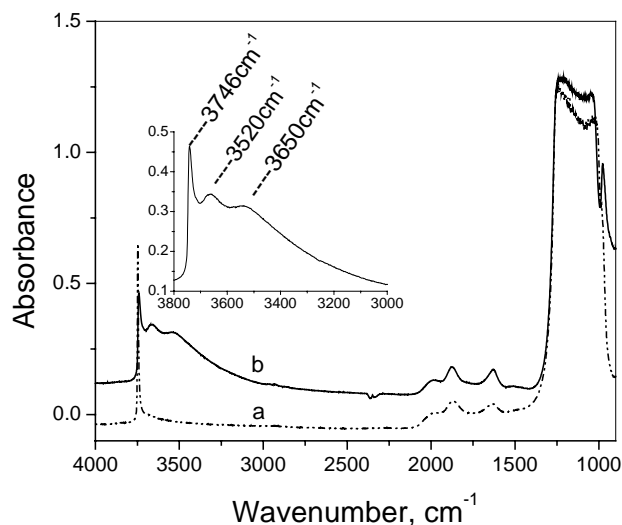
Figure 2-4   Infrared spectra show a distinct difference between Sylopol 948 analyzed after calcination at (a) 600 °C and (b) 250 °C.

Additionally, the band observed at 3650 cm^{-1} represents the presence of intraglobular silanols. As explained earlier (Section 2.1), these are silanols that are inaccessible to water. The main infrared band assignments for silica materials (related to the surface hydroxyl groups) are listed in Table 2-2, while additional band assignments (describing mainly the interaction of water with the silica surface) can be seen in Table 2-3.

Table 2-2   Stretching O-H band assignments typically observed for the functional groups present on silica surfaces[3].

Frequency (cm^{-1})	Species
3746	Free OH
3742	Geminal OH
3730-3720	Hydrogen perturbed OH (vicinal)
3650	Intraglobular OH
3520	Oxygen perturbed OH (vicinal)

Table 2-3   Additional infrared vibrations (mainly illustrating the interaction of water with surface silanols) observed for silica[3].

Frequency (cm^{-1})	Species
3400-3500	Molecular adsorbed H_2O
2000-1870	Skeleton (overtone) vibrations
1625	Bending O-H (molecular water)
1250-1020	Asymmetrical Si-O-Si stretching
970	Si-O(H…H_2O) bending
870	Bending O-H (silanol)
800	In-plane bending (geminal)[12]

It is clear, from the above data, that quite a range of hydroxyl groups and their interactions with water can be detected with IR spectroscopy. This method is therefore quite helpful in the analysis and characterization of silica materials.

2.3.4. Determination of Surface Hydroxyl Content

It was shown[13] that for several maximally hydrated silica's (with surface areas between 39 and 750 m^2/g), the concentrations of surface hydroxyl groups are more or less constant for a given drying temperature between 200 °C and 1000 °C. Fully hydroxylated silica contains 4.6 OH/nm^2 [2,7,8,14] and this can be regarded as a physicochemical constant that is independent of silica type and structural characteristics[3,15]. For the chemical dehydration of silica materials, various silanes and silazanes are employed (Scheme 2-2).
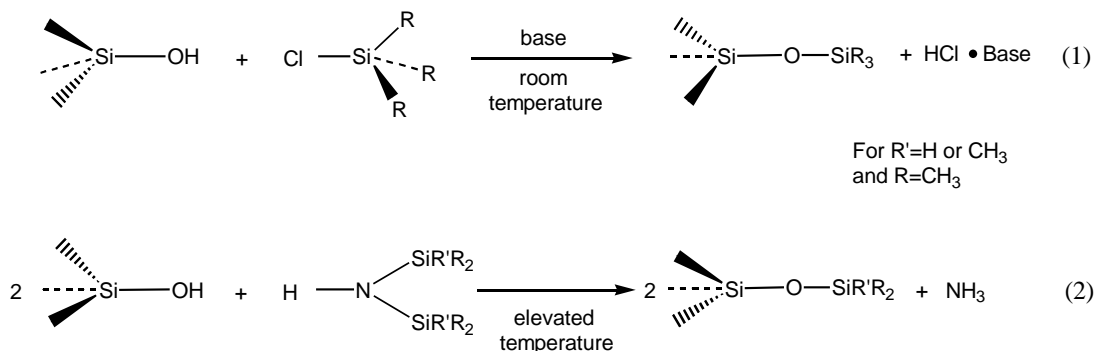
Scheme 2-2   Two main methods of sylilation, where (1) represents silane (e.g. trichloromethylsilane) and (2) silazane (e.g. hexamethyldisilazane) compounds.

In this specific study, the focus falls on surface hydroxyl group determination and not on modification of the surface itself (chemical dehydration). High temperatures are normally employed to break the Si-O-Si bonds on the surface on chemical dehydration. As we were only interested in the determination of the amount of surface OH-groups, a temperature slightly higher than room temperature (e.g. 50 °C) was employed for the reaction of Si-OH with hexamethyldisilazane (HMDS). After this reaction, the original amount of Si-OH groups can easily be deduced from the carbon content of the modified silica.

However, care should be taken here, as silica materials can be synthesized via a sol-gel process, typically with tetraethyl orthosilicate as precursor and ethanol as solvent[16]. It is therefore important, before the determination of the surface hydroxyl contents from the elemental analysis data of the HMDS-modified silica, to determine the wt % carbon residue that is already present in the virgin, non-modified silica's. (Table 2-4 indicates that indeed small amounts of carbon are present in all the virgin silica samples, for which the HMDS-modified silica's need to be corrected.)

Table 2-4   Traces of carbon present on the calcined silica's, as determined by elemental analysis.

Support	Silica	T_{cal} (ºC)	AES-ICP	
			C, wt %	Si, wt %
MS1	MS-3040	250	0.4	40
MS2		600	0.4	40
S1	Sylopol 948	250	0.2	41
S2		600	0.2	41

The four silica materials were modified with HMDS at 50 ºC and dried under vacuum. The elemental analysis and the subsequent quantification of the amount of silanol groups available for modification are summarized in Table 2-5. The carbon contents listed in this table have been corrected for the carbon content of the virgin silica materials, allowing a reliable calculation of the original amount of silanol groups present on the silica surface.

Table 2-5   Summary on the analysis results obtained for surface modification with hexamethyldisilazane (HMDS).

Support	AES-ICP		OH-groups (mmol/g)
	C, wt %	Si, wt %	
MS1	7.8	35	3.2
MS2	5.1	44	1.4
S1	8.7	45	2.4
S2	3.7	44	1.0

As would be expected, more silanols (available for modification) are detected with the 250 °C calcined materials compared to the 600 °C analogues. This is also supported by literature as Chien stated[11] that silica calcined at 200 °C has 2.3 mmol OH/ g, while silica calcined at 600 °C has 0.7 mmol OH/ g of silica. Okuda *et al*[17] estimated (via a thermogravimetric method[18]) the silanol content of Sylopol 948 calcined at 600ºC to be 1.18 mmol/g of silica. Hydroxyl content determination is strongly method dependent[3]. It is, however, vital to determine the amount of hydroxyl groups available for modification, as we would later need to calculate the amount of catalyst or cocatalyst required to react away as much of the silanols as possible, in order to ensure maximum activity of the catalyst. (The catalysts in question are very sensitive to polar groups and would easily react with them to result in the deactivation of these activated species.)
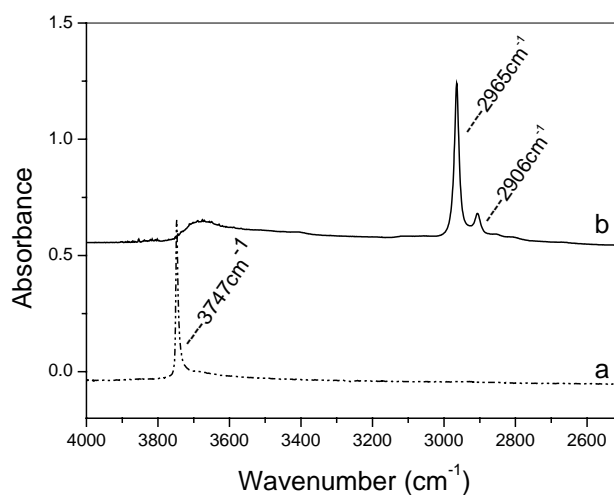
Figure 2-5   Infrared spectra of unmodified (a) and HMDS modified (b) Sylopol 948 calcined at 600ºC.

Hexamethyldisilazane (HMDS) reacts with the silica surface to form a very stable methylsilyl group (bands observed at 2906 cm^{-1} and 2965 cm^{-1} in the infrared spectrum in Figure 2-5) . HMDS is known to react exclusively with isolated hydroxyl groups on the silica surface, usually observed at 3746 cm^{-1} in the infrared spectrum[19-21] (Figure 2-5).

In contradiction to what is observed in the infrared spectra (Figure 2-5), it is postulated[22] that a maximum coverage of the silica after HMDS modification is not possible due to steric hindrance. Sindorf and Maciel[22] have calculated, on basis of molecular geometry and packing considerations, that a maximum coverage of 2.2-2.8 TMS groups/nm^2 (depending on the model) is possible. HMDS reacts initially very rapidly with the silica surface and the reaction is then retarded by steric hindrance. It is reported[22,23] that 1.5 TMS groups/nm^2 is the result of the fast reaction of the HMDS on the silica surface. The main advantage of HMDS above chlorosilanes is that no side reactions are detected.

2.4. CONCLUSIONS

The silica materials chosen appear to be porous and the amount of hydroxyl groups available for chemical modification can successfully be manipulated (1.0 – 3.2 mmol OH/g silica) in a reproducible manner with calcination. BET analysis gives a better understanding as to which properties of the silica material (and to what extent) have been influenced by chemical modification. (This will be illustrated in further detail in Chapter 4.) Infrared analysis proves to be quite a useful tool in the analysis of the extent of modification, while SEM provides clear images regarding the morphology of the support materials.

The silica characteristics and techniques introduced in this Chapter have successfully been employed in cocatalyst immobilization.

2.5. REFERENCES

1. Hlatky, G.G. *Chem. Rev.* **2000**, *100*, 1347.

2. Kislev, A. Kollodn. Zh. 1936, 2, 17.

3. Vansant, E.F.; Van Der Voort, P.; Vrancken, K.C. *Characterization and chemical modification of silica surface*; Elsevier: Amsterdam, **1995**.

4. Kellum, G.E.; Smith, R.C. *Anal. Chem.* **1967**, *39*, 341.

5. Gilpen, R.K.; Gangoda, M.E.; Jaroniec, M. *Carbon* **1997**, *35*, 133.

6. Costa, T.M.H.; Gallas, M.R.; Benvenutti, E.H.; daJornada, J.A.H. *J. Non-Cryst. Solids* **1997**, 220, 195.

7. Armistead, C.G.; Tyler, A.J.; Hambleton, F.H.; Mitchell, S.A.; Hockey, J.A. *J. Phys. Chem.* **1969**, *73*, 3947.

8. Fripiat, J.J.; Uytterhoeven, J. *J. Phys. Chem.* **1965**, *66*, 800.

9. Michael, G.; Ferch, H. *Tech. Bull. Pig.* **2001**, *11*, 41.

10. Ramos, M.A.; Gil, M.H.; Schact, E.; Matthys, G.; Mondelaers, W.; Figueiredo, M.M. *Powder Tech.* **1998**, *99*, 79.

11. Chien, J.C.W. *Top. Catal.* **1999**, *7*, 23.

12. Ogenko, V.M. *Reac. Kinet. Catal. Lett.* **1993**, *50*, 103.

13. Davydov, V.Y.; Kislev, A.V.; Zhuralev, L.T. *Trans. Faraday Soc.* **1964**, *60*, 2254.

14. Tayler, J.A.G.; Hockey, J.A.; Pethica, B.A. *Proc. Br. Ceram. Soc.* **1965**, *5*, 133.

15. Müller, R.; Kammler, H.K.; Wegner, K.; Pratsinis, S.E. *Langmuir* **2003**, *19*, 160.

16. Song, K.C.; Pratsinis, S.E. *J. Colloid. Inter. Sci.* **2000**, *231*, 289.

17. Musikabhumma, K.; Spaniol, T.P.; Okuda, J. *J. Macromol. Chem. Phys.* **2002**, *203*, 115.

18. Dissertation: Du Fresne von Hohenesche, C.; Mainz University: Mainz, Germany, **1999**.

19. Hertl, W.; Hair, M.L. *J. Phys. Chem.* **1971**, *75*, 2181.

20. Haukka, S.; Lakomaa, E.L.; Root, A. *J. Phys. Chem.* **1993**, *97*, 5085.

21. Haukka, S.; Root, A. *J. Phys. Chem.* **1994**, *98*, 1695.

22. Sindorf, D.W.; Maciel, E. *J. Phys. Chem.* **1982**, *86*, 5208.

23. Snyder, L.R.; Ward, J.W. *J. Phys. Chem.* **1966**, *70*, 3941.

CHAPTER 3

Effect of Immobilization Techniques on Support

and Polymer Properties[*]

SYNOPSIS: Homogeneous metallocene/MAO catalyst systems are not suitable for direct application in industry due to the lack of control over polymer morphology. Additionally, the large amount of MAO as cocatalyst that is required makes these systems quite expensive. A plausible solution to this is the immobilization of metallocene/MAO catalysts on suitable support materials such as silica. This not only allows for better control over particle morphology, but much lower cocatalyst (MAO) to catalyst ratios can be employed. However, immobilization is often accompanied by significant decreases in catalyst activity. Physical effects such as limited monomer diffusion through the growing polymer particle should also be taken into account, particularly in cases where incomplete immobilization of the catalyst can lead to blocking of the pores. The technique for the immobilization of these species on support materials is therefore a very important parameter in the industrial success of these materials.

The aim of this chapter is to provide a closer look to the challenges in the immobilization of single-center catalyst systems on silica for olefin polymerization. Homogeneous impregnation appears to be dependent, not only on the method, but also the type of silica.

Keywords: supports; immobilization; single-center catalysts; methylaluminoxane; polypropylene

3.1 Introduction

The combination of single-center catalysts with methylaluminoxane (MAO) as cocatalyst for olefin polymerization has, throughout the last two decades, been the subject of intensive research, as a result of high catalytic activity and versatile control of polymer structure and properties via manipulation of the ligand sphere surrounding the metal atom. A major challenge, however, lays in the adaptation of this system for implementation in industrial gas phase and slurry processes. Reactor fouling, polymers of low bulk densities and the high amount of methylaluminoxane required are problems confronting the use of homogeneous catalyst systems in polyolefin manufacture. The immobilization of methylaluminoxane (MAO)/catalyst systems on support materials, was first reported by Kaminsky[2] and Sinn[3] in the mid 1980's. A few key factors should always be kept in mind with the immobilization of these systems on support materials for olefin polymerization:

The catalyst systems should be thoroughly fixed on the support surface in order to prevent leaching of the catalyst into solution resulting in undesired homogeneous polymerization;

The method of immobilization should allow for the homogenous distribution of the activated catalyst species throughout the support particle to facilitate full particle fragmentation on polymerization. This will also prevent the formation of fines in the reactor setup;

The catalyst should retain its original characteristics observed in solution polymerization: tailoring the resulting polymer according to a predetermined molecular weight, molecular weight distribution, polydispersity and isospecificity (in case of polypropylene);

The catalyst should also retain the high, competitive activity observed in solution processes. (Incomplete activation of the immobilized catalyst often results in low activity systems on immobilization of the catalyst species).

An acceptable compromise between polymer particle morphology and catalyst activity is vital. High catalyst activities could result in large exotherms on the surface of the silica

particle, resulting in bad particle morphology (formation of fines or leaching of the catalyst into solution).

With the above in mind, various researchers set out to perfect the art of immobilization. These efforts are very well recapitulated in a recent review written by Ribeiro[4]. Although quite a number of variations exist, immobilization techniques can be divided into three main groups: Direct immobilization of the metallocene on a pretreated silica support[5-7]; Impregnation of the support with the methylaluminoxane followed by exposure to the catalyst species after tedious washing and drying of the support[5,8,9] (This method is based on the assumption that the catalyst species will "follow" the MAO that was impregnated on the support and thus all the species are activated.); Impregnation of the silica with the MAO-activated catalyst species[10]. The first method is the most simple, but the observed activities are low. The danger in this case is deactivation of the catalyst species when introduced to the polar surface hydroxyl groups[11,12]. Alternatively, the catalyst can be synthesized in situ on the support[13,14], minimizing the chance of leaching of the activated species into solution[15,16]. Comparisons between various reports in literature are often made with regard to this topic, but one must always keep in consideration that the handling of the sensitive catalyst species, the raw materials, the exact specification of the silica and the reactor system and conditions employed vary from one lab to another.

In this study, we have considered the immobilization of methylaluminoxane on Sylopol 948 and MS-3040 spheroidal silica, calcined at two different temperatures in order to control the amount of available hydroxyl groups. The homogeneity of the impregnation method and support characteristics will be discussed in terms of surface characteristics obtained from nitrogen adsorption data (BET), fourier transformed infrared spectroscopy (FTIR), scanning electron microscopy (SEM) and energy dispersive x-ray (EDX) element mapping. Polypropylenes, obtained through catalysis with a moderately and a highly isospecific catalyst precursor, were used to evaluate the influence of the method of immobilization and the type of silica on the degree of isotacticity, molecular weight distribution and the morphology of the resulting polymer particles.

3.2 Experimental

3.2.1. Materials

All reactions were carried out under argon atmosphere. Catalysts were handled in a glove box under an inert atmosphere with maximum O_2 and H_2O levels of 1 ppm and 0.3 ppm, respectively. A 10 wt-% solution of the methylaluminoxane (MAO) in toluene was obtained from Witco, while *racemic* ethylene-bridged bis(indenyl) zirconium dichloride (*rac*-Et(Ind)$_2$ZrCl$_2$) was purchased from STREM chemicals. *Racemic* dimethylsilyl-bridged bis(2-methyl-4-phenyl-indenyl) zirconium dichloride (*rac*-Me$_2$Si(2-Me-4Ph-Ind)$_2$ZrCl$_2$) was kindly donated by SABIC EuroPetrochemicals. Silica support materials, MS-3040 (PQ Corporation) and Sylopol 948 (Grace AG), were kindly donated by their respective suppliers. Toluene (Biosolve) was dried on alumina columns, while n-heptane was distilled over potassium before use. Tri*iso*butylaluminum (TIBA) was purchased from Akzo-Nobel as a 25 wt-% solution in toluene, while 1,1,1,3,3,3-hexamethyldisilazane (HMDS) was obtained from Sigma-Aldrich. Propylene (Hoekloos) was dried over columns containing activated copper catalyst (BTS) and alumina before introduction into the polymerization reactor.

3.2.2. Support synthesis

3.2.2.1. Calcination

See Section 2.2.2.1 for details.

3.2.2.2. Chemical modification for determination of available hydroxyl groups

See Section 2.2.2.2. for details.

3.2.2.3. MAO impregnation

In the first method, 1 g of each of the four silica materials (MS-3040 and Sylopol 948, calcined at 250 °C and 600 °C) was, respectively, slurried in 5ml of toluene. Impregnation was carried out by contacting the silica slurry with 3.12 mmol of MAO (diluted in 5 mL toluene) at room temperature over a period of 5 minutes. The slurry was left for two hours,

after which it was washed with 10 mL n-heptane and dried under vacuum to obtain a free-flowing powder.

In the second method, the MAO (3,12 mmol) was once again diluted in 5 mL toluene and slowly added to the silica (1 g of Sylopol 948, calcined at 250 °C and 600 °C, respectively) slurried in 5 mL of toluene. The slurry was subsequently heated to 110 °C and kept isothermal for 4 hours. It was then left for 18 hours at ambient temperature. The solid was separated from the solvent by decantation and was then contacted with 5 mL toluene (preheated to 90 ºC) and the slurry was left for 45 minutes and 90 °C. After decantation, 5 mL of fresh toluene were added and the slurry was left for 45 minutes at 90 °C. This procedure was repeated. The solvent was finally decanted again to obtain a "wet sand", which was then heated to 120 °C under a reduced pressure of 22 mbar. A free-flowing powder was obtained after an hour. Two additional supports, with increased amounts of MAO, were synthesized in the same manner with Sylopol 948, calcined at 250 °C (see Table 3-4).

The last method entailed the immobilization of MAO-activated catalyst on silica. A gram of silica was weighed off in the glove box, slurried in 1.5 mL toluene and placed in an ice bath. The catalyst (10 mg/g silica) was weighed off in the glove box and contacted with MAO (2 mL/g of silica). The catalyst solution was transferred to the fume cupboard and left for ten minutes to stir. The catalyst solution was slowly added to the silica slurry over a period of 5 minutes. The "wet sand" was slowly heated over a period of 6 hours from 0 °C to 63 °C under vacuum to obtain a free flowing powder.

3.2.3. Slurry Polymerization Procedure

Polymerization was carried out in a 200 mL Buchi glass reactor fitted with a pressure gauge, pressure relief valve, gaseous monomer inlet and an extra inlet for solvents. A hollow- shaft turbine stirrer was used. The catalyst (2.39 μmol), dissolved in 1 mL of toluene, was first pre-contacted with 1.8 mmol of the 25 wt-% TIBA solution. It was then aged at room temperature for 1 hour to ensure maximum alkylation. MAO impregnated silica (100 mg) was transferred to the reactor (under N_2 atmosphere) and contacted with the alkylated catalyst solution for 1 hour. The reactor was then charged with a solution of

100 mL dry n-heptane and 1.5 mmol of the 25 wt-% solution of TIBA in toluene (to serve as scavenger) under monomer atmosphere. The reactor temperature was raised to 50 °C (over 15 minutes) at a monomer pressure of 0.5 bar and a stirring speed of 700 rpm. The monomer pressure was raised to 4 bar after 15 minutes for the main polymerization. The reactor was degassed after 1 hour and the reaction slurry was quenched with acidic methanol.

3.2.4. Characterization techniques

Details regarding BET surface analysis, SEM imaging, elemental analysis and infrared spectroscopy are given in Section 2.2.3. Polypropylene tacticity was determined by ^{13}C NMR (125.69MHz) spectroscopy at 120 ºC on a Varian Unity Inova 500 NMR spectrometer. The polymer (150-200 mg) was dissolved in 1,2,4-trichlorobenzene with deuterated tetrachloroethane as lock solvent. Analyses were performed in 10mm NMR tubes at a flip angle of 74 °, an acquisition time of 1.3 seconds and a delay time of 4 seconds. A Q100 (TA Instruments) differential scanning calorimetric equipment was used for the determination of melting temperatures. Samples (1.5-2.5 mg) were heated to 160 °C at a rate of 10 °C/ minute and cooled down at the same speed to 50 °C. This was repeated and the second heating cycle was used for data analysis. High temperature gel-permeation chromatography (GPC) was carried out in 1,2,4-trichlorobenzene at 135 ºC on a PL-GPC 210 High Temperature chromatograph. The instrument was equipped with 4 PL-Gel Mixed A columns, a RALLS light scattering detector, H502 viscometer, refractive detector and DM400 data manager (Viscotek)**.**

3.3 Results and Discussion

3.3.1. Calcination and characterization of silica supports

Two different silica supports, PQ (MS-3040) and Grace (Sylopol 948), with average particle sizes of 90 μm and 50 μm, respectively, were selected for this study. Calcination was carried out at two different temperatures (250 °C and 600 °C) and the surface area, mean pore diameter and pore volume, of each calcined silica, was determined with BET analysis. The residual hydroxyl content (Table 2-5) was determined by carbon analysis

after treatment with hexamethyldisilazane (HMDS), as described in Section 2.2.2.2. It was concluded that MS-3040 has a larger surface area and pore volume than Sylopol 948.

3.3.2. Simple MAO impregnated silica

The calcined silica materials were contacted with MAO at room temperature, washed and then dried under vacuum to obtain orange, free-flowing powders. Surface analysis (Table 3-1) of these Al-modified silica's (MS-3040 and Sylopol 948) indicated a moderate decrease in BET surface areas (30-80 m^2/g), BJH pore diameters (5-10 nm) and BJH pore volumes (0.5-0.7 cm^2/g) in comparison to their calcined, non-impregnated analogues (see Table 2-1). Little effect of calcination temperature on the Al content of the impregnated supports was observed, but the Al contents of the supports prepared from MS-3040 were somewhat higher than those observed for Sylopol 948-based support materials.

Table 3-1 Characteristics of MAO impregnated supports (reference to surface and elemental analysis).

Silica	T_{cal}[a] (°C)	Support	Surface area (m^2/g)	Pore diameter (nm)	Pore volume (cm^3/g)	Al (mmol/g silica)	AES-ICP	
							Al (wt %)	Si (wt %)
MS-3040	250	MS$_{250}$	351	22	2.1	4.08	11	36
MS-3040	600	MS$_{600}$	405	18	2.0	3.71	10	31
Sylopol 948	250	S$_{250}$	274	15	1.2	2.96	8	31
Sylopol 948	600	S$_{600}$	276	14	1.1	3.34	9	35

[a]Calcination temperature

The results obtained suggest that MAO has reacted with the free silanols on the surface, as well as in the pores of the silica particles. The higher amount of aluminum detected on the MS-3040 silica's, in comparison to the Sylopol 948 silica's, is in agreement with the larger amount of hydroxyl groups (Table 2-5) available for modification on these materials.

In order to visualize the effect of catalyst behavior as a function of type of silica material and calcination temperature, emphasis was placed on the synthesis of polypropylene (PP) with a moderately isospecific catalyst (*rac*-Et(Ind)$_2$ZrCl$_2$). Prior to contact with the support, a toluene solution of the catalyst was first contacted with an

excess of AliBu$_3$ (Al/Zr 750) for 1 hour to effect alkylation of the metallocene[17]. The polymer properties, as summarized in Table 3-2, indicate that the activity of the homogeneous systems (with a catalyst to cocatalyst mol ratio of 1:130) is at least five times higher than that observed for the supported catalyst systems.

Table 3-2   Polypropylene properties, resulting from propylene polymerization with rac-Et(Ind)$_2$ZrCl$_2$ on MAO-impregnated silica.

Support	Al:Zr[a]	Activity[b]	mmmm (%)	T$_m$ (°C)	M$_w$ (g/mol)	M$_n$ (g/mol)	Mw/Mn
none	1000:1	12 772	67	124	11 250	4 700	2.4
none	130:1	1 197	82	131	25 000	9 600	2.6
MS$_{250}$	130:1	252	85	136	46 400	25 400	1.8
MS$_{600}$	130:1	52	91	141	73 800	29 200	2.5
S$_{250}$	130:1	216	87	132	30 400	15 300	2.0
S$_{600}$	130:1	152	85	137	56 800	31 400	1.8

[a]Intended catalyst to cocatalyst mol ratios

[b]Activity in kg PP / (mol catalyst.hour)

The polypropylenes synthesized using the immobilized catalysts are more isotactic than the polymers obtained under homogeneous conditions. The exotherm observed for the homogeneous polymerization at MAO/Zr of 1000 was around 10 ℃, while the exotherm of the supported polymerization system was about 2 ℃. This significant difference in temperature could explain the large difference in tacticity between the supported and the homogeneous systems[18]. However, in the ^{13}C NMR spectra of the homogeneously prepared polymer (Figure 3-1), the presence of atactic sequences was observed, possibly due to photo-induced rac/meso isomerization in metallocene solutions exposed to light[19]. It was reported by Kaminsky et al[19] that the final rac/meso proportion and interconversion rate is dependent on the specific metallocene structure. In the case of the immobilized catalyst, ^{13}C NMR revealed the presence of only isolated stereoirregularities arising from enantiomorphic site control (irregular insertions), leading to a typical 2:2:1 distribution of mmmr, mmrr and mrrm pentads. The second homogeneous system (with the lower catalyst to cocatalyst mol ratio) showed a lower exotherm of 5 ℃ and only traces of atactic sequences were observed. The very low

molecular weights of the homogeneously prepared polymers should also be taken into account, as the relatively high proportion of chain-ends will lead to changes in the chemical shifts of the methyl groups in pentads close to the chain-ends.
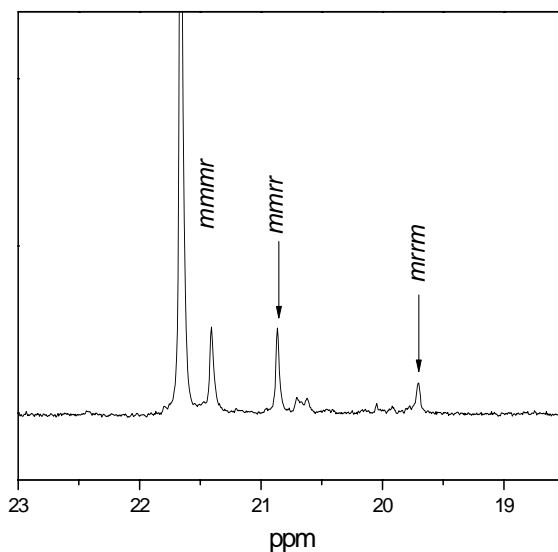
Figure 3-1   A ^{13}C NMR spectrum (methyl region) of PP synthesized with the homogeneous catalyst system (catalyst to cocatalyst mol ratio of 1000:1), indicating chain irregularities.

The narrow molecular weight distributions serve as an indication of the retention of single-center behavior throughout this series. The higher molecular weights observed for the supported systems could be explained by the lower probability of chain transfer to aluminum. (Taking into account the differences in the amount of MAO present and the contribution of chain transfer to aluminum of AlMe$_3$ present in MAO, unless removed by chemical or physical means[20].) Polypropylene synthesized homogeneously with a catalyst to cocatalyst ratio of 1:130 also displays a molecular weight of at least double the amount observed for the homogeneous system where 8 times more MAO was used. This supports the idea that chain transfer to aluminum plays a significant role as method of chain termination in these systems. In general, higher activities are observed with 250 °C calcined silica systems compared to those with the 600 ºC calcined systems, although the latter result in polymers with higher molecular weights and isotacticities. Possible reasons for this phenomenon are discussed below.

In the case of the more isospecific *rac*-Me$_2$Si(2-Me-4Ph-Ind)$_2$ZrCl$_2$, the influence of support type and calcination temperatures on isospecificity was observed to a lesser extent (Table 3-3).

Table 3-3   Polypropylene properties, resulting from propylene polymerization with *rac*-Me$_2$Si(2-Me-4Ph-Ind)$_2$ZrCl$_2$ on MAO-impregnated silica.

Support	Al:Zr[a]	Activity[b]	mmmm (%)	T$_m$ (°C)	M$_w$ (g/mol)	M$_n$ (g/mol)	Mw/Mn
MS$_{250}$	130:1	720	96	146	729 300	242 800	3.0
MS$_{600}$	130:1	72	97	147	368 500	116 700	3.2
S$_{250}$	130:1	640	95	146	497 500	144 300	3.5
S$_{600}$	130:1	276	95	146	466 000	148 600	3.1

[a]Intended catalyst to cocatalyst mol ratio's

[b]Activity in kg PP / (mol catalyst.hour)

The only chain irregularities detectable by C^{13} NMR resulted from isolated regioirregular (2,1 erythro) insertions (Figure 3-2).
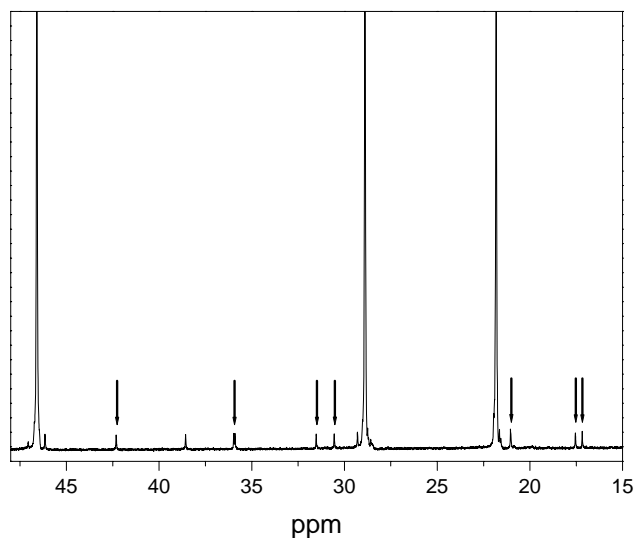
Figure 3-2 ^{13}C NMR spectra (methyl region) of polypropylene, synthesized on support S$_{250}$ with *rac*-Me$_2$Si(2-Me-4Ph-Ind)$_2$ZrCl$_2$ as catalyst precursor, illustrating the presence of 2,1 *erythro*-regio defects (indicated by the arrows in the spectra).

The above chain irregularities are a characteristic feature in PP synthesized with this particular catalyst[21]. This more stereospecific metallocene gave high molecular weight, highly isotactic polymers with DSC melting temperatures in the range of 146-147 °C. Variance in calcination temperature appeared to show the same trend as observed for *rac*-Et(Ind)$_2$ZrCl$_2$ derived PP.

In order to support or better understand our findings above, we turned to IR spectroscopy and EDX element mapping of aluminum on individual particles of the MAO impregnated support samples. Figure 3-3 illustrates the infrared spectra obtained of 1 or 2 of the most representative support particles, as obtained after analysis of 20-30 individual particles of each support with a transmission microscope.

a)   b)

c)   d)
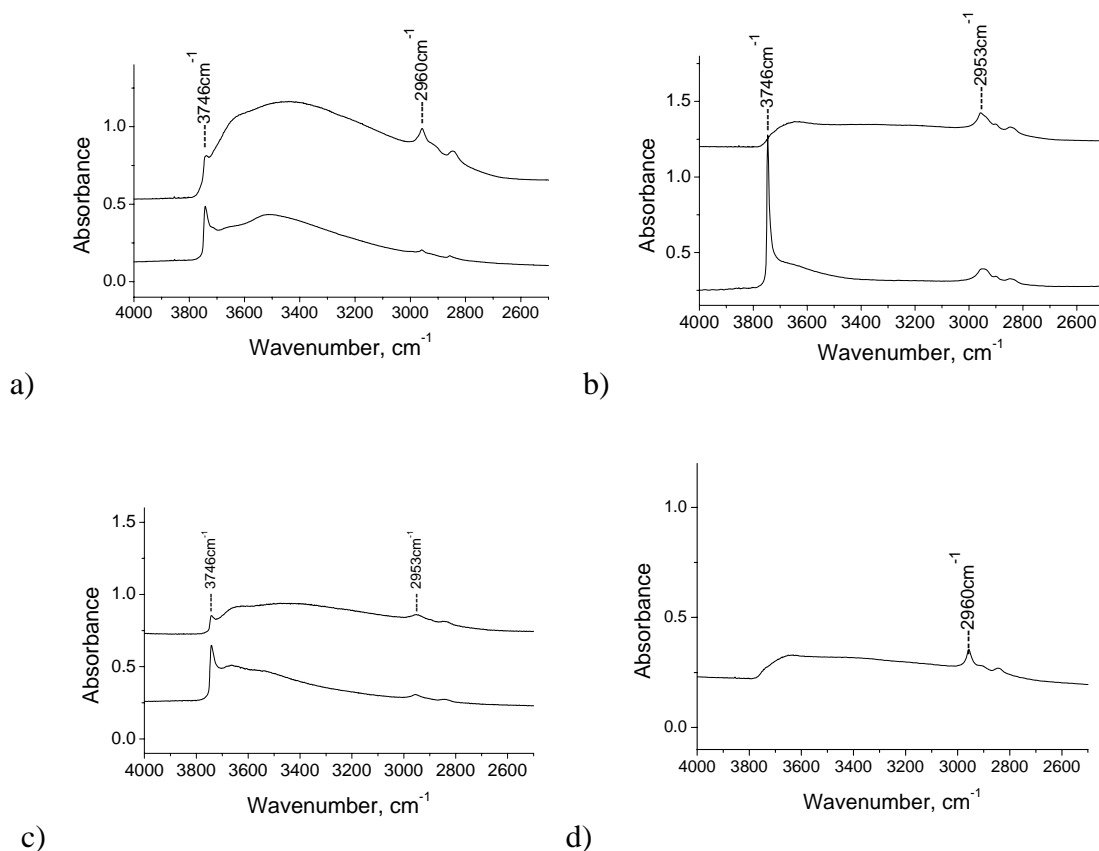
Figure 3-3   Infrared spectra, as observed for MAO-impregnated silica's (MS$_{250}$ (a) MS$_{600}$ (b), S$_{250}$ (c) and S$_{600}$ (d)). Each IR curve represents the analysis of one particular silica particle isolated from each of these supports.

According to literature[22], only the isolated silanol groups on silica react during the immobilization of species. Peaks observed in the 2960-2850cm^{-1} region represent the C-H stretching vibration as observed for methyl groups. Infrared spectra of the MAO-impregnated supports indicate the presence of methyl groups, representing methylaluminoxane, in all the particles analyzed. The difference in isolated silanols detected between two or more silica particles within a sample, MS_{250}, MS_{600} and S_{250}, suggests an inhomogeneous distribution of MAO throughout the support sample. The only exception to this is observed for the MAO-impregnated Sylopol 948 calcined at 600 ˚C (S_{600}). In the latter case, only one type of spectrum (indicating the absence of isolated silanol groups (3746 cm^{-1})) was detected for all particles analyzed.

EDX element mapping of aluminum distribution across individual support particles was carried out after imbedding the support in an epoxy resin, after which samples were cut for cross-sectional analysis. Figure 3-4 shows a homogeneous distribution of aluminum throughout the silica particle in the case of S_{600}, thus supporting the IR data.

(a)   (b)

(c)   (d)
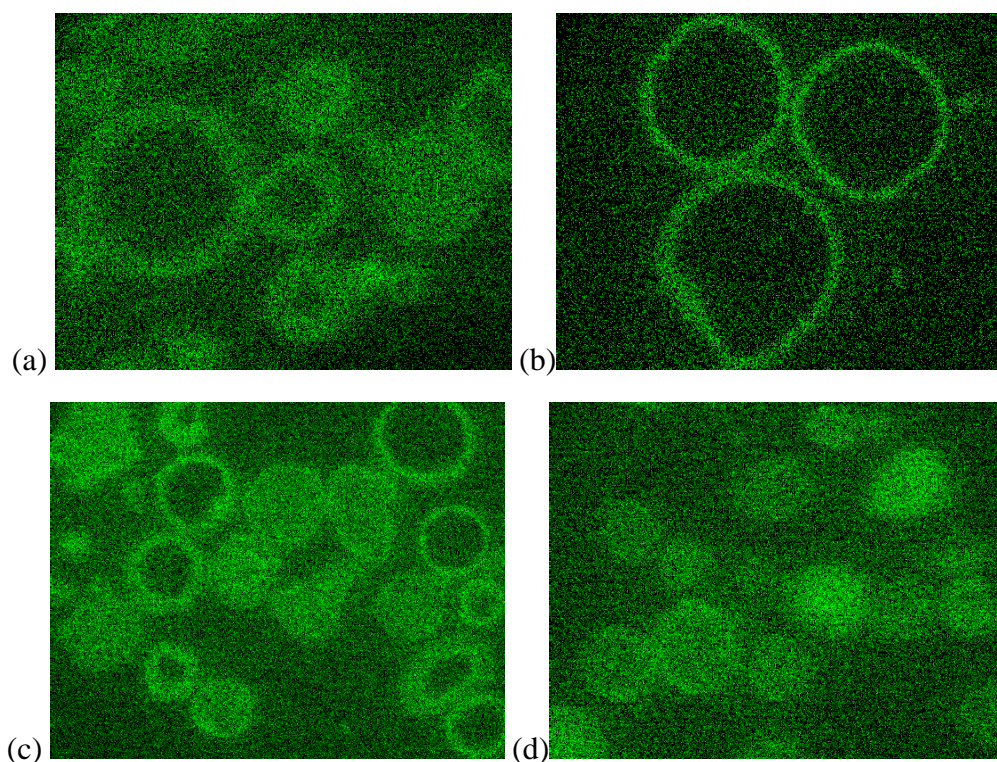
Figure 3-4   EDX mapping of aluminum for supports MS_{250} (a), MS_{600} (b), S_{250} (c) and S_{600} (d) (see Table 3-1 for details).

The MS-3040 silica's (MS_{250} and MS_{600}) and Sylopol 948, calcined at 250 °C (S_{250}) seem to have core-shell distributions of aluminum (the Al being present in the shell). A non-uniform Al distribution in a SiO_2/MAO/zirconocene system has also been noted by Fink and coworkers[23]. A core-shell distribution, implying efficient removal of hydroxyl groups only near the surface of the silica particle, is in agreement with the presence of residual OH-groups on the MAO treated silica's calcined at 250 °C (as observed in IR spectra given in Figure 4(a)). The catalyst activities obtained with the 250 °C calcined silica's were higher than those obtained with the silica's calcined at 600 °C. The trend of the increasing polymer isotacticity and polymer molecular weight with decreasing catalyst activity (Table 3-2) indicates that the low activities are not due to monomer diffusion limitation. A low local monomer concentration as a result of diffusion limitation would, as demonstrated previously[1], lead to a decrease in isotacticity as a result of epimerization of the last inserted monomer unit[24].

The differences in the degree of homogeneity of MAO impregnation in the various supports could contribute to the observed differences in catalyst activity. A core-shell distribution in which the concentration of MAO is the highest at or near the support surface will lead to a significantly higher effective Al/Zr ratio, taking into account that the zirconocene is itself likely to become immobilized at or near the support surface. This might explain, at least in the case of Sylopol 948, the higher activities obtained after calcination at 250 °C rather than 600 °C.

Fragmented particles were observed with SEM imaging (Figure 3-5).
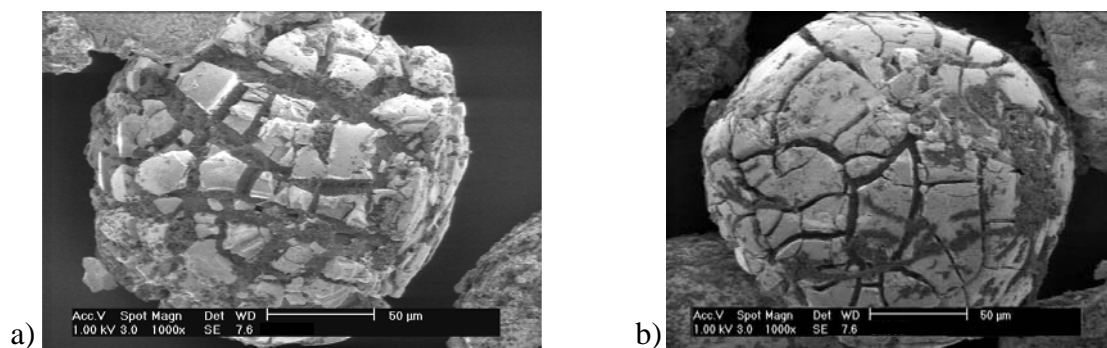
Figure 3-5   SEM images of two individual PP particles prepared using MS_{600} (Table 4-3).

The fragmentation of the support is, however, only partially complete after an hour polymerization time. This is supported by the low activity data on these systems. EDX elemental mapping (as given in Figure 3-6), taken of another fragmented particle shows that the outer surface of the particle comprises of fragmented islands of silica (containing also Al) under which the polymer phase can be seen.

a) b) c) d)
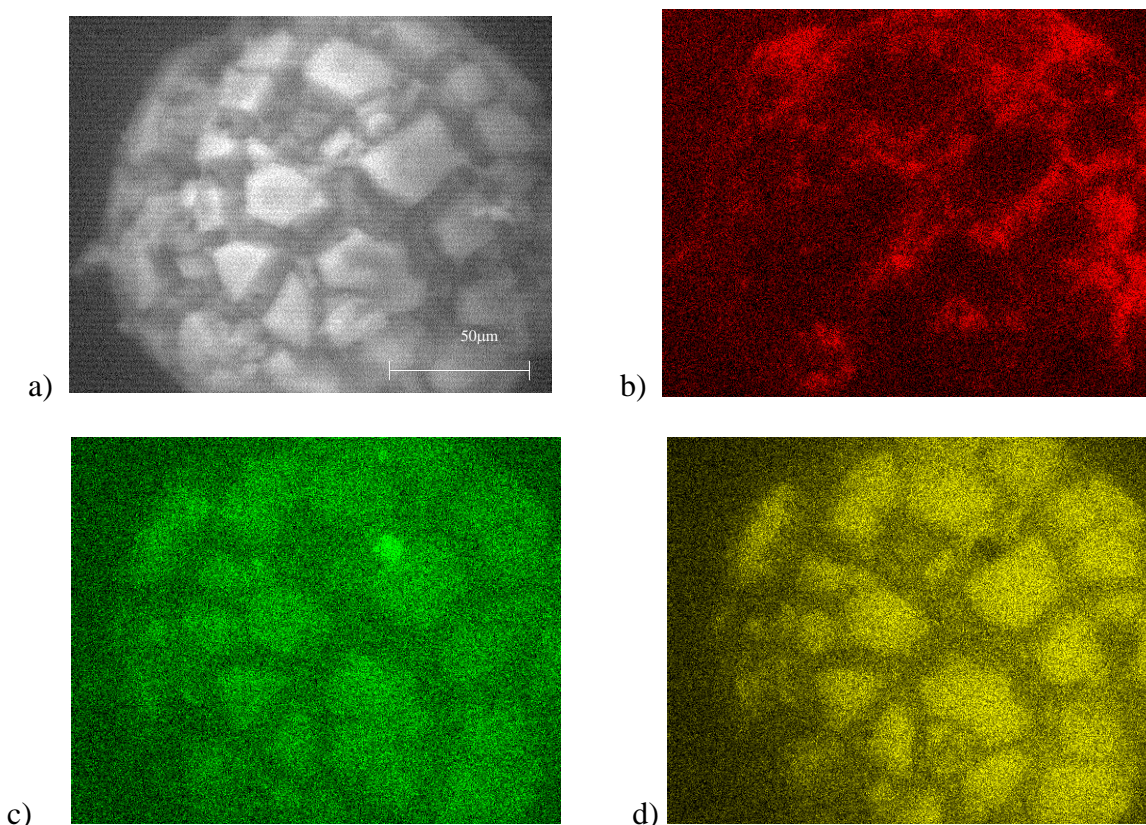
Figure 3-6 EDX elemental mapping illustrating the presence of carbon ((b) red), aluminum ((c) green) and silica ((d) yellow) in the expanding catalyst particle after propylene polymerization, as synthesized with S_{600} (Table 3-2).

3.3.3. "Improved" MAO impregnated silica

Simple contact of MAO with calcined silica at room temperature does not seem to be sufficiently effective to synthesize uniformly impregnated support materials for subsequent catalyst immobilization. We therefore turned our attention to a more rigorous impregnation procedure in which silica was contacted with an increasing amount of MAO

at an elevated temperature (110 °C). Subsequently, it was washed (toluene at 90 °C) to remove all non-immobilized MAO before volatiles removal under reduced pressure. The use of a relatively high temperature for the preparation of MAO impregnated silica may be expected to improve the chemical fixation of MAO on the support .

Support materials $S1_{250}$ and $S1_{600}$ were synthesized with the same amount of MAO as used in the previous section, while $S2_{250}$ and $S3_{250}$ were synthesized with double and triple the original amounts, respectively. The surface characteristics of these modified silica's seem to be more or less the same (Table 3-4) as observed for the first method of MAO impregnation (Table 3-1).

Table 3-4   Surface and Elemental analysis data obtained for the "improved" MAO impregnated silica (Sylopol 948) support materials.

T_{cal}^{a} (°C)	Support	Surface area (m^2/g)	Pore diameter (nm)	Pore volume (cm^3/g)	Al (mmol/g silica)	AES-ICP	
						Al (wt %)	Si (wt %)
250	$S1_{250}^{b}$	299	14	1.3	2.59	7	36
250	$S2_{250}^{c}$	290	13	1.0	4.08	11	32
250	$S3_{250}^{d}$	286	13	1.0	4.08	11	32
600	$S1_{600}^{b}$	342	13	1.2	2.59	7	37

[a]Calcination temperature

[b] Impregnation using 3.1 mmol MAO/ g SiO_2

[c] Impregnation using 6.2 mmol MAO/ g SiO_2

[d] Impregnation using 9.4 mmol MAO/ g SiO_2

IR analysis of these "improved" support materials shows the presence of residual isolated OH groups only for $S1_{250}$ (Figure 3-7 (a), 3746 cm^{-1}), indicating a homogeneous immobilization of MAO over the range of particles observed for samples $S2_{250}$, $S3_{250}$ and $S1_{600}$.
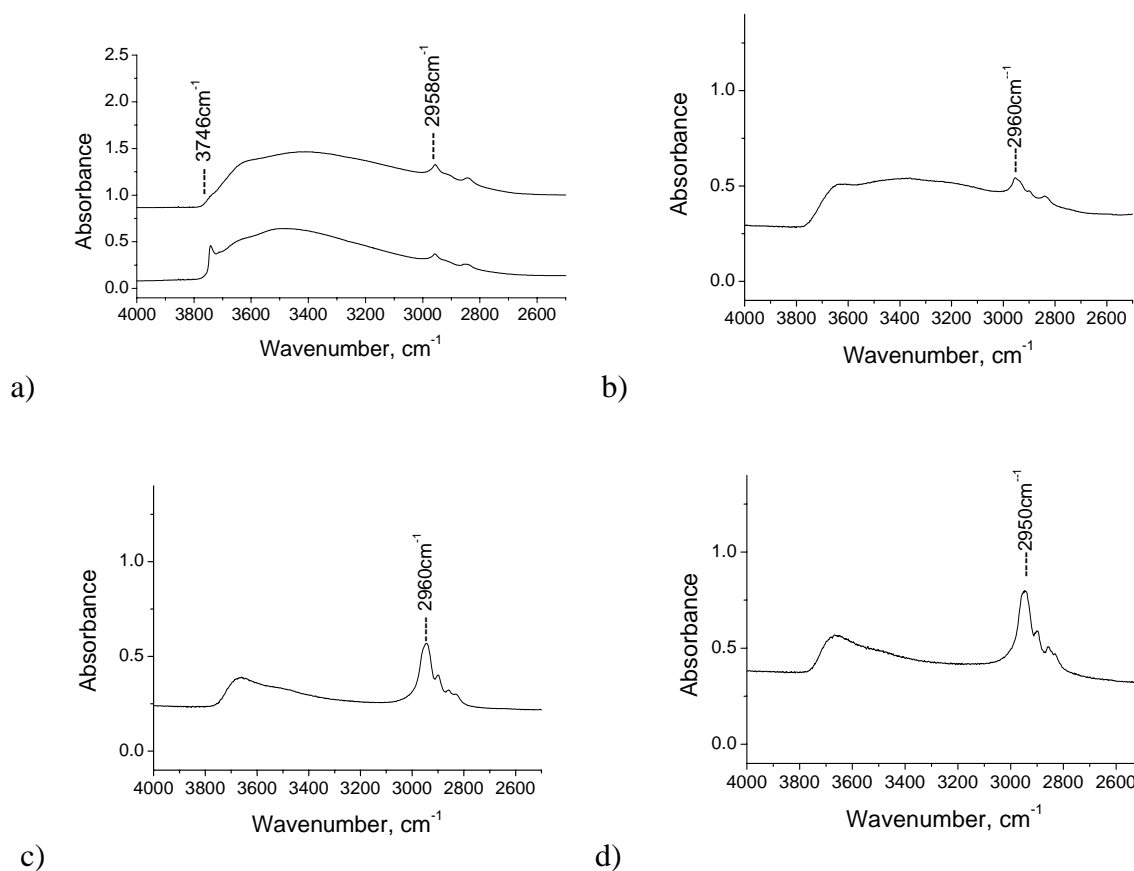
Figure 3-7   Infrared spectra, as observed for supports $S1_{250}$ (a), $S2_{250}$ (b), $S3_{250}$ (c) and $S1_{600}$ (d).

EDX element mapping of these materials ($S1_{250}$, $S2_{250}$, $S3_{250}$ and $S1_{600}$) confirms that a more homogeneous distribution of the cocatalyst is observed throughout the whole silica particle and the entire sample (Figure 3-8).
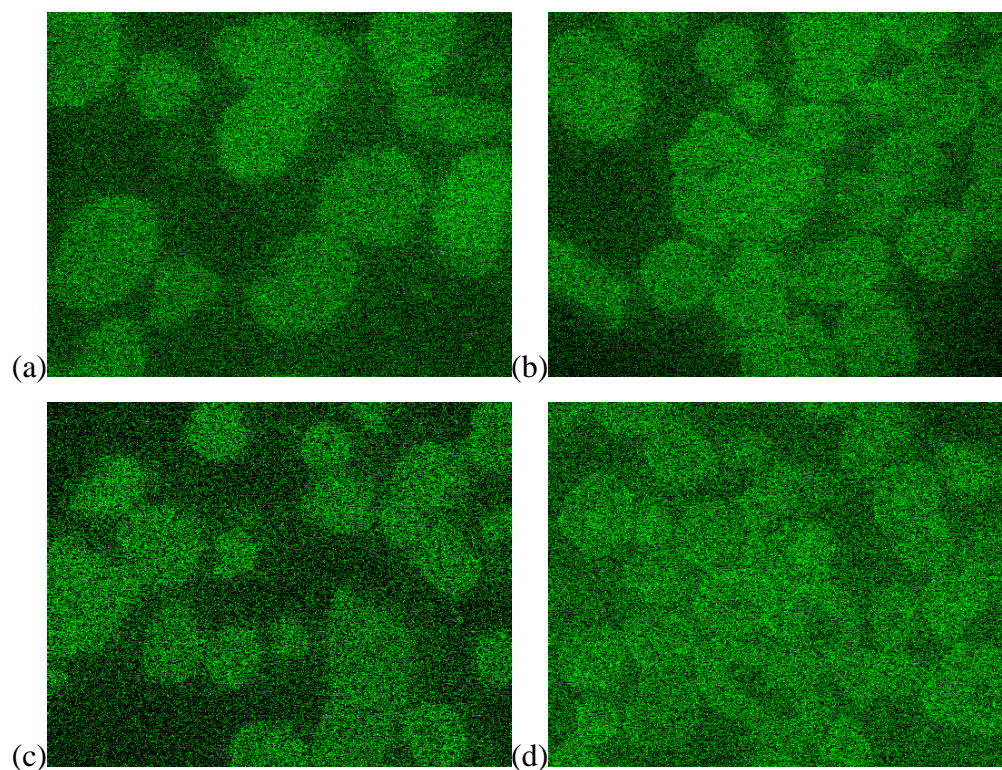
Figure 3-8 EDX element mapping of aluminum for supports $S1_{250}$ (a), $S2_{250}$ (b), $S3_{250}$ (c) and $S1_{600}$.

The results of propylene polymerizations carried out using these "improved" MAO impregnated systems, with *rac*-Et(Ind)$_2$ZrCl$_2$/ Al*i*Bu$_3$ as catalyst precursor, are shown in Table 3-5.

Table 3-5 Polypropylene properties, resulting from propylene polymerization with *rac*-Et(Ind)$_2$ZrCl$_2$ on MAO-impregnated silica.

Support	Al:Zr[a]	Activity[b]	mmmm (%)	T_m (°C)	M_w (g/mol)	M_n (g/mol)	Mw/Mn
$S1_{250}$	130:1	116	88	141	65 000	31 300	2.0
$S2_{250}$	260:1	564	83	142	50 700	24 500	2.1
$S3_{250}$	390:1	956	87	140	44 000	20 600	2.1
$S1_{600}$	130:1	124	83	140	57 200	30 000	1.9

[a]Intended catalyst to cocatalyst mol ratio's
[b]Activity in kg PP/ (mol catalyst.hour)

It is apparent that increasing the quantity of MAO used in the SiO$_2$/ MAO immobilization leads to a significant increase in catalyst activity, despite the fact that the

Al contents in both S2$_{250}$ and S3$_{250}$ appear to be 11 wt %. It appears that the silica surface is saturated with MAO and would thus explain why the Al detected with elemental analysis does not increase with a further increase in MAO added during impregnation. The increase in activity does, unfortunately, go together with a deterioration in particle morphology, which was revealed with SEM imaging (Figure 3-9).
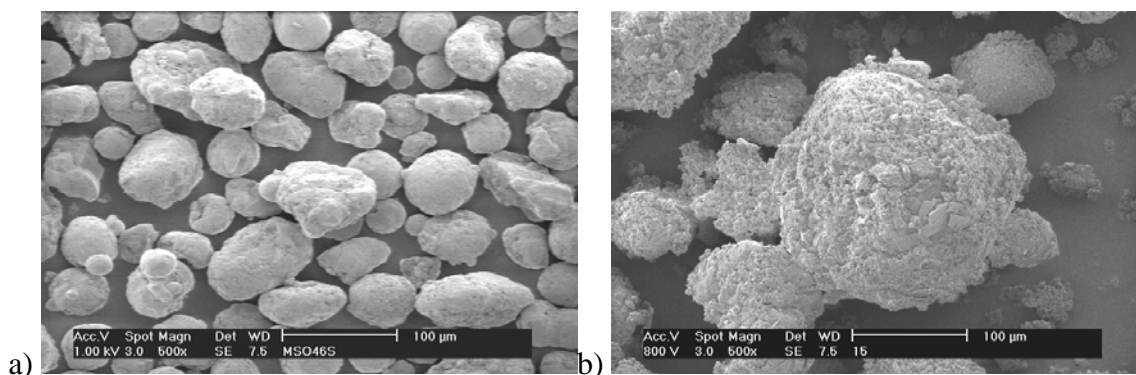
Figure 3-9   Particle morphology of (a) MAO-impregnated support S4 and (b) the resulting polypropylene (Table 3-5).

Again, the molecular weight distribution indicates the retention of the single-center characteristics of the catalyst. A decrease in molecular weight with increasing amount of MAO used in immobilization is apparent, supporting the higher probability of chain termination reactions via chain transfer to aluminum. It is also clear, as was the case for the experiments listed in Table 3-2, that there is an inverse relationship between catalyst activity and polymer molecular weight in this series.

The activity of 956 kg/mol catalyst.h obtained using S3$_{250}$ approaches that obtained in homogeneous polymerization (Table 3-2) at a Al/Zr of 130. However, the fact that this improvement in activity was accompanied by irregular particle growth indicates that in these experiments simple contact between the support and the catalyst solution prior to polymerization was insufficient to achieve good particle morphology. Attention was therefore turned to the impregnation of silica with a pre-contacted mixture of MAO and zirconocene, aiming for a uniform distribution of both Al and Zr throughout the support.

3.3.4. MAO-activated catalyst immobilized on silica (temperature program)

In this third approach to catalyst immobilization on silica, the zirconocene was first pre-activated by contacting with MAO, after which the resulting solution was used to impregnate the silica. A minimum amount of solvent was used, in order to effect efficient pore filling of the support, leading to a mixture having the consistency of wet sand. The solvent was then removed under reduced pressure in the temperature range 0-63 ℃, in order to immobilize the catalyst and cocatalyst on the support. The characteristics of the supports prepared in this way are given in Table 3-6.

Table 3-6   Characteristics of MAO-activated *rac*-Et(Ind)$_2$ZrCl$_2$ impregnated supports (surface and elemental analysis).

Silica	T_{cal}[a] (°C)	Support nr	Surface area (m^2/g)	Pore diameter (nm)	Pore volume (cm^3/g)	AES-ICP		
						Zr (wt %)	Al (wt %)	Si (wt %)
MS-3040	250	MS1$_{250}$	319	23.6	1.9	0.16	8.2	35.7
	600	MS1$_{600}$	375	22.2	2.1	0.10	6.7	32.9
Sylopol 948	250	S4$_{250}$	258	17.1	1.1	0.17	8.7	34.9
	600	S2$_{600}$	270	17.3	1.2	0.17	8.6	39.2
	600	S3$_{600}$[b]	269	16.3	1.1	-	11.1	43.2

[a]Calcination temperature
[b]MAO impregnated reference reaction synthesized with the same temperature program as method 3 (Section 3.2.2.3.)

For the purpose of comparison, a reference silica/MAO support was prepared under the same conditions, but without the zirconocene. The Al distribution in cross-sectional images of the MAO/zirconocene-impregnated supports are shown in Figure 3-10, which indicates the presence of both homogeneously and inhomogeneously impregnated particles in all the samples prepared.
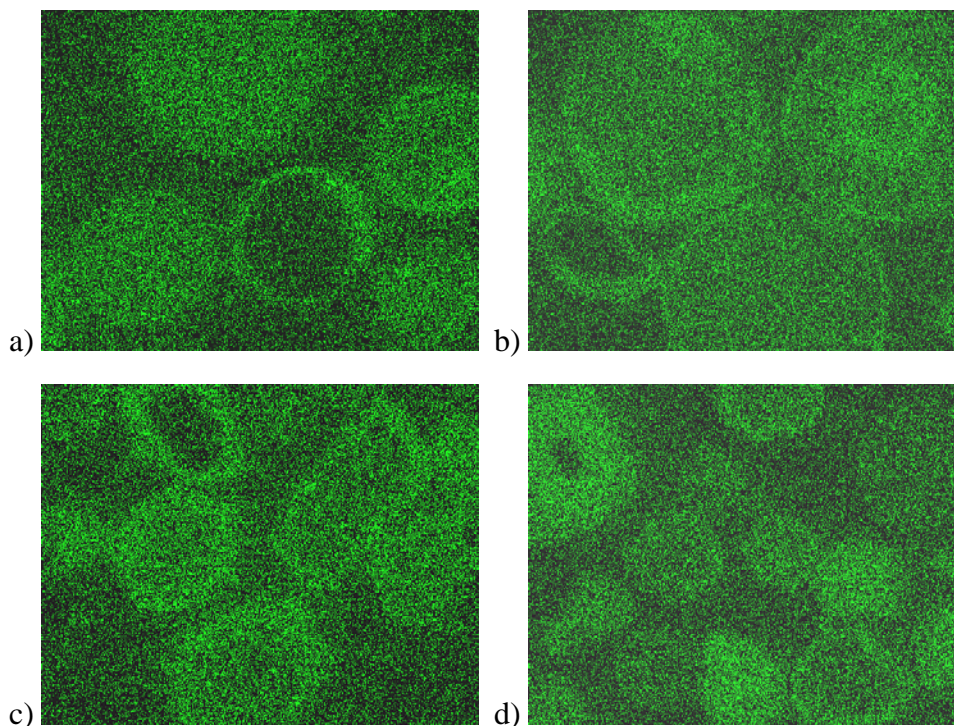
Figure 3-10 EDX mapping for aluminum for supports MS1$_{250}$ (a), MS1$_{600}$ (b), S4$_{250}$ (c) and S2$_{600}$ (d) (Table 3-6).

The results of propylene polymerizations carried out using these immobilized catalysts are given in Table 3-7.

Table 3-7 Polypropylene properties, resulting from polymerization with *rac*-Et(Ind)$_2$ZrCl$_2$ on MAO-impregnated silica.

Support	Activity[a]	mmmm (%)	T$_m$ (°C)	M$_w$ (g/ mol)	M$_n$ (g/mol)	Mw/Mn
MS3	720	79	133	35 500	17 600	2.0
MS4	1210	82	134	36 000	17 200	2.1
S7	1090	76	133	41 300	18 800	2.2
S8	860	82	133	40 700	20 000	2.0
S9[b]	290	88	135	40 200	20 800	1.9

[a]Activity in kg polymer / (mol catalyst.hour) with 130:1 intended Al:Zr in all cases
[b]MAO-impregnated Sylopol 948 (calcined at 600°C); *rac*-Et(Ind)$_2$ZrCl$_2$/Al*i*Bu$_3$ added separately prior to polymerization

On comparison of the results summarized in Table 3-7 with those shown in Table 3-5, for the MAO-impregnated silica materials, it is apparent that significantly higher polymerization activities were observed for the MAO-activated metallocene systems

impregnated on silica (results given in Table 3-7). This is also apparent from the lower activity obtained with support S9, in which MAO impregnation of the silica was carried out using the same conditions as used for support S8, but in the absence of the zirconocenes (the catalyst was added separately prior to polymerization). Again a trend of decreasing polypropylene isotacticity with increasing polymerization activity is observed, possibly due to a temperature exotherm of up to 5 ℃ with the most active systems. These polymers had similar molecular weights (Mw approx. 40000 g/mol) and narrow molecular weight distribution (Mw/Mn = 1.9-2.2), indicative of retention of the single-center behavior of the catalyst.

SEM investigation of polymers obtained revealed large differences (Figures 3-11 (a) and (b)) in particle morphology, dependent on the silica used in the support preparation.
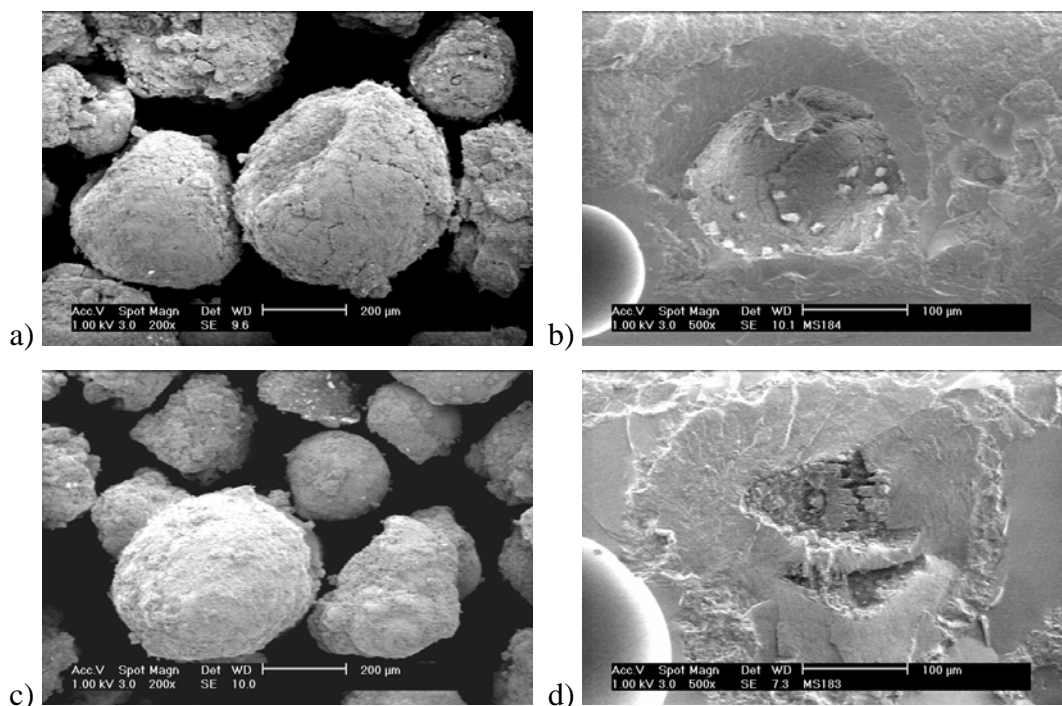
Figure 3-11a   Particle morphology and cross-section images of polymers synthesized with supports $MS1_{250}$ (a and b) and $MS1_{600}$ (c and d).

Supports $MS1_{250}$ and $MS1_{600}$, prepared with MS-3040 silica, gave spheroidal polymer morphology. In contrast, the use of Sylopol 948 resulted in significant fine particle formation, indicative of some leaching of catalyst from the support during the course of polymerization. Differences in internal polymer particle morphology were also apparent.
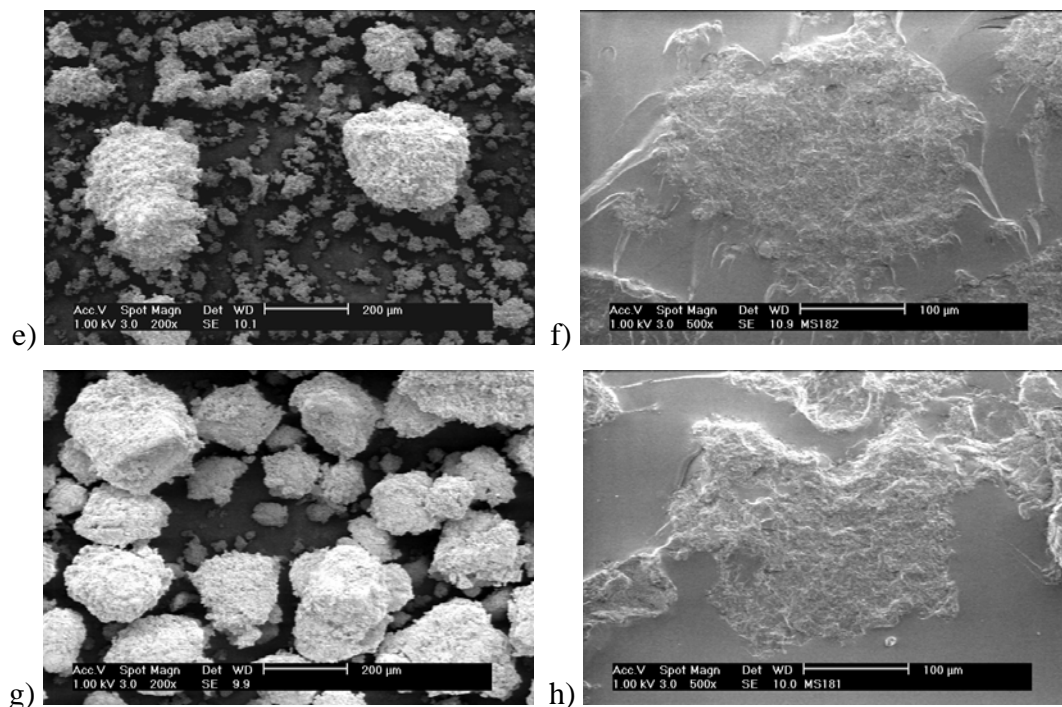
Figure 3-11b   Particle morphology and cross-section images of polymers synthesized with supports $S4_{250}$ (e and f) and $S2_{600}$ (g and h).

Cross-section imaging of polymers obtained with MS-3040 silica revealed void formation at the particle center and the compact polymer growth in the rest of the particle. A more uniform fragmentation, without void formation, was apparent in the polymers prepared with Sylopol 948, although the images indicate a more porous polymer structure.
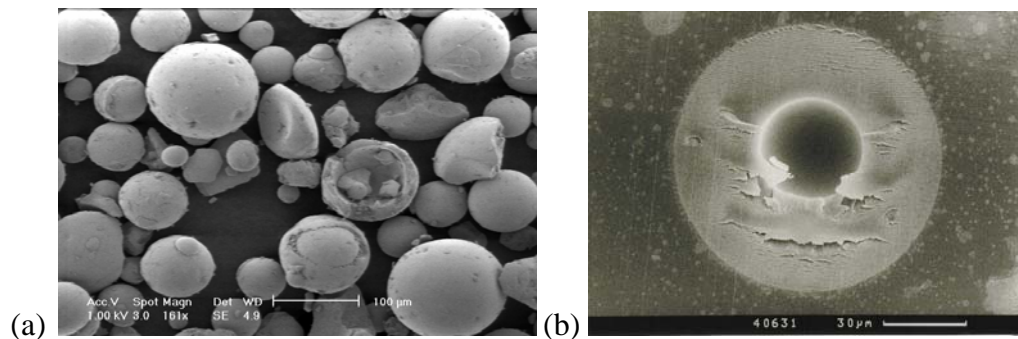
Figure 3-12   Unmodied particle morphology of MS-3040, as given by SEM imaging (a) and cross-section TEM imaging (b). (These images were kindly donated by Basell Polyolefins)

SEM images of the unmodified MS-3040 (Figure 3-12) suggest that some of these particles are indeed hollow, indicating that the voids observed in the polymers may result from replication of the internal morphology of the silica rather than from inhomogeneous catalyst impregnation.

3.4 Conclusions

Uniform impregnation of a SiO_2 support with methylaluminoxane is difficult to achieve simply by contacting the support with MAO in toluene at ambient temperature. Generally, this leads to a core-shell type distribution, with relatively high Al content at and near the particle surface and a much lower Al content towards the center of the particle. Homogeneous impregnation of silica with MAO can be achieved under rigorous conditions at elevated temperatures. Increasing the quantity of MAO used results in the removal of residual hydroxyl groups from the silica and leads to significant increases in catalyst activity in propylene polymerizations (following contact of such supports with *rac*-Et(Ind)$_2$ZrCl$_2$/Al*i*Bu$_3$). The polymers obtained had narrow molecular weight distribution, indicative of retention of the single-center behavior of the catalyst.

A more efficient catalyst immobilization procedure, requiring less MAO for increased polymerization activity, comprises the impregnation of silica with pre-contacted MAO and zirconocenes. Polymer particle growth characteristics and the incidence of leaching of catalyst from the support was dependent on the silica used.

3.5 Acknowledgements

3.6 References

1. Zechlin, J.; Steinmetz, B.; Tesche, B.; Fink, G. *Macromol. Chem. Phys.* **2003**.

2. Kaminsky, W.O.; Hähnsen, H.; Külper, K.; Woldt, R.; Hoechst, **1985**, p US 4542199.

3. Sinn, H.W.; Kaminsky, W.O.; Vollmer, H.-J.; Woldt, R.; BASF, **1983**, p US 4403344.

4. Ribeiro, M.R.; Deffieux, A.; Portela, M.F. *Ind. Eng. Chem. Res.* **1997**, *36*, 1224.

5. Kaminsky, W.O.; Renner, F. *Macromol. Rapid Commun.* **1993**, *14*, 239.

6. Soga, K.; Kaminaka, M. *Makromol. Chem.* **1993**, *194*, 1745.

7. Kaminaka, M.; Soga, K. *Macromol. Rapid Commun.* **1991**, *12*, 367.

8. Chien, J.C.W.; He, D. *J. Polym. Sci., Part A Polym. Chem.* **1991**, *29*, 1603.

9. Chen, Y.-X.; Rausch, M.D.; Chien, J.C.W. *J. Polym. Sci., Part A Polym. Chem.* **1995**, *33*, 2093.

10. Steinmetz, B.; Tesche, B.; Przybyla, C.; Zechlin, J.; Fink, G. *Acta Polym.* **1997**, *48*, 392.

11. Collins, S.; Kelly, W.M.; Holden, D.A. *Macromolecules* **1992**, *25*, 1780.

12. Sacchi, M.C.; Zucchi, D.; Tritto, I.; Locatelli, P.; Dall'Occo, T. *Macromol. Rapid Commun.* **1995**, *16*, 581.

13. Lee, D.-H.; Yoon, K.-B. *Macromol. Rapid Commun.* **1997**, *18*, 427.

14. Suzuki, N.; Asami, H.; Nakamura, T.; Hihn, T.; Fukuoka, A.; Ichikawa, M.; Saburi, M.; Wakatsi, Y. *Chem. Lett.* **1999**, 341.

15. Bonds, W.D.; Brubaker, J.C.H.; Chandrasekaran, E.S.; Gibbons, C.; Grubbs, R.H.; Kroll, L.C. *J. Am. Chem. Soc.* **1975**, *97*, 2128.

16. Petrucci, M.G.L.; Kakkar, A.K. *J. Chem. Soc., Chem. Commun.* **1995**, 1577.

17. Götz, C.; Rau, A.; Luft, G. *J. Mol. Catal. A Chem.* **2002**, *184*, 95.

18. Resconi, L.; Cavallo, L.; Fait, A.; Piemontesi, F. *Chem. Rev.* **2000**, *100*, 1253.

19. Kaminsky, W.; Schauwienhold, A.-M.; Freidanck, F. *J. Mol. Catal.* **1996**, *112*, 37.

20. Busico, V.; Cipullo, R.; Cutillo, F.; Friederichs, N.; Ronca, S.; Wang, B. *J. Am. Chem. Soc.* **2003**, 125, 12402.

21. Lahelin, M.; Kokko, E.; Lehmus, P.; Pitkänen, P.; Löfgren, B.; Seppälä, J. *Macromol. Chem. Phys.* **2003**, *204*, 1232.

22. Vansant, E.; Van Der Voort, P.; Vrancken, K. *Characterization and chemical modification of silica surface*; Elsevier: Amsterdam, **1995**.

23. Knoke, S.; Korber, F.; Fink, G.; Tesche, B. *Macromol. Chem. Phys.* **2003**, *204*, 607.

24. Busico, V.; Cipullo, R. *J. Am. Chem. Soc.* **1994**, *116*, 9329.

CHAPTER 4

Methylaluminoxanes as Cocatalysts

for ∝-Olefin Polymerization

SYNOPSIS: *The discovery of MAO by Sinn and Kaminsky in 1976 marked a new era of high activity, single-center catalyst systems for olefin polymerization. Not only does MAO alkylate and activate the catalyst precursor for olefin polymerization, but it also serves as a scavenger, protecting the metal center from reacting with poisonous, polar compounds leading to subsequent deactivation of the catalyst species. Typically, 1000-5000 equivalents of MAO are used in a homogeneous metallocene system, making them quite expensive. On immobilization, however, 50-600 equivalents of MAO are commonly employed. In general, a MAO solution will also contain small amounts of trimethylaluminum (TMA), where the latter is often detrimental to the catalysts in a homogeneous metallocene polymerization system.*

This chapter aims to provide a better understanding of the role of MAO in the heterogeneous metallocene catalyst systems for α-olefin polymerization. More stable, industrially available methylaluminoxanes, as well as the role of trialkylaluminums in olefin polymerization systems will be discussed. It appears that trialkylaluminums protect the activated catalyst species against deactivation on reaction with the polar silica surface.

4.1 Introduction

Methylaluminoxane[1] is an oligomeric compound (with a molecular weight of 1000-1500 g/mol) resulting from the partial hydrolysis of trimethylaluminum (TMA). Although considerable research efforts have, over the last two decades, been focused on the synthesis and structural characterization of MAO, quite a few questions still remain. Linear and cyclic structures[2] have been proposed for this oligomer, while the latest theory given by Sinn *et al*[3] is that MAO consists of cage-like structures (Figure 4-1) with trimethylaluminum dispersed throughout the complex. It is known that a certain amount of TMA is always present in MAO. The degree of oligomerization[4,5] and the presence of TMA has a significant influence on catalyst activity[3,6-8] in olefin polymerization.
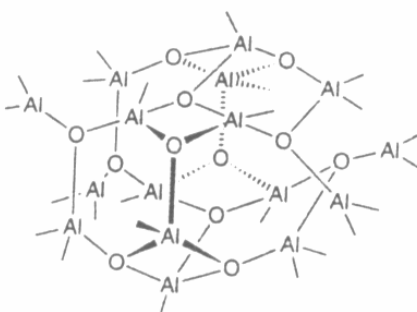
Figure 4-1   Suggested structure for methylalumoxane, clusters and cages, by Sinn *et al.* [3,6-8].

The main requirement for a good cocatalyst is its capability of forming a weakly bound anion with reference to the activated catalyst species. The cocatalyst's Lewis acidity plays therefore a significant role during the formation of the cation-like active centers. It is, however, given that all the aluminum atoms in the cage-like structure are tetra-coordinated and can therefore not possess significant acidity. Barron introduced the concept of latent Lewis acidity of aluminoxanes[9], where aluminoxanes only display Lewis acidity on reaction with zirconocenes. Zirconocene cleaves the Al-O bonds in the cage-like aluminoxane and the methyl group of the zirconocene binds with the aluminum atom of the aluminoxane, while the zirconocene binds to the oxygen atom of the cocatalyst (Scheme 4-1).
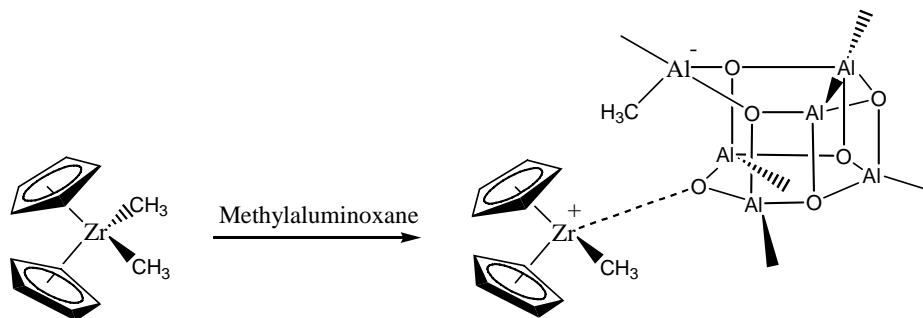
Scheme 4-1   Reaction scheme to illustrate the activation of an alkylated zirconocene by methylaluminoxane to obtain an active species for olefin polymerization.

The presence of TMA in MAO has also raised quite a few questions. It has been suggested that TMA is responsible for the first methylation step in catalyst activation[10]. Resconi *et al*[11] stated that it is responsible for total activation of the zirconium catalyst precursor, although this has been contradicted elsewhere in literature[12]. A possible "poisoning effect" on the activated catalyst species as a result of the presence of TMA in these systems has also been reported[13,14]. The presence of trialkylaluminums in the polymerization systems also often leads to chain termination via chain transfer to Al (Scheme 4-2).
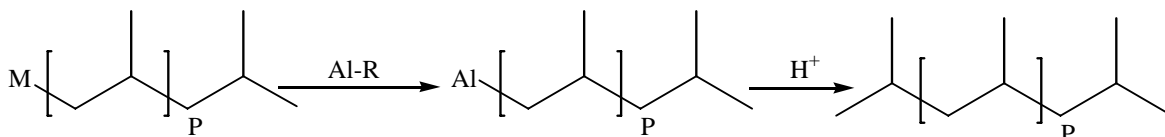
Scheme 4-2   Illustration of chain transfer to Al, a common chain transfer method resulting in chain termination in metallocene/MAO systems.

The formation of the resulting inactive dinuclear complexes will be discussed in Section 4.2.6. Additional drawbacks of MAO are its poor solubility in aliphatic hydrocarbons (used as solvents in olefin polymerization setups) and its instability with regard to long-term storage as it is prone to gel formation (resulting in a non-homogeneous product).

In this work, we considered the effect of a variation in TMA content with reference to the total amount of aluminum present in MAO-activated single center catalyst systems immobilized on silica. This was achieved by comparing the more stable MAO variations, namely modified MAO (MMAO-7), poly-MAO (PMAO-IP) and TMA-"trapped" MAO[15], with the traditional 10 wt % MAO in toluene (as supplied by Witco). The resulting

support systems were characterized with SEM/ EDX elemental mapping and elemental analysis, while the polymers were characterized in terms of isotacticity (^{13}C NMR spectroscopy), thermal properties (differential scanning calorimetry) and molecular weights (gel-permeation chromatography).

4.2 Experimental

4.2.1. Materials

All reactions were carried out under argon atmosphere. Catalysts were handled in a glove box under an inert atmosphere with maximum O_2 and H_2O levels of 1 ppm and 0.3 ppm, respectively. A 10 wt % solution of the methylaluminoxane (MAO) in toluene was obtained from Witco, while *racemic* ethylene-bridged bis(indenyl) zirconium dichloride (*rac*-Et(Ind)$_2$ZrCl$_2$) was purchased from STREM chemicals. *Racemic* dimethylsilyl-bridged bis(2-methyl-4-phenyl-indenyl) zirconium dichloride (*rac*-Me$_2$Si(2-Me-4Ph-Ind)$_2$ZrCl$_2$) was kindly donated by SABIC EuroPetrochemicals. Silica support materials, MS-3040 (PQ Corporation) and Sylopol 948 (Grace AG), were donated by their respective suppliers. Toluene (Biosolve) was dried on alumina columns, while n-heptane (Biosolve) was distilled over potassium before use. Poly-methylaluminoxane (PMAO-IP), modified methylaluminoxane (MMAO-7) and tri*iso*butylaluminum (TIBA), as a 25 wt % solution in toluene, were purchased from Akzo-Nobel. 2,6-di-tert-butyl-4-methylphenol (butylated hydroxy toluene, BHT) was obtained from Sigma-Aldrich and degassed. Propylene (Hoekloos) and ethylene (Air Liquide) were dried over columns containing activated copper catalyst (BTS) and alumina before introduction into the polymerization reactor.

4.2.2. Support synthesis

4.2.2.1. Calcination

See Section 2.2.2.1. for details.

4.2.2.2. MAO impregnation

BHT crystals, as obtained from the supplier, were degassed and transferred to the glove box. A BHT stock solution was prepared by dissolving 13.28 g of the BHT crystals in 20 mL of toluene at ambient temperature. The various MAOs were left for an hour at room

temperature under stirring to react with BHT, after which they were directly added to the catalyst for activation. Table 4-1 summarizes the amounts of BHT employed for modification of the various systems.

Table 4-1			Details of support preparation to obtain 2:1 BHT to Al_{free} ratios	
Methylaluminoxane	**Volume (mL/g silica)**	**$[Al_{free}]$ (mmol/mL)**	**BHT (mL/g silica)**	**Additional toluene (mL)**
10 wt% MAO	2.0	0.537	3.0	-
MMAO-7	0.8	0.732	0.2	1
PMAO-IP	0.7	0.585	0.3	1

This study was based on a mol ratio cocatalyst to catalyst of $\pm$ 100. Note that the total volume of the methylaluminoxane was always rounded off to 2 mL so that the total amount of solvent with which the silica was contacted was 4 mL. See the last method (*wet sand*) in Section 3.2.2.3.

4.2.3. Slurry Polymerization Procedure

Refer to Section 3.2.3. for a complete description.

4.2.4. Characterization techniques

See Section 3.2.4. for a complete description.

4.3 Results and Discussion

4.3.1. Methylaluminoxanes

4.3.1.1. Introduction and catalyst/support characteristics

MAO is industrially produced through partial hydrolysis of trimethylaluminum[16] and a certain amount of TMA is always present in MAO. The residual TMA is referred to as the amount of "free" aluminum present in the product. It is also given that, if all the TMA is removed through removal of volatiles in the system, TMA will form again on storage due to the equilibrium between the "free" and "associated" trialkyls (Scheme 4-2):

$$[Al(Me)O]_n \cdot + \; xAlMe_3 \;\rightleftharpoons\; [Al(Me)O]_n \bullet (x\text{-}y) \; AlMe_3 + yAlMe_3$$

$$\text{"associated"} \qquad\qquad \text{"free"}$$
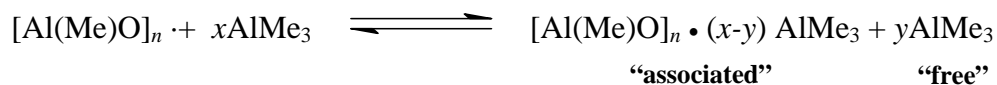
Scheme 4-2   Proposed equilibrium between trimethylaluminum (present in methylaluminoxane (MAO) solutions) with MAO[16].

Akzo-Nobel produces MAO via a non-hydrolytic route (Scheme 4-3)[17], called PMAO-IP and their modified MAOs contain hydrocarbon modifiers that enhance storage stability and the solubility of MAO in hydrocarbons.

$$Me_3Al + 0.8Me_3COH \rightarrow Me_{2.2}Al(OCMe_3)_{0.8} + 0.8MeH$$

$$\text{Al-C/} \qquad\qquad \text{Al-O}$$

$$\longrightarrow Me_{1.4}AlO_{0.8} + \; hydrocarbons$$
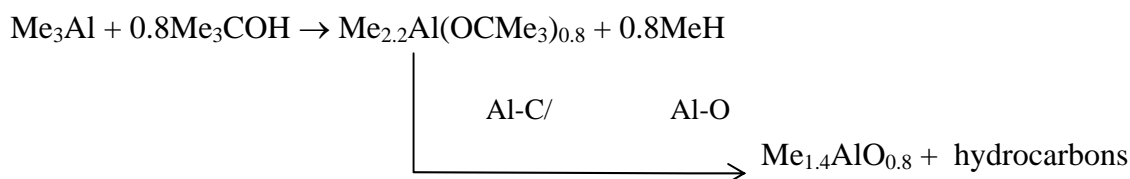
Scheme 4-3   A non-hydrolytic route to obtain methylaluminoxane[17].

The characteristics of the MAOs, as given by their respective suppliers, are summarized in Table 4-2.

Table 4-2   Industrially available methylaluminoxanes and their characteristics.

Cocatalyst	Approximate Molecular formula	Method of Synthesis	$M_w{}^a$ (g/mol)	Al_{total} (mmol/mL)	Al_{free} (mmol/mL)	Al_{free} (%)
10wt%MAO	$[MeAlO\text{-}]_n$	Hydrolytic	1 000	1.6	0.5	31
MMAO-7	$[Me_{0.86}n\text{-}Octyl_{0.14}AlO\text{-}]_n$	Non-Hydrolytic	±4 000	3.9	0.7	18
PMAO-IP	$[MeAlO\text{-}]_n$	Non-Hydrolytic	1 500-2 000	4.5	0.6	13

^{a} Determined cryoscopically in benzene by their respective suppliers

MMAO-7 en PMAO-IP contain higher concentrations of total aluminum (Al_{total}), although the TMA content (free aluminum (Al_{free})) is relatively low in relation to the total amount of aluminum in the products.

The above-mentioned methylaluminoxanes were used to activate *rac*-Et(Ind)$_2$ZrCl$_2$ before immobilization on silica or employed directly in homogeneous polymerization systems. The activated catalyst species were immobilized in a *wet sand* fashion. Sylopol 948, calcined at 600 °C, was used in these systems due to academic and industrial interest. The aim being to understand the role of MAO and the residual TMA in the cocatalyst

system, in a heterogeneous metallocene setup for olefin polymerization. The characteristics of these support materials are given in Table 4-3.

Table 4-3   Characteristics (in terms of elemental analysis) of the individual support materials synthesized for this study.

Methylaluminoxane	AES-ICP		
	Al (wt %)	Zr (wt %)	Si (wt %)
10 wt % MAO	8.1	0.18	35.7
MMAO-7	10.1	0.14	31.7
PMAO-IP	7.7	0.14	37.6

In all cases, both catalyst (Zr) and cocatalyst (Al) were successfully immobilized on silica. One of the drawbacks in the heterogenization of MAO/catalyst systems is the loss in catalyst activity after immobilization on a solid support. In this work, we will therefore also list results of the analogous homogeneous reactions carried out at the same Al:Zr.

4.3.1.2. Propylene polymerization

The results of propylene polymerizations carried out with the different MAOs, under both homogeneous and heterogeneous conditions, are given in Table 4-4.

Table 4-4   Polypropylene properties obtained with various methylaluminoxane activated rac-Et(Ind)$_2$ZrCl$_2$ catalysts on Sylopol 948, calcined at 600 °C.

Cocatalyst	System[a]	Activity[b]	%mmmm	Mw (g/mol)	Mw/Mn	T$_m$ (°C)
10 wt% MAO	Homogeneous	12 800	67	19 500	2.1	124
	Slurry	500	78	42 900	2.0	136
MMAO-7	Homogeneous	6 700	70	42 900	2.1	131
	Slurry	100	82	50 600	1.8	132
PMAO-IP	Homogeneous	9 800	69	42 800	2.0	129
	Slurry	<100	n.o.[c]	n.o.	n.o.	132

[a]All reactions were carried out with an intended catalyst to MAO ratio of 1: 130

[b]Activity is expressed in terms of kg polymer/((mol cat.hour))

[c]Not obtainable

Comparing homogeneous to heterogeneous systems, one immediately notes the higher activities of the homogeneous system despite the fact that the same Al to Zr ratios

were applied (130:1). The systems containing a very low Al_{free} concentration (MMAO-7 and PMAO-IP, Table 4-2) show exceptionally low activities on heterogenization. One of the concerns of immobilization is the possibility of catalyst deactivation on contact with the polar surface. As all other variables were kept equal as far as possible, one can propose that TMA (which is less bulky than MAO) can effectively access the excess OH groups on the silica surface and consume them thoroughly, thus protecting the activated catalyst species. Although the presence of TMA in homogeneous systems is undesired, it appears as if it could serve to "protect" the heterogenized activated species against the polar silica/support surface. Thus, explaining the extremely low catalyst activities observed for the heterogenized MAO (Table 4-4). It is also apparent that, for heterogeneous systems, significantly higher activities were obtained with MAO than with PMAO-IP and MMAO-7, the latter aluminoxanes having relatively low contents of TMA (Al_{free}) with respect to Al_{tot} (Table 4-2).

Despite the lower activities observed, heterogenization does result in more isotactic polymers (as illustrated earlier in Chapter 3) with higher molecular weights. (Keep in mind that the generally low Mw values observed are characteristic[18] of this catalyst precursor in propylene polymerization systems and are not a result of the variables studied in this work). The higher Mw values observed in Table 4-4 for the heterogenized catalyst systems could be ascribed to the hindered diffusion of the trialkylaluminum (present as scavenger or introduced through MAO), resulting in less chain transfer to Al as chain termination possibility. It is also noteworthy that the Mw of the heterogeneous 10 wt % MAO system (containing the most amount of Al_{free} with reference to PMAO-IP and MMAO-7) is significantly higher (23 400 g/mol) than its homogeneous analogue, whereas a difference of only 7 300 g/mol was observed for the MMAO-7 systems.

The fact that narrow molecular weight distributions are obtained serves as an indication of the effectiveness of the immobilization method for this single-center catalyst, as single-center behavior was retained in all the heterogeneous systems.

4.3.1.3. Ethylene polymerization

Polyethylenes obtained with these catalyst/MAO systems (Table 4-3) are listed in Table 4-5. Molecular weights 10 times higher than those observed for the polypropylene

systems were observed, although activities for the homogeneous systems appear to be 12 times lower. The formation of higher molecular weight polymers in ethylene polymerization (compared to propylene) is characteristic for such catalysts and has been reported previously[19,20]. Also noteworthy is that the activity for the heterogeneous 10 wt % MAO system is almost double that of the homogeneous analogue, indicating the effectiveness of the immobilization method.

Table 4-5   Polyethylene properties obtained with various methylaluminoxane activated *rac*-Et(Ind)$_2$ZrCl$_2$ catalysts on Sylopol 948, calcined at 600 ℃.

Cocatalyst	System	Activity[a]	Mw (g/mol)	Mw/Mn	T$_m$ (℃)
10 wt% MAO	Homogeneous	1 000	471 900	5.0	136
	Slurry	1 900	475 500	4.5	132
MMAO-7	Homogeneous	1 200	298 700	3.2	135
	Slurry	700	n.o.[b]	n.o.	132
PMAO-IP	Homogeneous	700	389 800	5.9	134
	Slurry	300	n.o.	n.o.	133

[a]Activity is expressed in terms of kg polymer/((mol cat)(hour))
[b]Not obtainable by GPC analysis

It has been reported[21] that PMAO-IP shows improved performance in comparison to the hydrolytic MAO (produced by Akzo-Nobel, 10 wt % MAO) in homogeneous ethylene polymerization. In our systems, these two cocatalysts result in systems of similar activity, although the 10 wt % MAO shows much higher activity on heterogenization. The difference in performance of these two cocatalysts with respect to what has been reported for homogeneous systems, might relate to the difference in polymerization conditions and the different MAO products employed, as we used Witco as supplier for the 10 wt % MAO used. The conditions used by Malpass[21] might favor the PMAO-IP system. Also keep in mind that the traditional 10 wt % MAO solution is unstable with reference to its composition and the latter is influenced by various factors, thus influencing its performance.

The broad molecular weight distributions (also in the case of the homogeneous systems) and the low activities observed for these polyethylenes are most likely to be

explained through the presence of a *diffusion limitation* resulting from the highly crystalline polyethylene precipitating from solution or forming on the support during the first minutes of polymerization. The lower melting temperatures observed for the heterogeneous systems may be caused by residual silica acting as an impurity.

In comparing the activity values of the various homogeneous systems, it is interesting to see that the MMAO-7 system shows activity of the same magnitude as the 10 wt % MAO system. A rather low activity is observed for PMAO-IP. It appears that the PMAO-IP- activated catalyst systems incorporate propylene easier and the MMAO-7 systems seem to favor ethylene. The higher activity observed for the heterogenized 10 wt % MAO system would support our theory regarding the protective role of alkylaluminums in heterogenized metallocene systems, as proposed for the results in Table 4-4.

4.3.2. Trapping of TMA with BHT

4.3.2.1. Introduction and catalyst/support characteristics

TMA is known to form a methyl-bridged dinuclear species (Scheme 4-4) on contact with transition metal complexes. The resulting species are believed to be either inactive or to promote chain transfer that could result in the formation of oligomers instead of high molecular weight polymers.
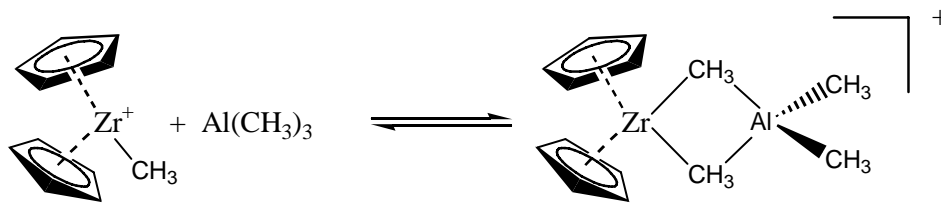
Scheme 4-4   Formation of dinuclear species due to the presence of TMA in the activated metallocene system[13,14,22].

Various ways of eliminating TMA present in MAO have been proposed, as discussed earlier (see Section 4.2.5). Recently, Busico *et al*[15] reported on the efficient "trapping" of TMA molecules in MAO through the addition of a sterically hindered phenol such as 2,6-di-*tert*-butylphenol (${}^{t}Bu_2Ph$-OH). They report higher catalyst productivity, polymer stereoregularity and/or molar mass in propylene systems with MAO and PMAO-IP.

It is known[23], that the phenolic functionality of butylated hydroxy toluene (BHT) reacts quite rapidly with aluminum alkyls to liberate alkanes and give the following sterically hindered aluminum phenoxides (Scheme 4-5):

$$H_3C-\underset{\underset{CH_3}{|}}{\overset{\overset{CH_3}{|}}{Al}}-CH_3 \xrightarrow[-CH_4]{H\text{-}BHT} (CH_3)_2AlBHT \xrightarrow[-CH_4]{H\text{-}BHT} (CH_3)AlBHT_2$$
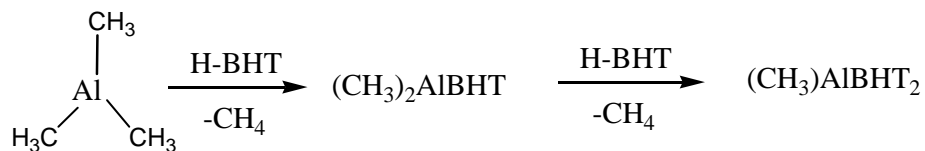
Scheme 4-5   Reaction between TMA and butylated hydroxy toluene.

Shreve *et al.*[23] also stated that a ratio of alkylaluminum to BHT of 1:2 should be used, as MeAl-(O-Ph(^{t}Bu)$_2$)$_2$ is more stable. Me$_2$Al-O-Ph(^{t}Bu)$_2$ will disproportionate to the latter and TMA.

MAO (10 wt % solution), PMAO-IP and MMAO-7 were contacted with the desired amount of BHT solution, as given in Table 4-6, for an hour at ambient temperature before being used for the activation of *rac*-Et(Ind)$_2$ZrCl$_2$. The activated catalyst species were immobilized in a *wet sand* fashion on Sylopol 948, calcined at 600 °C (see details in the Experimental Section in Chapter 3). The compositions of these materials are listed in Table 4-6.

Table 4-6   Characteristics (in terms of elemental analysis) of the individual BHT-modified support materials synthesized for this study.

Methylaluminoxane	AES-ICP		
	Al (wt %)	Zr (wt %)	Si (wt %)
10 wt % MAO/ BHT[a]	6.3	0.14	34.0
MMAO-7/ BHT	7.9	0.19	35.7
PMAO-IP/ BHT	7.0	0.12	36.5

[a]A 2:1 BHT to Al solution was used.

The data in Table 4-6 show that Zr (catalyst) and Al (cocatalyst) have effectively been immobilized on silica in more or less the same amounts. The homogeneity of the immobilization of the activated catalyst species, modified with BHT, is compared to that of the non-modified systems in terms of EDX aluminum mapping (Figure 4-3).
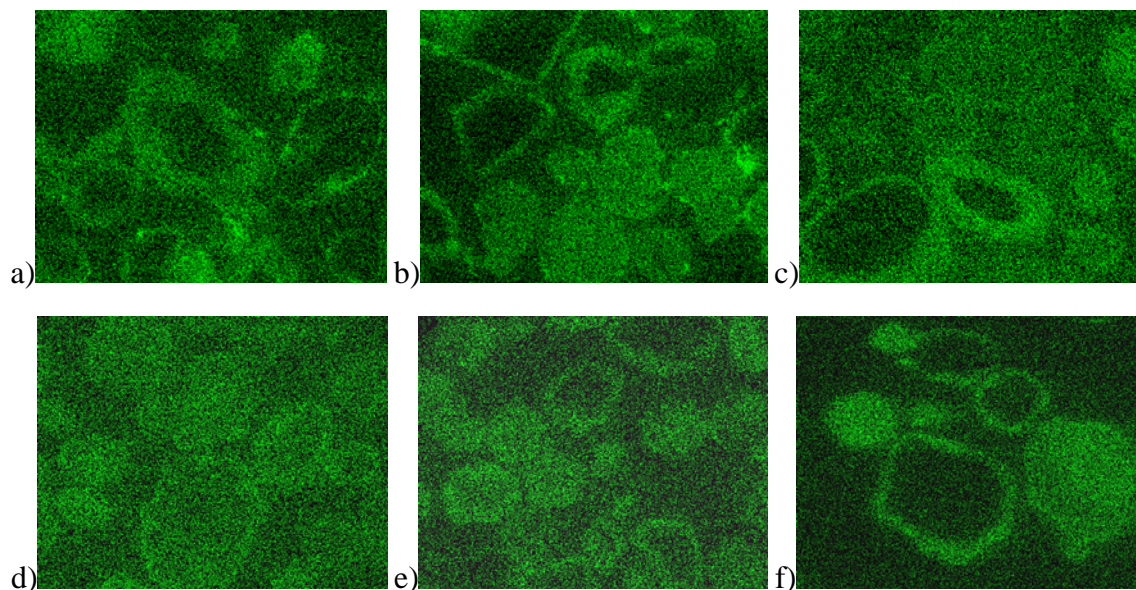
Figure 4-3   EDX aluminum mapping of a) MAO (10 wt % solution); b) MMAO-7; c) PMAO-IP; d) BHT-modified MAO (10 wt % solution); e) BHT-modified MMAO-7; f) BHT-modified PMAO-IP used in the activation of EBI before impregnation on Sylopol 948, calcined at 600 °C.

Modification of the 10 wt % MAO and MMAO-IP systems with BHT seems to improve the homogeneity of the aluminum distribution across the individual silica particles.

4.3.2.2. Propylene polymerization

Once again, the performance of the homogeneous catalyst systems is also listed in order to serve as reference in relation to the performance of the heterogeneous metallocene systems in olefin polymerization. All reactions were carried out under the same conditions with the same intended Al: Zr. Polypropylene polymer properties obtained with these systems are summarized in Table 4-7.

Table 4-7   Polypropylene properties obtained with various BHT-modified methylaluminoxane activated *rac*-Et(Ind)$_2$ZrCl$_2$ on Sylopol 948, calcined at 600 °C.

Cocatalyst	System	Activity[b]	%mmmm	Mw (g/mol)	Mw/Mn	T$_m$[d] (°C)
10 wt% MAO	Homogeneous[a]	8 400	51	47 800	2.2	130
	Homogeneous	18 900	73	18 800	3.0	119
	Slurry	<100	n.o.[c]	n.o.	n.o.	132
MMAO-7	Homogeneous	1 800	77	48 000	2.0	135
	Slurry	<100	74	79 100	2.3	136
PMAO-IP	Homogeneous	12 000	79	35 300	2.2	127
	Slurry	<100	71	151 800	4.8	137

[a]2:1 ratio of BHT:Al$_{tot}$

[b]Activity is expressed in terms of kg polymer/((mol cat.hour))

[c]Not obtainable

[d]Melting temperature of second heating cycle of DSC

The first 10 wt % MAO homogeneous system quoted differs from the rest as it was made with a Al$_{total}$: BHT ratio of 1:2, instead of a Al$_{free}$ to BHT ratio of 1:2. All other factors being equal, the Mw increased by more than a factor of 2 suggesting the effective removal of TMA in the system. The narrow molecular weight distribution was retained, although a material of higher melting temperature was observed. The low % *mmmm* is probably a result of the presence of atactic sequences, possibly due to photo-induced *rac*/*meso* isomerization in metallocene solutions exposed to light[24] (as discussed in Section 3.3.2.).

In general, comparing the data in Tables 4-4 and 4-7, polypropylenes of higher polydispersites and lower melting temperatures were observed with the BHT-modified methylaluminoxane systems (MMAO-7 being the exception). The only system that shows comparable activities to those of the unmodified systems is PMAO-IP. An activity of 9800 kg PP/mol catalyst.hour (Table 4-4) for the unmodified homogeneous system compares quite well to the 12000 kg PP/mol catalyst.hour activity obtained for the BHT-modified homogeneous system with low melting temperatures of 129 °C (Table 4-4) and 127 °C, respectively. The good correlation between the two homogeneous systems would suggest that the PMAO-IP activated catalyst species is not influenced by the 2:1 addition of BHT.

This can be explained by the low amount of Al_{free} with reference to Al_{tot} present in this system. (There is thus not that much Al_{free} available to be trapped by BHT.) With TMA being trapped by BHT, negligible activities were obtained for all the heterogenized systems, thus supporting the theory regarding the role of TMA in heterogenized metallocene/MAO systems for olefin polymerization (Section 4.2.5.). A very low melting temperature of 119 °C was observed for the 10 wt % MAO system treated with a 2:1 ratio of BHT to Al_{free}. The fact that the material shows a very low molecular weight of 18800 g/mol might influence the thermal analysis and thus the DSC results. The large difference (10 °C) in the melting temperatures of the homogeneous and heterogeneous polypropylene systems is surprising, taking into account the respective pentad contents.

Polymer properties, as obtained for the polyethylenes produced with the BHT-modified cocatalysts are given in Table 4-8.

Table 4-8   Polyethylene properties obtained with BHT-modified methylaluminoxane activated *rac*-Et(Ind)$_2$ZrCl$_2$ on Sylopol 948, calcined at 600 °C.

Cocatalyst	System	Activity[b]	Mw (g/mol)	Mw/Mn	T_m^d (°C)
10 wt% MAO	Homogeneous[a]	700	338 400	4.2	136
	Homogeneous	700	n.o.[c]	n.o.	134
	Slurry	300	422 100	2.2	134
MMAO-7	Homogeneous	800	304 700	3.5	137
	Slurry	200	n.o.	n.o.	132
PMAO-IP	Homogeneous	600	317 800	3.2	138
	Slurry	300	888 000	5.4	132

[a] 2:1 ratio of BHT:Al_{tot}
[b] Activity is expressed in terms of kg polymer/((mol cat)(hour))
[c] Not obtainable by GPC analysis
[d] Melting temperature of second heating cycle of DSC

In general, lower activities (compared to the unmodified cocatalyst systems (Table 4-5)) were mostly observed for ethylene polymerization. Although the activities of the heterogenized systems were low, they were significantly better than those observed for the propylene systems. This trend was also observed for the non-BHT systems. Higher melting temperatures, compared to the non-BHT modified systems (Table 4-5) were observed for the homogeneously produced polymers. The heterogeneously produced PEs

showed similar melting temperatures to those observed for the non-modified BHT systems, but somewhat lower than those observed for the homogeneously produced PEs. Once again the presence of residual silica might provide an explanation.

The results shown in Tables 4-4, 4-5, 4-7 and 4-8 reveal that in propylene polymerization the immobilized catalysts gave much lower activities than observed for the homogeneously produced polymers systems. This was surprisingly not the case in ethylene polymerization. An explanation for this effect could be that the "homogeneous" systems quickly become heterogeneous as the polymer formed precipitates from solution. This can lead to the active catalyst becoming encapsulated in a solid mass of polymer, which can prevent effective mass transport of the monomer. As will be discussed in subsequent Chapters, monomer diffusion limitations are more prevalent in ethylene than in propylene polymerization and in the case of the "homogeneous" ethylene polymerization may be exacerbated by the high molecular weight of the polymer being formed.

Comparison of the results in Tables 4-5 and 4-8 reveals that similar activities were obtained with the unmodified and BHT-modified PMAO-IP/catalyst systems. As mentioned before, PMAO-IP contains the least amount of Al_{free}. These activities were, however, generally the lowest, compared to the other systems. It is also interesting to note that the data in Table 4-8 reveal similar molecular weights and melting points for the polymers obtained using PMAO-IP and MMAO-7. This was incidentally also the case for the non-modified MAO systems in propylene polymerization.

4.3.3. The role of AlR_3 in heterogeneous catalysis

In section 4.2.6, we have noticed that Al_{free}-poor systems (either due to the way they were synthesized or as a result of BHT modification) show exceptionally low activities on heterogenization. The theory proposed was that TMA protects the activated catalyst species against deactivation due to the polar silica surface. The work of Lo *et al*[25] contradicts this, as they state that the pretreatment of a support with TMA diminishes catalyst activity.

Putting our theory to the test, we pretreated 10 g of Sylopol 948 (calcined at 600 ºC, (slurried in 60 mL *n*-heptane) with 5.601 mmol of TEA (diluted in 20 mL *n*-heptane) over a period of 90 minutes. The silica slurry was left overnight to ensure maximum

modification. The support was then washed (with 20 mL of *n*-heptane) and dried for 120 minutes at 60 ºC under vacuum before impregnation of the MAO-activated catalyst species. (TEA is essentially inactive towards breaking siloxane linkages[26] and will only react with the isolated silanols.) The properties of the resulting polyethylenes are given in Table 4-9. These polymerizations were carried out with a tenth of the normal amount of scavenger (tri*iso*butylaluminum, TIBA) used.

Table 4-9   Polyethylene properties obtained with methylaluminoxane activated *rac*-Et(Ind)$_2$ZrCl$_2$ on TEA-modified Sylopol 948, calcined at 600ºC.

Reaction	Details	Support	Activity[b]	Mw (g/mol)	Mw/ Mn	$\Delta H_{m,2}$ (J/g)	Tm (onset, °C)	Tm[c] (°C)
SM1	10 wt % MAO	SiO$_2$	900	480 300	2.0	169.9	121.8	131.8
SMT	10 wt % MAO[b]	TEA/SiO$_2$	1 700	n.o[d]	n.o.	188.9	125.2	134.6
SBM	BHT[a]/ 10 wt % MAO	SiO$_2$	300	422 300	2.2	113.9	123.3	134.0
SBMT	BHT[a]/ 10 wt % MAO	TEA/SiO$_2$	1 300	319 500	2.9	181.3	124.9	135.0

[a]2:1 ratio of BHT:Al$_{tot}$

[b]Activity is expressed in terms of kg polymer/((mol cat)(hour))

[c]Melting temperature of second heating cycle of DSC

[d]Not obtainable with GPC analysis

SMT and SBMT show significant enhancement in catalyst activity due to the pretreatment of silica with TEA. The greater productivity obtained after pre-treatment with TEA is also apparent from the different values obtained for the heat of fusion (ΔH); at low catalyst productivity, the heat of fusion will be limited by a high proportion of silica residue in the polymer. Molecular weight distributions from 2.0 to 2.9 were observed and can be regarded as acceptable for single-center catalyst systems. A slight depreciation in Mw of the polymers produced with the BHT-modified catalyst systems, as also noted in Section 4.2.6.3., is observed in Table 4-9.

The TEA impregnated silica systems also appear to be quite robust, as these systems are even active in the absence of an additional scavenger, traditionally required in MAO polymerization systems (Table 4-10).

Table 4-10   Polyethylene properties obtained with methylaluminoxane activated *rac*-Et(Ind)$_2$ZrCl$_2$ on TEA-modified Sylopol 948, calcined at 600ºC (no additional scavenger).

Details	Activity[b]	Mw (g/mol)	Mw/ Mn	$H_{m,2}$ (J/g)	Tm (onset, °C)	Tm[c] (°C)
BHT[a]/ 10 wt % MAO	200	494 200	3.9	155.9	121.5	133.6
10 wt % MAO	300	425 100	3.3	143.0	120.7	132.8

[a] 2:1 ratio of BHT:Al$_{tot}$

[b] Activity is expressed in terms of kg polymer/((mol cat)(hour))

[c] Melting temperature of second heating cycle of DSC

4.4 Conclusions

Experimental evidence was given to suggest that the presence of TMA in MAO is actually desired in heterogenized systems, as it protects the activated catalyst species against the polar silica surface. The more stable MAO species (containing less TMA (Al$_{free}$)) appear therefore to be less effective in heterogenized catalyst systems and in these systems the removal of residual TMA from MAO via reaction with butylated hydroxyl toluene led to decreased activity. The immobilization of MAO-activated catalyst species on TEA-modified silica resulted in higher activity systems for olefin polymerization. It was also shown that TEA coated silica materials deliver more robust catalyst species after the immobilization of MAO-activated catalyst systems, as no additional scavenger is required to obtain an active catalyst system.

4.5 References

1. Andresen, A.; Cordes, H.; Herwig, W.; Kaminsky, W.; Merch, A.; Pein, J.; Sinn, H.; Vollmer, H. *Angew. Chem., Int. Ed. Engl.* **1976**, *16*, 630.

2. Kaminsky, W.; Linderhof, N. *Bull. Soc. Chim.* **1990**, 99, 1103.

3. Sinn, H. *Macromol. Symp.* **1995**, *97*, 27.

4. Gianetti, E.; Nicoletti, R.; Mazzochi, R. *J. Polym. Sci., Polym. Chem. Ed.* **1985**, *23*, 2117.

5. Peng, K.; Xiao, S. *J. Mol. Catal.* **1994**, *90*, 201.

6. Reddy, S.; Shaashider, G.; Sivaram, S. *Macromolecules* **1993**, *26*, 1180.

7. Reiger, B.; Janiak, C. *Makromol. Chem.* **1994**, *215*, 35.

8. Tritto, I.; Mealares, C.; Sacchi, M.; Locatelli, P. *Macromol. Chem. Phys.* **1997**, *198*, 3963.

9. Barron, A.R. *Macromol. Symp.* **1995**, *97*, 15.

10. Cam, D.; Giannini, U. *Makromol. Chem.* **1992**, *193*, 1049.

11. Resconi, L.; Bossi, S.; Abis, L. *Macromolecules* **1990**, *23*, 4489.

12. Tritto, I.; Li, S.; Sacchi, M.; Zanonni, G. *Macromolecules* **1993**, *26*, 7111.

13. Bochmann, M.; Lancaster, S.J. *Angew. Chem. Int. Ed. Engl.* **1994**, *33*, 1634.

14. Petros, R.A.; Norton, J.R. *Organometal. Commun.* **2004**, *23*, 5106.

15. Busico, V.; Cipullo, R.; Cutillo, F.; Friederichs, N.; Ronca, S.; Wang, B. *J. Am. Chem. Soc.* **2003**, *125*, 12402.

16. Barron, A.R. *Organometallics* **1995**, *14*, 3581.

17. Smith, G.; Palmaka, S.; Rogers, J.; Malpass, D., **1998**, US 5831109.

18. Spaleck, W.; Küber, F.; Winter, A.; Rohrmann, J.; Bachmann, B.; Antberg, A.; Dolle, V.; Paulus, E.F. *Organometallics* **1994**, *13*, 954.

19. Kaminsky, W. *Angew. Makromol. Chem.* **1986**, *145/146*, 149.

20. Van Reenen, A.J. 2nd Annual UNESCO training School, Stellenbosch, South Africa, **1999**.

21. Malpass, D. Akzo Nobel **2003**, 1.

22. Bochmann, M.; Lancaster, S.J. *Angew. Chem.* **1994**, *106*, 1715.

23. Shreve, A.; Mülhaupt, R.; Fultz, W.; Calabrese, J.; Robbins, W.; Ittel, S. *Organometallics* **1988**, 7, 409.

24. Kaminsky, W.; Schauwienhold, A.-M.; Freidanvk, F. *J. Mol. Catal.* **1996**, *112*, 37.

25. Lo, F.Y.; Pruden, A.L., **1995**, PCT Int. Appl. 95/11263.

26. Tao, T.; Maciel, G.E. *J. Am. Chem. Soc.* **2000**, 3118.

CHAPTER 5

Effect of comonomer incorporation on particle growth[*]

SYNOPSIS: *In an ideal heterogeneous polymerization system, the monomer will diffuse through the thin layer of polymer, formed on the catalyst particle after initiation of polymerization, through to the narrow pores of the catalyst to reach all the active polymerization species. The polymer chains inside the pores will grow and the catalyst particle will start to fragment as a result of hydraulic forces. The fragments will, however, be kept together by the adhesive forces of the polymer. The resulting polymer particle will be an exact replica of the original catalyst particle. This is defined as particle growth. In reality, however, various complications do exist in the use of solid catalysts for olefin polymerization. In the case of highly crystalline materials, the monomer might have difficulty diffusing through the thin layer of crystalline polymer on the catalyst surface and this will delay polymerization at the active species inside the pores, thus delaying particle fragmentation and influencing catalyst productivity, as well as polymer properties such as molecular weight and chemical composition distributions.*

In this Chapter, the effect of the addition of small amounts of comonomer to ethylene homo- and copolymerization systems are studied in terms of catalyst activity, polymer properties and morphology. These characteristics were strongly influenced by the diffusion limitation and filter effect observed in heterogeneous homo- and copolymerization systems, respectively.

Keywords: supports; polymer growth; metallocene catalysts; methylaluminoxane; poly(propylene)

5.1 Introduction

The copolymerization of ethylene with higher α-olefins has commercial importance in the production of elastomers and linear low density polyethylene (LLDPE) materials. Multi-sited Ziegler-Natta catalysts, probably the most important as they result in the broadest range of products on the market, produce copolymers with broad molecular weight (MWD) and short chain branching distributions (SCBD) with limited control. Metallocene-based linear low density polyethylenes (mLLDPE's) are random copolymers with a narrow MWD and comonomer compositional distribution[1-7]. These properties play an important role in processing and it is therefore important to determine structure property relationships[8].

Rate enhancement on the addition of higher ∝-olefins to ethylene polymerization systems is well-known in Ziegler-Natta catalysts[9-18]. Plausible reasons given include an increase in rate constant by the heterogeneous catalyst, while others suggest that the particular comonomer plays a key role in the activation of catalyst species. Tait proposes that the rate enhancement is due to an increase in the number of active centers[19,20].

Similarly, this effect has also been noted for metallocene-based ethylene polymerization systems[5,21-23]. Various possible reasons for this have also been published. The most plausible (in the case of crystalline materials such as polyethylene and isotactic polypropylene) is the existence of a diffusion limitation. A *diffusion limitation* is observed in the formation of crystalline polymers in which case a crystalline polymer mass forms around the catalyst/ support particle directly after initiation of polymerization. The monomer diffuses very slowly through this crystalline mass up to a stage where enough polymer has formed inside the catalyst particle to allow for particle fragmentation. The addition of a small amount of comonomer has proven to be enough to break this crystalline envelope, thus enhancing polymer productivity. The addition of comonomer to the homopolymerization systems also provides for some complications, known as the *filter effect*. Fink *et al*[24] described this effect in ethylene/ 1-hexene copolymers where an ethylene/1-hexene copolymer shell forms around the silica particles during the initial stages of polymerization; small ethylene molecules diffuse through easily, while the larger

1-hexene diffuses through very slowly. Thus, a copolymer shell is formed around a polymer mass consisting mainly of ethylene homopolymer. A broad chemical composition distribution, compared to the homogeneous analogue, is observed for these copolymer systems. Additionally, the presence of a comonomer could result in either a positive or negative comonomer effect in which case the addition of comonomer either results in an enhancement or depreciation of catalyst activity, respectively.

In this study, we provide a closer look at the properties of polymers obtained at various stages of ethylene polymerization, as well as the influence of comonomer (mainly 1-hexene) incorporation in various amounts. The aim is to give a more in-depth look into the so-called *comonomer* and *filter* effect. The system used was obtained by the immobilization of methylaluminoxane-activated *racemic* ethylene-bridged bis(indenyl) zirconium dichloride (*rac*-Et(Ind)$_2$ZrCl$_2$) on Sylopol 948, calcined at 600 °C, exhibiting 1.0 mmol OH groups/ g of silica for modification. Polymer properties are discussed in terms of thermal characteristics (differential scanning calorimetry (DSC)), chemical composition distribution (crystallization analysis fractionation (CRYSTAF)), and morphology (SEM and EDX elemental mapping).

5.2 Experimental

5.2.1. Materials

All reactions were carried out under argon atmosphere. Catalysts were handled in a glove box under an inert atmosphere with a sensitivity of 1 ppm O$_2$ and H$_2$O. Support materials were handled in a glove box of 0.1 ppm O$_2$ and H$_2$O sensitivity. A 10 wt % solution of the cocatalyst methylaluminoxane (MAO) in toluene was obtained from Witco, while *racemic* ethylene-bridged bis(indenyl) zirconium dichloride (*rac*-Et(Ind)$_2$ZrCl$_2$) was purchased from STREM chemicals. The silica support material, Sylopol 948, was kindly donated by Grace AG. Toluene (Biosolve) was dried on alumina columns, while n-heptane was distilled over potassium before use. Tri*iso*butylaluminum (TIBA) was purchased from Akzo-Nobel as a 25 wt % solution in toluene. Propylene (Hoekloos) and ethylene (Air Liquide) were dried over columns containing activated copper catalyst (BTS) and alumina before introduction into the polymerization reactor.

5.2.2. Support synthesis

5.2.2.1.   Calcination

See Section 2.2.2.1.

5.2.2.2.   Immobilization of MAO-activated catalyst on silica

MAO-impregnation was carried out according to the *wet sand* method, as described in Section 3.2.2.3.

5.2.3. Slurry Polymerization Procedure

The polymerization was carried out in a 1 Litre PREMEX stainless steel reactor, equipped with a hollow-shaft turbine stirrer and a temperature controlled heating/cooling mantle. 400 mL of n-heptane was charged to the reactor under argon atmosphere. After heating to 50 °C, an ethylene monomer pressure of 2.4 bar (±0.1 bar) was applied and the reactor contents were stirred for 30 minutes at 1000 rpm to ensure maximum dissolution of the gaseous monomer. 1.8 mmol of TIBA was transferred to the reactor, along with the desired amount of comonomer and 75 mL of n-heptane.   After 15 minutes, the catalyst/support (150 mg) was transferred (via a pressure injector system) into the reactor with 75 mL n-heptane. After 1 hour polymerization at 50 °C, the reactor was degassed and the slurry was quenched with acidic methanol. The polymer was dried for at least three days in a vacuum oven at 60 °C.

5.2.4. Characterization techniques

The main characterization techniques are described in Section 3.2.4. and only additional methods will be described here. Crystallinity was determined as described by Inoue[25] with the ΔH_f° of polyethylene as 269.87 J/g. The samples have been analyzed using a GPC PL 220 from Polymer Laboratories (Church Stretton) with refractive index (RI) detection. A column system consisting of 5 polystyrene columns of the following specification were used: PSS SDV 10^7, 10^6, 10^5, 10^3, 100 Å. 1,2,4-Trichlorobenzene was the eluent at a flow rate of 1 mL/min and operating temperature of 140 °C. A calibration vs. polystyrene standards was applied. A CRYSTAF model 200 from PolymerChar SA

(Valencia) was used for the analysis. The sample was dissolved at 160 °C in 1,2,4-trichlorobenzene, the solution was stabilized at 100 °C and cooled down at 0.1 °C/min to 20 °C. The sample concentration was 0.5 mg/mL.

5.3 Results and Discussion

5.3.1. Support characteristics

Methylaluminoxane-activated *racemic* ethylene-bridged bis(indenyl) zirconium dichloride (*rac*-Et(Ind)$_2$ZrCl$_2$)) was immobilized on silica (Sylopol 948, calcined at 600 °C) at elevated temperatures via a *wet sand* procedure. This method was chosen because of its excellent reproducibility (see Chapter 3) and lifetime of the activated support. The characteristics of the support material are summarized in Table 5-1.

Table 5-1 Characteristics of the unmodified and MAO-activated *rac*-Et(Ind)$_2$ZrCl$_2$ impregnated on Sylopol 948, calcined at 600 °C.

Sylopol 948	OH content (OH/g SiO$_2$)	Surface area (m^2/g)	Pore diameter (nm)	Pore volume (cm^2/g)	AES-ICP	
					Al (wt %)	Zr (wt %)
Unmodified	1.0	304	24	1.8	n.a.	n.a.
Impregnated silica	n.a.[a]	270	17	1.2	8.6	0.17

[a]not applicable

Immobilization of the activated species is apparent from the decrease in the values obtained for the individual surface characteristics, as well as for the elemental analysis data, indicating that the support now also contains Al and Zr.

5.3.2. Ethylene homopolymer (PE)

5.3.2.1. Polymer Properties

Low monomer pressure (2.5 bar) was used to facilitate the study of catalyst activity, particle morphology and polymer properties at various stages of polymerization. These results are summarized in Table 5-2.

Table 5-2   Properties of ethylene homopolymer systems.

| Sample | Time (min) | Activity[a] | Mw (g/mol) | Mn (g/mol) | Mw/Mn | Tm | | Crystallinity[b] (%) | TGA |
						Peak (°C)	Onset (°C)		Polymer (wt %)
E1	6	1 700	475 900	151 900	3.1	127.2[c]	116.8	30.0	55
E2	10	1 700	541 500	139 400	3.9	129.4[c]	117.7	35.5	61
E3	30	800	539 700	140 700	3.8	130.6	120.0	50.2	89
E4	60	700	558 000	160 900	3.5	130.6	120.8	53.0	87
E5	300	400	496 300	144 600	3.4	131.1	122.2	60.8	86

[a]Activity is given as kg PP/ (mol catalyst.hour)

[b]Determined as described by Inoue[7]

[c]Melting peak of first heating cycle showed a shoulder

Thermal gravimetric analysis was carried out in order to obtain a better idea of the composition of the polymer particle in terms of polymeric versus silica material, as residual silica might also influence for instance the DSC data. TGA analysis, carried out (after an hour of ethylene polymerization and 72 hours in a vacuum oven at 60 °C) over a temperature range of 25-600 °C showed that the particle is made up of 87 % polymer and 13 % silica. The decrease in activity values, expressed per hour, on going from very short to long polymerization times, is indicative of a diminishing activity throughout the course of polymerization.

The molecular weight distribution data of the polyethylene homopolymers, tabulated in Table 5-2, are somewhat broad and not consistent with ideal single-center behavior (± 2). We have, however, shown (Chapter 4) that the heterogenization of this particular catalyst with the *wet sand* method does result in polyolefins (polypropylenes) with narrow molecular weight distributions. The molecular weight distribution curves of the ethylene homopolymers (Figure 5-1) are unimodal, indicating that the broad MWD's observed are most probably not the result of different active species.
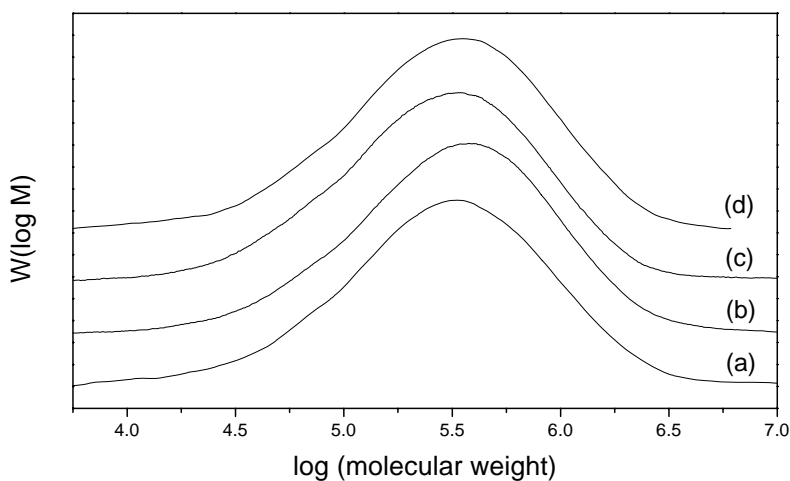
Figure 5-1   Molecular weight distributions of polyethylene at various stages of polymerization ((a) 6 minutes; (b) 30 minutes; (c) 60 minutes and (d) 300 minutes).

Ray et al[26,27] illustrated the possibility of diffusion controlled reactions and broadening of molecular weight distributions, as a result of large concentration gradients in the growing polymer particle, in their work on the multigrain model. In order to check whether this phenomenon could explain the broadening of the MWD of PE with respect to that of PP (see Chapter 3), the particle morphology was studied.

5.3.2.2.   Polymer morphology

Free-flowing polymeric particles of 120 – 240 μm in size were obtained after ethylene polymerization for 60 minutes. Stretching of polymeric material, leading to fibril formation on the particle surface, as seen in Figure 5-2 (e), is typically indicative of a growing particle in a diffusion-controlled reaction. In such a reaction, a crystalline PE layer will form around the catalyst/silica particle due to polymerization that mainly takes place on the surface at the early stages in polymerization. Eventually, enough ethylene might diffuse through to the active catalyst species in the pores of the silica particle. Polymerization is now also initiated in the center of the silica particle, to such an extent as to result in particle fragmentation. The polymeric material on the silica surface will thus stretch in order to facilitate this.
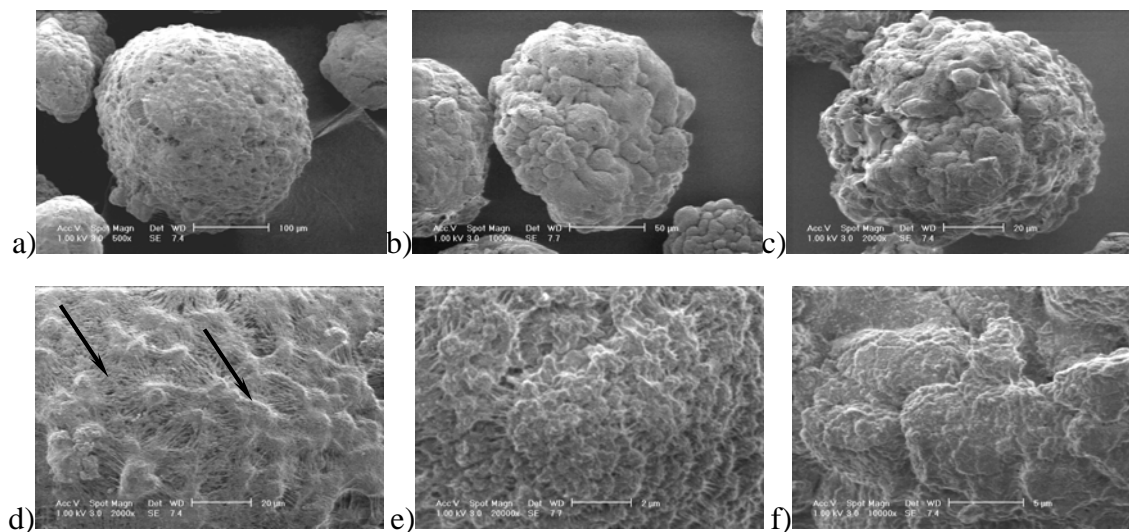
Figure 5-2   Particle morphology at magnifications of 500 (E1 (a); E4 (b) and E5 (c)) and 2000 (E1 (d); E4 (e) and E5 (f)).

The barrier of crystalline material, formed around the catalyst/ silica particle 6 minutes into polymerization, is illustrated in cross-section SEM imaging in Figure 5-3 (a). One can clearly distinguish between the solid silica catalyst particle and the polymer phase building up on the surface. This theory is further strengthened by the fact that cross-section SEM imaging of the polymer particles, even after 60 minutes of polymerization time (Fig 5-3 (b)), still shows two distinct phases. Incomplete particle fragmentation after 60 minutes of polymerization is observed. It does, however, appear as if this barrier is overcome to a certain extent after a long polymerization time of 300 minutes (Figure 5-3 (c)).
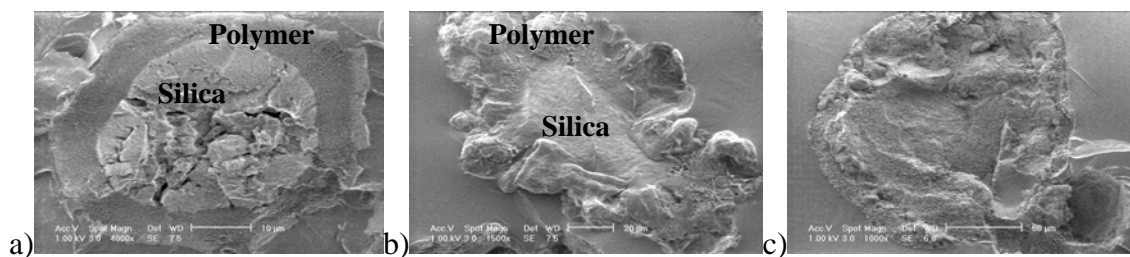

Figure 5-3   Cross-section imaging (SEM) of polyethylene particles during various stages of polymerization (E1 (a); E4 (b) and E5 (c)).

In this case, a definite silica core was not observed with SEM cross-section analysis, indicative of a fully fragmented polymer particle.   The study of polymer particle

morphology is not only important in the prevention of reactor fouling, but also gives insight into the extend of particle fragmentation during polymer growth. Incomplete fragmentation due to the diffusion limitation will influence important characteristics of a polymerization setup such as catalyst activity and polymer properties.

5.3.3. Ethylene/1-hexene copolymers (PEH)

5.3.3.1.   Polymer properties

The effect of comonomer addition on catalyst activity and particle morphology, with special reference to the overcoming of the above-mentioned diffusion limitation, forms the focus of this section. The observed polymer properties are given in Table 5-3.

Table 5-3   Properties of poly(ethylene-co-hexene) copolymers, as produced at various stages of polymerization.

Sample	Comonomer (mmol/cm^3)	mol %	Time (min)	Activity[a]	Mw (g/mol)	Mn (g/mol)	Mw/Mn	Tm[b] Peak (°C)	Onset (°C)	Crystallinity[c] (%)	Polymer (wt %)
EH1	0.05		6	800	223 400	86 600	2.6	112	84	19	57
EH2			30	700	270 800	89 000	3.0	120	110	39	90
EH3		0.5	60	800	313 600	69 300	4.5	120	112	55	96
EH4			300	700	316 500	66 800	4.7	123	113	53	99
EH5	0.09		6	900	193 800	74 200	2.6	103 (118)	60	29	72
EH6			30	700	230 900	76 100	3.0	119 (100)	105	28	n.d.
EH7		1.0	60	1 400	303 700	85 100	3.6	97 (117)	64	37	99
EH8			300	800	n.d.	n.d.	n.d.	121 (97)	112	58	99
EH9	0.17		6	1 000	349 300	81 400	4.3	83 (123)	29	21	75
EH11		2.9	60	600	326 600	86 500	3.8	85 (121)	35	44	93
EH12	0.35		6	3 600	n.d.	n.d.	n.d.	80 (123)	20	23	65
EH13		3.3	60	400	296 700	76 800	3.9	(84) 124	114	38	85

[a]kg Polymer/ (mol catalyst.hour)
[b]Thermal characteristics from second heating cycle in DSC; Values in brackets indicate peak maxima of shoulder peaks observed
[c]Determined as described by Inoue[7]
[d]Not determined

In this study, 1-hexene concentrations were increased from 0.05 to 0.35 mmol.cm^{-3} in the ethylene polymerization autoclave, while polymerization times varied between 6 and

300 minutes. In the case where two melting temperatures were observed for a particular polymer, the secondary peak is listed in brackets.

Table 5-3 shows that an increase in 1-hexene concentration to 0.09 mmol/cm^3 results in a system that shows an increase in activity at almost all studied polymerization stages. (In Table 5-2 a mere activity of 700 kg PE/(mol catalyst.hour) was observed for homopolyethylene after 60 minutes polymerization time.) A further increase in 1-hexene concentration does, however, result in a decrease in catalyst activity recorded after a polymerization time of 60 minutes (Figure 5-4). The enhancement in activity is thus dependent on the comonomer concentration. In metallocene systems, in contradiction to traditional Ziegler-Natta catalyst systems, the *comonomer effect* can either manifest itself as a slight rate enhancement[17,28-31] or even a rate depression[4,32] (as illustrated in Figure 5-4).
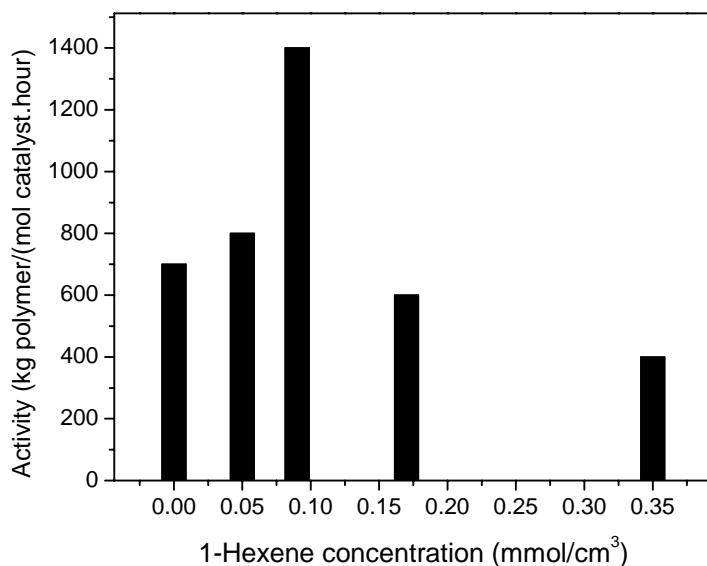

Figure 5-4   Catalyst activity as a function of comonomer concentration, recorded for a polymerization time of 60 minutes.

Table 5-3 further shows the general trend that the enhancement of catalyst activity in crystalline materials, due to the addition of comonomer, goes hand-in-hand with a decrease

in crystallinity. An optimum activity of 1 400 kg PEH/ (mol of catalyst.hour) is obtained after 60 minutes polymerization time at a monomer concentration of 0.09 mmol/cm^3.

The molecular weights of the various copolymers appear to be 100000 to 200000 g/mol lower than those observed for the homopolymers. This is characteristic for metallocene-based catalyst systems[24,33]: comonomer insertion promotes chain termination. The molecular weight distributions observed are still extremely broad. During the process of particle fragmentation, the monomer concentration at the various activated catalyst sites, on the support particle, is different. Also, considering that the outer shell of the polymer particle may consist mainly of 1-hexene-rich copolymer chains, whilst the center of the particles are more likely to be composed of ethylene-rich polymer chains, the broad distributions are understandable (see the molecular weight shoulders observed in Figure 5-5).
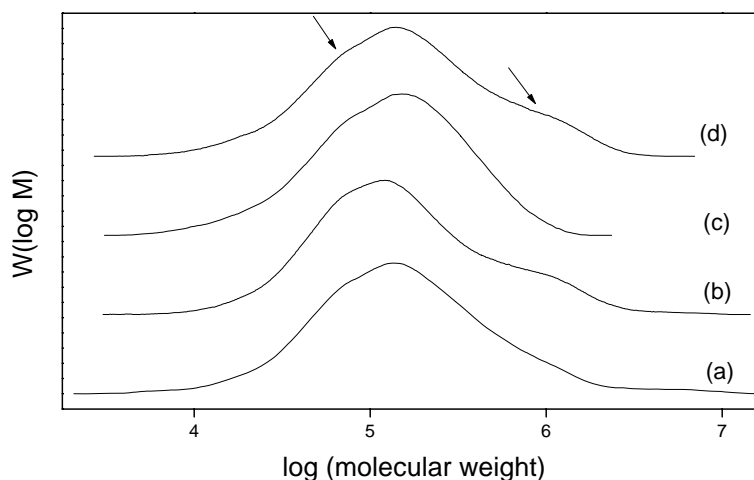

Figure 5-5   Molecular weight distributions observed for poly(ethylene-1-hexene) copolymers at 0.17mmol/cm^3 1-hexene ((d) 60 and (c) 6 minutes polymerization time) and at 0.09mmol/cm^3 1-hexene ((b) 60 and (a) 6 minutes polymerization time).

The type of polymer chains that might be responsible for the shoulder observed in the MWD curve (Figure 5-5) could be determined with size exclusion chromatography coupled fourier transform infrared spectroscopy (SEC-FTIR). With this technique, also

referred to as LC-transform, the FTIR interface allows the combination of high resolution GPC or gradient HPLC together with the good identification capabilities of FTIR spectroscopy[34].

TGA analysis of these materials at various stages of polymerization shows that the wt % polymer detected in a sample, for a specific polymerization time is, for most of the copolymers, higher than that observed for the homopolymer. (In Table 5-2, a PE produced after 60 minutes polymerization time, consisted of 87 wt % polymer.) It appears that comonomer incorporation results in an enhancement of particle growth, independent of the catalyst activity for that specific system.

CRYSTAF is a fractionation technique, which has been introduced into polymer analysis in the early nineties. The fractionation uses the dependence of the crystallization temperature on the chemical composition. Based on the Flory-Huggins theory, a linear correlation between the comonomer content and the crystallization temperature for random copolymers can be deduced.

For the analysis, the polymer is dissolved in a suitable solvent (typically 1,2,4-trichlorobenzene or 1,2-dichlorobenzene) at elevated temperatures. After stabilization at a given temperature, the solution is slowly cooled down while the concentration of the polymer in solution is measured with an infrared detector. During the crystallization step, the concentration of the polymer in solution is measured using an infrared detector. As a result a concentration profile over the temperature is obtained. The first derivative of this profile is referred to as the chemical composition distribution[35,36]. Polymers with fewer short chain branches will precipitate at higher temperatures and chains with more short chain branches (such as 1-hexene-rich copolymer chains) stay dissolved longer and will precipitate at lower temperatures. The peak temperature in CRYSTAF chromatograms is controlled by the longest sequence in the chain[37] and is correlated to the comonomer content. The chemical composition distributions of copolymers prepared using 1-hexene concentrations of 0.05 mmol/cm^3 and 0.09 mmol/cm^3 are shown in Figure 5-6.
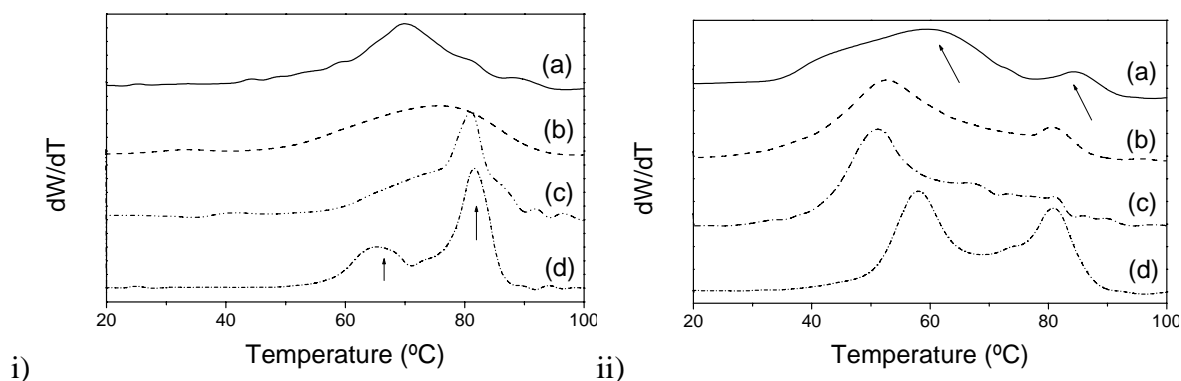
Figure 5-6   Chemical composition distribution, as given by CRYSTAF analysis of copolymers (with initial 1-hexene concentration of (i) 0.05 mmol/cm^3 and (ii) 0.09 mmol/cm^3)after (a) 6, (b) 30, (c) 60 and (d) 300 minutes of polymerization.

In the case of the copolymers synthesized with the lower concentration of 1-hexene (Figure 5-6 (i)), the crystallizable fractions are observed in the temperature range of 47 ºC to 87 ºC and a crystallization peak in the highly crystalline region is observed for polymerization times of 60 minutes or more. The copolymers from experiments with a higher 1-hexene concentration in the feedstream (Figure 5-6 (ii)) show crystallizable fractions in the 31 ºC to 90 ºC temperature range. Two distinct fractions can be noticed even at the initial stage of polymerization (6 minutes). In both cases, two defined insoluble fractions (one 1-hexene-rich and the other ethylene-rich) were observed after a polymerization time of 300 minutes. At a 1-hexene concentration of 0.09 mmol/cm^3, a more 1-hexene-rich copolymer was observed at a temperature of 58 ºC, while the 0.05 mmol/cm^3 copolymer showed the presence of a copolymer which contains only small amounts of comonomer crystallizing at 87 ºC. As would be expected, a system of higher 1-hexene content will give polymers of higher 1-hexene incorporation. The pure polyethylene fraction (for ethylene homopolymerized under the same polymerization conditions for 300 minutes) is observed at 88 ºC. (It is to be kept in mind that the experimental error of T_{peak}, in CRYSTAF analysis is ± 1 ºC[38].)

Soares *et al* proposed[39,40] that bimodality in CRYSTAF chromatograms of ethylene/1-hexene copolymers is indicative of the existence of more than one active center on the heterogenized metallocene catalyst. However, the MWD of the 0.09 mmol/cm^3

1-hexene sample after 6 minutes of polymerization, is 2.6 and thus indicative of single-center behavior. It is therefore not likely that the appearance of dual peaks in the CRYSTAF profile is due to the presence of two types of active centers on the silica catalyst system. The fact that we observe a change in crystalline behavior at various stages of polymerization and at various 1-hexene concentrations, is indicative that the bimodality observed in this work can be best described by the *filter effect*[24]. In the initial stages of copolymerization (after 6 minutes), the first peak observed at the low temperature side in the CRYSTAF chromatograms correlates to 1-hexene rich fractions, as best illustrated by the sample with a 1-hexene concentration of 0.05 mmol/cm^3. In the *filter effect* theory, one assumes that 1-hexene rich polymer chains will form initially on the surface of the solid catalyst particle. Diffusion of the small ethylene monomer with time will be faster than that of the much larger 1-hexene comonomer, thus resulting in polymer particles with more polyethylene-rich cores. The shells will mainly consist of 1-hexene rich polymer chains.

Caution should be taken with the interpretation of DSC data, as the presence of large amounts of residual silica will influence the accurateness of these measurements. On consideration of the polymers produced after 60 minutes polymerization time, a general decrease in Tm from 120 °C to 85 °C was observed for an increase of 1-hexene concentration from 0.05 mmol/cm^3 to 0.17 mmol/cm^3.

5.3.3.2. Particle Morphology

The effect of comonomer incorporation on particle morphology is illustrated by the comparison of SEM images of ethylene homopolymer particles with those of ethylene/1-hexene copolymer particles (Figure 5-7). Quite a change in particle morphology is observed in images a) (homopolyethylene) and b) (polyethylene-co-1-hexene) of Figure 5-7. Cross-section SEM images ((c) and (d)) also indicate that full fragmentation of the catalyst particle after merely 6 minutes of polymerization is observed upon on the addition of 1-hexene.
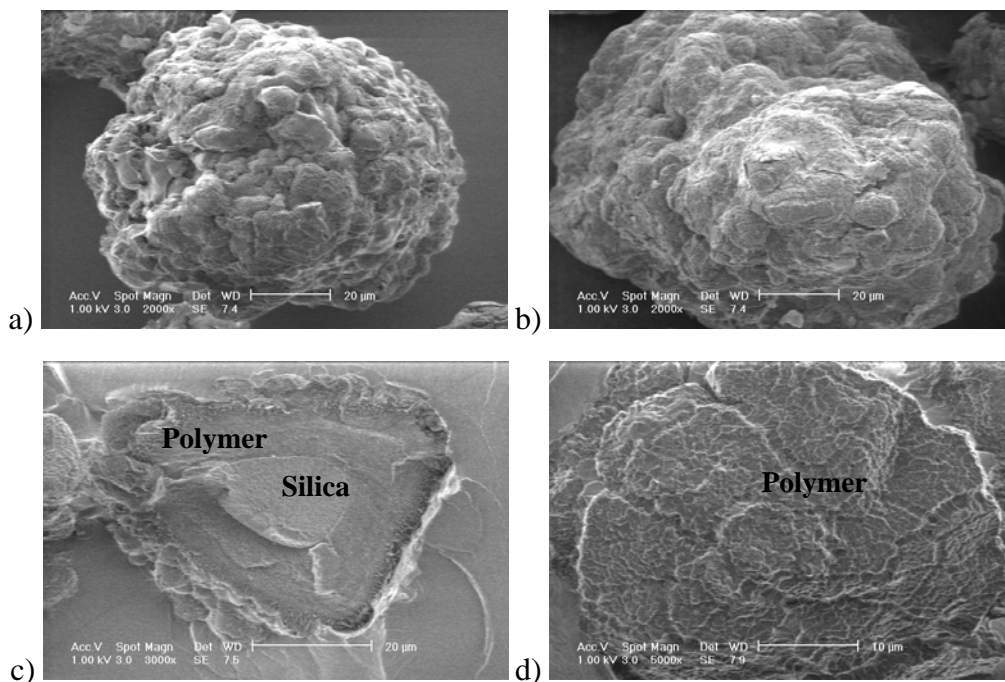
Figure 5-7   SEM imaging illustrates the difference in morphology observed for homopolyethylene (a and c, Table 5-2) and polyethylene-co-1-hexene (b and d, Table 5-3) particles.

5.3.4. Ethylene/1-octene copolymers (PEO)

 For comparison and verification of our hypothesis, we also considered the effect of 1-octene incorporation into polyethylene chains.

5.3.4.1.   Polymer properties

The polymerizations were carried out in the same manner (with the same monomer concentrations) as for the 1-hexene copolymers and the polymer properties are listed in Table 5-4. The polymers listed were obtained after 60 minutes polymerization time. A rather different trend in activity values is observed: activity seems to increase from 300-700 kg polymer/(mol catalyst.hour)) for an increase in comonomer concentration from 0.09-0.34 mmol/cm^3. An increase in Mw is also observed with an increase in comonomer concentration.   This is typical for ethylene/α-olefin copolymers synthesized with metallocene chemistry[41].

Table 5-4   Characteristics of ethylene/1-octene copolymers obtained at various comonomer concentrations after 60 minutes polymerization time.

Sample	Comonomer (mmol/cm³)	Time (min)	Activity[a]	Mw (g/mol)	Mw/Mn	Tm[b] Peak (°C)	Onset (°C)	Crystallinity[c] (%)	Polymer (wt %)
EO1	0.09	60	300	189 000	2.7	123	114	48	93
EO2	0.17	60	600	361 000	3.7	(93)122	115	37	91
EO3	0.34	60	700	nd[d]	nd	(93)122	115	34	nd

[a]kg Polymer/ (mol catalyst.hour)
[b]Thermal characteristics from second heating cycle in DSC
[c]Determined as described by Inoue[7]
[d]not determined

Keeping in mind that the catalytic activity for the homopolymerization of ethylene is 700 kg polymer/(mol catalyst.hour), see Figure 5-4 and Table 5-3, no enhancement of catalyst activity is observed with the addition of 1-octene as comonomer in the ethylene polymerization systems.
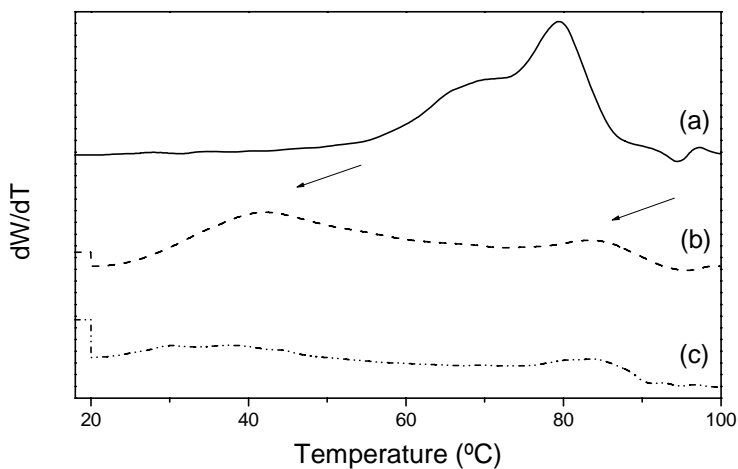

Figure 5-8   Chemical composition distribution, as given by CRYSTAF analysis of 1-octene copolymers (with initial 1-octene concentration of (a) 0.09 mmol/cm³, (b) 0.17 mmol/cm³ and (c) 0.34 mmol/cm³) after 60 minutes of polymerization time.

CRYSTAF analysis (Figure 5-8) does indicate the formation of two definite fractions: one being ethylene-rich (around 84 °C) with the other being 1-octene-rich (29 °C – 50 °C).

5.3.4.2. Particle Morphology

SEM images obtained for the 1-octene copolymers are shown in Figure 5-9. It appears that the addition of 1-octene is not as effective as the addition of 1-hexene, as the silica core is still observed in the SEM cross-section images. Large partially fragmented silica segments are also still observed, even at low magnification. This could also explain why no well-defined peak of an ethylene-rich fraction is observed around 80 °C could be seen in Figure 5-9, as was the case for ethylene/1-hexene copolymers in Figure 5-6.
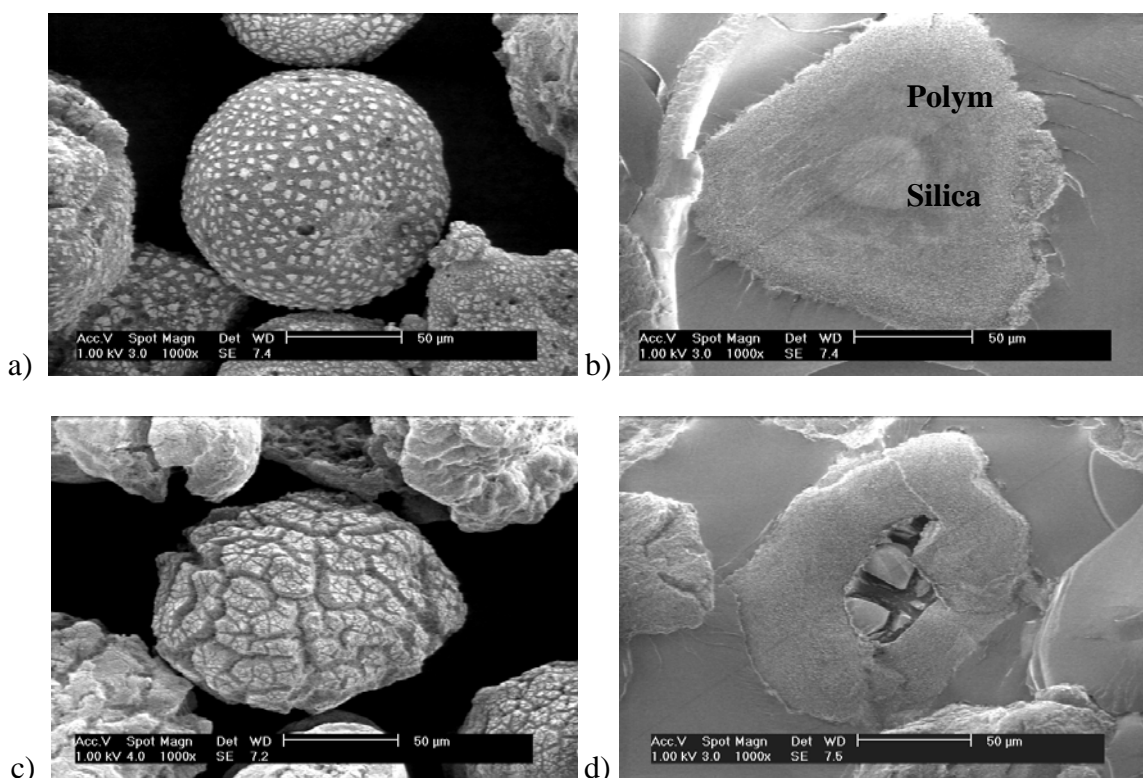

Figure 5-9   SEM imaging of poly(ethylene-co-octene) copolymer particles after 60 minutes of polymerization at 0.09 mmol/cm^3 (a and b) and 0.17 mmol/cm^3 (c and d) comonomer concentrations, respectively. ((a) and (b) show particle morphology; (c) and (d) show cross-sections.)

5.4 Conclusions

The presence of a diffusion limitation in ethylene polymerization is clearly illustrated by the incomplete particle fragmentation evident from SEM analysis of polymer particles formed at most stages in the polymerization process. An enhancement of catalyst activity and particle fragmentation and growth was observed with the addition of small amounts of 1-hexene. Broadening of the molecular weight and copolymer chemical composition distributions with increasing polymerization time provides evidence for the presence of a *filter effect*, in which ethylene diffuses more rapidly than 1-hexene through a copolymer outer shell, resulting in the formation of a polyethylene fraction with low comonomer content. Control of these characteristics is vital for processing and application considerations. In Chapter 6 we will discuss alternative routes to enhance catalyst activity, and thus particle fragmentation, to obtain systems retaining the original designed single-center characteristics of the catalyst and giving polymers of uniform composition.

5.5 Acknowledgements

5.6 References

1. Chien, J.C.W.; He, D. *J. Polym. Sci: Polym. Chem.* **1991**, *29*, 1585.

2. Kaminsky, W.; Miri, M. *J. Polym. Sci. Polym. Chem. Ed.* **1985**, *23*, 2151.

3. Kaminsky, W.; Drögemüller, H. *Makromol. Chem., Rapid Commun.* **1990**, *11*, 89.

4. Chien, J.C.W.; Xu, B.-P. *Macromol. Chem., Rapid Commun.* **1993**, *14*, 109.

5. Herfert, N.; Montag, P.; Fink, G. *Macromol. Chem., Rapid Commun.* **1993**, *194*, 3167.

6. Yu, Z.-P.; Marques, M.; Rausch, M.D.; Chien, J.C.W. *J. Polym. Sci., Part A: Polym. Chem.* **1995**, *33*, 2795.

7. Marques, M.; Yu, Z.-P.; Rausch, M.D.; Chien, J.C.W. *J. Polym. Sci., Part A: Polym. Chem.* **1995**, *33*, 2707.

8. Gabriel, C.; Lilge, D. *Polymer* **2001**, *42*, 297.

9. Pino, P.; Cioni, P.; Wei, J.; Rotzinger, B.; Arizzi, S. *Poceedings of the International Symposium on Transition Metal Catalyzed Polymerization*, Cambridge, **1986**, pp 1.

10. Fink, G.; Kinkelin, E. *Proceedings of the International Symposium on Transition Metal Catalyzed Polymerization*, Cambridge, **1986**, pp 161.

11. Spitz, R.; Duranel, L.; Masson, P.; Darricades Llauro, M.F.; Guyot, A. *Proceedings of the International Symposium on Transition Metal Catalyzed Polymerization*, Cambridge, **1986**, pp 719.

12. Calaro, D.C.; Lo, F.Y. *Proceedings of the International Symposium on Transition Metal Catalyzed Polymerization*, Cambridge, **1986**, pp 729.

13. Tait, P.J.T.; Donns, W.; Akibami, A.A. *Proceedings of the International Symposium on Transition Metal Catalyzed Polymerization*, Cambridge, **1986**, pp 834.

14. Munoz-Escalona, A.; Alarion, C.; Albornoz, A.; Fuentes, A.; Seguera, J.A. In *Olefin Polymerization*; Kaminsky, W.; Sinn, H., Eds.; Springer-Verlag: Berlin, **1988**, p 417.

15. Tait, P.J.T. In *Olefin Polymerization*; Kaminsky, W.; Sinn, H., Eds.; Springer-Verlag: Berlin, **1988**, p 309.

16. Kaminsky, W.; Hahnsen, H. *Advances in Polyolefins*; Plenum: New York, **1987**.

17. Tsutsui, T.; Kashiwa, N. *Polym. Commun.* **1988**, *29*, 180.

18. Soga, K.; Yanagihara, H.; Lee, D.-H. *Makromol. Chem.* **1989**, *190*, 995.

19. Tait, P.J.T.; Downs, G.W.; Akibami, A.A. In *Transition Metal Catalyzed Polymerizations*; Quirk, R.P., Ed.: Cambridge, **1988**, p 834.

20. Tait, P.J.T.; Berry, I.G. *Surf. Sci. Catal.* **1994**, *89*, 55.

21. Suhm, J.; Schneider, M.J.; Mülhaupt, R. *J. Polym. Sci., Part A: Polym. Chem.* **1997**, *35*, 735.

22. Widmer, A. *Chem. Rundsch.* **1994**, *47*, 4.

23. Schneider, M.J.; Mülhaupt, R. *Macromol. Chem. Phys.* **1997**, *198*, 1121.

24. Przybyla, C.; Tesche, B.; Fink, G. *Macromol. Rapid. Commun.* **1999**, *20*, 328.

25. Inoue, M. *J. Polym. Sci. Polym., Part A; Polym. Chem.* **1963**, *1*, 2697.

26. Nagel, E.J.; Kirillov, V.A.; Ray, W.H. *I & EC Prod. Res. Dev.* **1980**, *19*, 372.

27. Yuan, H.G.; Taylor, T.W.; Choi, K.Y.; Ray, W.H. *J. Appl. Polym. Sci.* **1982**, *27*, 1961.

28. Uozumi, T.; Soga, K. *Makromol. Chem.* **1992**, *193*, 823.

29. Koivomäki, J.; Seppälä, J. *Macromolecules* **1993**, *26*, 5535.

30. Koivomäki, J.; Fink, G.; Seppälä, J. *Macromolecules* **1994**, *27*, 6254.

31. Karol, F.; Kao, S.-C.; Wasserman, E.; Brady, R. *New J. Chem.* **1997**, *21*, 797.

32. Tait, P.; Awudza, J.; Terano, M., Ed.; Technology and Education Publishers: Tokyo, **2000**, p 214.

33. Chu, K.J.; Li Pi Shan, C.; Soares, J.B.P.; Penlidis, A. *Macromol. Chem. Phys.* **1999**, *200*, 2372.

34. Gagel, J.; Biemann, K. *Anal. Chem.* **1986**, *58*, 2184.

35. Monrabal, B. *J. Appl. Polym. Sci.* **1994**, *52*, 491.

36. Monrabal, B. *Macromol. Symp.* **1996**, *110*, 81.

37. Beigzadeh, D.; Soares, J.; Duever, T. *J. Appl. Polym. Sci.*, in Print.

38. Ananatawaraskul, S.; Soares, J.B.P.; Wood-Adams, P.M.; Monrabal, B. *Polymer* **2003**, *44*, 2393.

39. Kim, D.J.; Soares, J.B.P. *Macromol. Rapid. Commun.* **1999**, *20*, 347.

40. Chu, K.J.; Zi Pi Chan, C.; Soares, J.B.P.; Penlidis, A. *Macromol. Chem. Phys.* **1999**, *200*, 2372.

41. Seppälä, J.; Koivumäki, J.; Liu, X. *J. Polym. Sci., Part A: Polym. Chem.* **1993**, 31, 3447.

CHAPTER 6

Enhancement of ethylene polymerization activity

through pre-polymerization with propylene[*]

SYNOPSIS: Rate enhancement on addition of a small amount of a higher ∝-olefin such as 1-hexene is a commonly observed phenomenon in ethylene polymerization. In Chapter 5, we considered the effect of this "comonomer activation" on both polymer properties and polymer morphology. Activity values doubled with a comonomer concentration of only 0.09 mmol/cm³. Although the so-called "diffusion limitation" appeared to be overcome, lower molecular weight products displaying a definite influence of the comonomer on polymer properties were observed. Ideally, one would prefer a simple method to enhance catalyst activity that has a minimum influence on the original polymer properties. This will allow much more control over the end product, thus making it much more suitable for industrial application.

In this chapter, we consider novel, simple pre-polymerization techniques to enhance catalyst activity, while retaining the original catalyst performance characteristics. Additionally, we will show that pre-polymerization before a main ethylene copolymerization results in polymers with narrower chemical composition distributions (CCDs).

Keywords: support; immobilize; metallocenes; pre-polymerization; poly(ethylene)

6.1 INTRODUCTION

Rate enhancement following the introduction of a comonomer in ethylene polymerization with Ziegler-Natta systems, is a well-established phenomenon[1,2]. In metallocene systems, however, the *comonomer effect* can either manifest itself as a slight rate enhancement[3-7] or even a rate depression[8,9](as also illustrated in Chapter 5).

Traditionally, single-center catalysts produce random copolymers with narrow molecular weight (MWDs) and chemical composition distributions (CCDs)[6,9-14]. We have, however, seen in Chapter 5 that broad distributions are observed for the heterogenized ethylene homo- and copolymerization products. This was partially explained by the *diffusion limitation* and *filter effect*. Narrow MWDs observed for polypropylenes obtained with the same catalyst systems (Chapter 3) indicate that single-center behavior is retained on immobilization of the MAO-activated catalyst systems with the *wet sand* method. Chien *et al*[15] also reported that the activity and copolymerization reactivity of the homogeneous and heterogeneous MAO-activated *racemic* ethylene-bridged bis(indenyl) zirconium dichloride (*rac*-Et(Ind)$_2$ZrCl$_2$) are the same.

Another way to enhance the activity of a catalyst system is known as pre-polymerization. The latter refers to a polymerization process, at very mild conditions, of a monomer other than ethylene before main polymerization is initiated. This also limits the formation of a *diffusion limitation* and thus facilitates particle fragmentation. Prepolymerization can also prevent local overheating of the catalyst particle caused by large exotherms in the early stages of polymerization. Fusing or melting of particles, bad particle morphology and adhesion of molten polymer to reactor walls are a few factors that interfere with heat transfer in the reactor. This is not very practical and often results in the broadening of MWDs and CCDs. Pre-polymerization aims to reduce the surface exotherm resulting from high initial catalyst activity combined with a small surface area of the initial support particle. Ideally, it allows controlled particle fragmentation.

A positive effect on ethylene homopolymerization activity after a brief pre-polymerization with Ziegler-Natta catalyst with either ethylene/propylene or ethylene/1-butene, followed by the removal of the monomer, has been reported by Wu *et al.*[16]. Recently, Zakharov *et al*.[17] have found that diffusion limitation in ethylene

polymerization using a MgCl$_2$-supported Ziegler-Natta catalyst can be greatly alleviated by carrying out a pre-polymerization with propylene, which resulted in a large increase in productivity. Very little has been published in open literature on pre-polymerization with heterogeneous metallocene catalyst systems. In this work, we will explore the *comonomer effect* in terms of propylene and ethylene/1-hexene pre-polymerization prior to ethylene and ethylene/∝-olefin main polymerization setups. In theory, if pre-polymerization before a main ethylene polymerization could enhance particle fragmentation, it might also reduce the so-called *filter effect* and promote the formation of ethylene copolymers with narrow MWDs and CCDs. Results will be discussed in terms of particle morphology (SEM imaging), and polymer properties with special reference to CRYSTAF analysis for the study of the chemical composition distribution (CCD) in copolymers.

6.2 Experimental

6.2.1. Materials

All reactions were carried out under argon atmosphere. Catalysts were handled in a glove box under an inert atmosphere with a sensitivity of 1ppm O$_2$ and H$_2$O. Support materials were handled in a glove box of 0.1 ppm O$_2$ and H$_2$O sensitivity. A 10 wt % solution of the cocatalyst methylaluminoxane (MAO) in toluene was obtained from Witco, while *racemic* ethylene-bridged bis(indenyl) zirconium dichloride (*rac*-Et(Ind)$_2$ZrCl$_2$) was purchased from STREM chemicals. The silica support material, Sylopol 948, was kindly donated by Grace AG. Toluene (Biosolve) was dried on alumina columns, while n-heptane was distilled over potassium before use. Triisobutylaluminum (TIBA) was purchased from Akzo-Nobel as a 25 wt % solution in toluene. Propylene (Hoekloos) and ethylene (Air Liquide) were dried over columns containing activated copper catalyst (BTS) and alumina before introduction into the polymerization reactor.

6.2.2. Support synthesis

6.2.2.1.   Calcination

See Section 5.2.2.1.

6.2.2.2. *Immobilization of MAO-activated catalyst on silica*

See Section 5.2.2.2. for full description.

6.2.3. Pre-polymerization

6.2.3.1. *1-Hexene*

400 mL n-Heptane were transferred into the Premex reactor and were placed under a 2.4 bar ethylene pressure for 30 minutes. 1.8 mmol of the TIBA solution were added to the reactor with 75 mL n-heptane containing 1 mL 1-hexene. The reactor mixture was left to stir for 15 minutes, after which 150 mg of catalyst were transferred with 75 mL n-heptane. The reaction was left for 30 minutes and then the main polymerization was started.

6.2.3.2. *Propylene*

100 mL n-Heptane were transferred to the Premex reactor and placed under 0.3 bar propylene overpressure while stirred for 30 minutes. The propylene feed was then stopped. 1.8 mmol of the TIBA solution was then transferred with 75 mL n-heptane, followed by the addition of 250 mg catalyst with another 75 mL n-heptane. The reaction was left for 90 minutes before the main polymerization was started with the transfer of 300 mL n-heptane into the reaction vessel and increase of overpressure with 2.5 bar ethylene.

6.2.4. Slurry Polymerization Procedure

The polymerization was carried out in a 1 L PREMEX stainless steel reactor, equipped with a hollow-shaft turbine stirrer and a temperature controlled heating/cooling mantle. The reactor temperature was kept at 50 °C and 400 mL of n-heptane were transferred under argon atmosphere into the PREMEX reactor. The reactor pressure was raised to 2.4 bar (±0.1 bar) monomer pressure and left under stirring for 30 minutes at 1000 rpm to ensure maximum dissolution of the gaseous monomer. 1.8 mmol of the TIBA solution were transferred to the reactor with the desired amount of comonomer and 40 mL of n-heptane. After 15 minutes, the catalyst (150 mg) was transferred into the reactor with 22 mL n-heptane. Time was noted and the reactor was degassed after an hour and the slurry quenched with acidic methanol. The polymer was dried in a vacuum oven at 60 °C.

6.2.5. Characterization techniques

See Section 5.2.4. for a full description of all the analysis techniques employed in this study.

6.3 RESULTS AND DISCUSSION

6.3.1. Characterization of the heterogeneous metallocene catalyst

The heterogeneous catalyst used in this study was prepared via the immobilization of methylaluminoxane-activated *racemic* ethylene-bridged bis(indenyl) zirconium dichloride (*rac*-Et(Ind)$_2$ZrCl$_2$)) on silica (Sylopol 948, calcined at 600 °C) at elevated temperatures as a *wet sand*. As described earlier[18,19], this method was chosen for its excellent reproducibility and storage lifetime of the activated support. The characteristics of the support material are summarized in Table 6-1.

Table 6-1   Characteristics of the unmodified and MAO-activated *rac*-Et(Ind)$_2$ZrCl$_2$ impregnated on Sylopol 948, calcined at 600 °C.

Sylopol 948	OH content (mmol OH/g SiO$_2$)	Surface area (m^2/g)	Pore diameter (nm)	Pore volume (cm^2/g)	AES-ICP	
					Al (wt %)	Zr (wt %)
Unmodified	1.0	304	24	1.8	n.a.	n.a.
Activated silica	n.a.[a]	270	17	1.2	8.6	0.17

[a]not applicable

Successful immobilization of both the catalyst and cocatalyst is illustrated by the simultaneous presence of aluminum (8.6 wt %) and Zr (0.17 wt %). The marked decrease in surface area, pore diameter and pore volume also illustrates to this.

6.3.2. Pre-polymer morphology

In this study, we developed simple pre-polymerization techniques that exclude traditional washing or tedious refluxing of the pre-polymer to ensure effective removal of the pre-polymerization monomer[16,20]. A 90-minute propylene pre-polymerization was carried out at a very low propylene concentration at 50 ℃ in 150 mL n-heptane, after dissolution of 0.3 bar propylene in 100mL n-heptane for 30 minutes. The main polymerization was initiated, after degassing, with the addition of 300 mL n-heptane and the application of the desired ethylene pressure.

As discussed in Chapter 5, particle morphology and particle fragmentation are two important variables in heterogeneous metallocene catalysis that influence catalyst activity and polymer properties directly. The pre-polymers were therefore first analyzed using scanning electron microscopy (SEM) to obtain information regarding pre-polymer morphology. The propylene pre-polymer (Figure 6-1) was obtained as a free-flowing powder with good morphology.
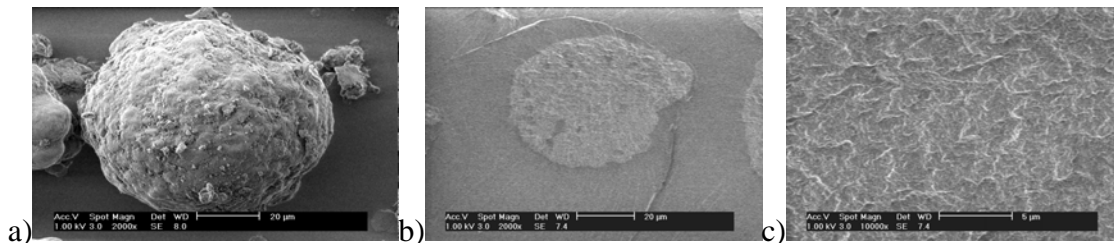

a)   b)   c)

Figure 6-1   Polypropylene pre-polymer particle, as depicted by SEM imaging (singular particle (a), microtome cross-section (b) and a close-up 100000 magnification) of the cross-section morphology (c)).

Although the particles illustrated in Figure 6-1 (a) are small (*ca.* 80μm), cross-section analysis at a magnification of 100000 reveals morphology that is typical for polypropylene on silica (as illustrated in Figure 3-11 in Section 3.3.4.).

We have also noticed the activation effect of the presence of a small amount of 1-hexene in an ethylene pre-polymerization system. The positive effect of such an addition on particle morphology is clearly illustrated by the SEM images of granular silica-based polyethylene particles (Figure 6-2). The image on the left (of PE) illustrates various fibrils, a typical indication of a diffusion limitation. The image on the right was made from PE particles that had been pre-polymerized with a combination of ethylene and 1–hexene as monomers.
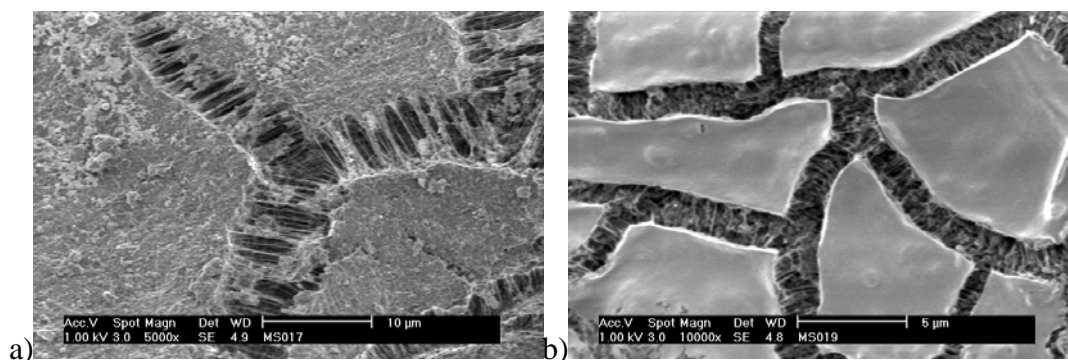
Figure 6-2   SEM images of polyethylene (a) and polyethylene-co-hexene (b) synthesized on granular silica.

A drastically smoother granular surface is observed for the PEH copolymer particles with the minimization of fibrils, in comparison to that observed for the homo PE particles. SEM images of the PEH pre-polymer used in this work are given in Figure 6-3.
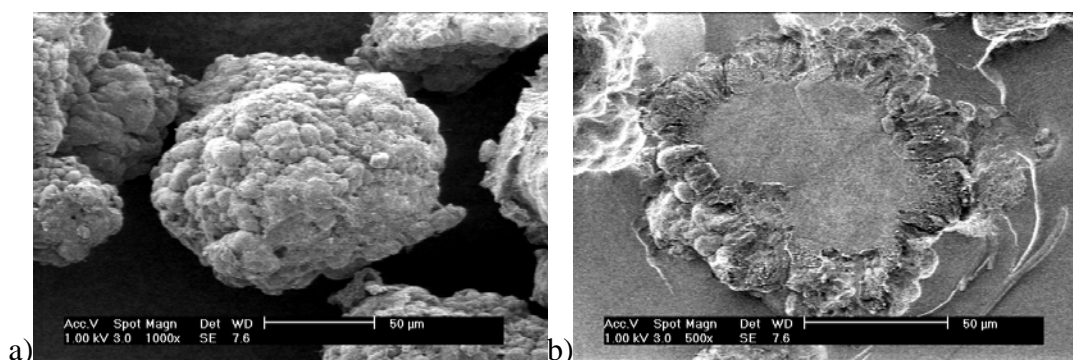

Figure 6-3   SEM images of the PEH pre-polymer synthesized.

Although the particle given in Figure 6-3 (a) is quite large (*ca.* 130μm), a definite diffusion limitation is observed on cross-section analysis (Figure 6-3 (b)) of these PEH pre-polymer particles. In order to determine the effectiveness of the pre-polymerization step, ethylene homo- and copolymers were synthesized and the polymer properties were subsequently determined.

6.3.3. Characteristics of resulting polymers

6.3.3.1.   Polyethylene properties

Table 6-2 summarizes the polyethylene properties, as obtained after simple ethylene polymerization (PE), pre-polymerization with propylene (ppPE) and pre-polymerization with 1-hexene (pehPE) before ethylene main polymerization.

According to ^{13}C NMR, very low amounts of comonomer (0.24-0.35 mol %), resulting from pre-polymerization, were incorporated in the polymer particle. Pre-polymerization with either propylene or an ethylene/1-hexene combination results in a significant enhancement of catalyst activity for the ethylene main polymerization, especially with the propylene pre-polymerized polyethylene system. This appears, however, to go hand-in-hand with major drops in the molecular weight values, and polymers with Mw values of *ca*. 279000-386000 g/mol are obtained, compared to 558000 g/mol for the non-prepolymerized PE sample. A possible reason for this might be the increased particle porosity as a result of pre-polymerization. This is, however, pure speculation.

Table 6-2 Polyethylene properties obtained with and without pre-polymerization before main polymerization.

| Sample | mol % comonomer | | Activity[a] | Mw (g/mol) | Mn (g/mol) | Mw/Mn | Tm[b] | |
	propylene	1-hexene					Peak (°C)	Onset (°C)
PE			400	558 000	160 900	3.5	130.6	120.8
ppPE	0.35		1 100	278 600	58 600	4.8	127.6	118.2
pehPE		0.24	600	385 900	142 100	2.7	124.8	113.7

[a]kg Polymer/(mol catalyst.hour)

[b]Melting peak from second heating cycle in DSC analysis

The same is true for the number-average molecular weight value of the propylene pre-polymerized PE, resulting in a broad molecular weight distribution of 4.8 (unacceptable for single-center catalyst behavior). We have shown (in Chapter 3) that the impregnation of MAO-activated *rac*-Et(Ind)$_2$ZrCl$_2$ in a *wet sand* fashion, results in catalyst species producing PP with narrow MWDs (*ca*. 2.1). *rac*-Et(Ind)$_2$ZrCl$_2$ is thus successfully immobilized with this method as to retain single-center behavior and the broad molecular weight distribution observed appears not to be the result of ineffective immobilization of a single-center catalyst. Narrow MWDs are, however, not ideal for processing, thus making the above polymers more ideal for industrial application. The pehPE sample shows a MWD of 2.7, which is more expected behavior for single-center catalysts, compared to the 3.5 obtained for the PE homopolymer.

The melting temperature observed for polyethylene (130.6 °C) is characteristic of this catalyst (see Table 5–2 in Section 5.3.2.) at a monomer pressure of 2.4 bar. Propylene pre-polymerization does lower the melting temperature of the resulting polyethylene, although it should be noted that this is observed to a lesser extent compared to that observed for the ethylene/1-hexene pre-polymerized polyethylene system (single melting peaks with no shoulders were observed in both cases). It is important for HDPE (high density polyethylene) that one should retain polyethylene characteristics after pre-polymerization and not have materials with copolymer characteristics. The thermal analysis data are supported by results obtained from CRYSTAF analysis (Figure 6-4).
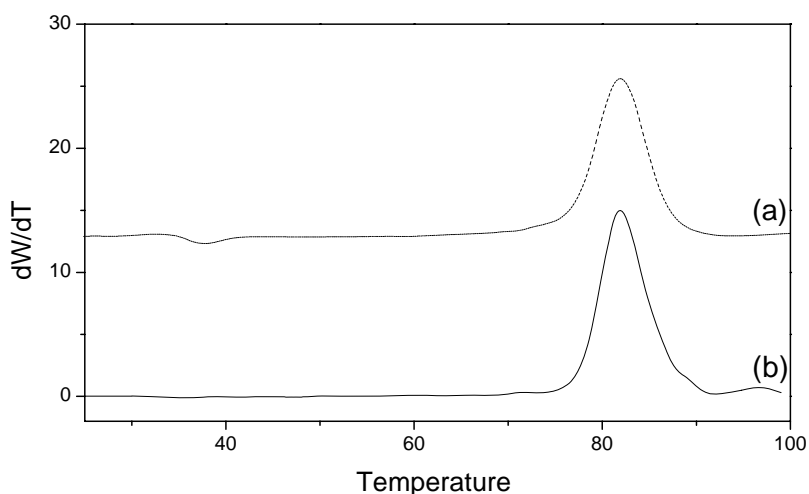

Figure 6-4   CRYSTAF   chromatograms,   as   obtained   for   ethylene/1-hexene (a) and propylene (b) pre-polymerized polyethylene materials.

Only one crystallization peak is observed for the propylene (0.35 mol % propylene) and ethylene/1-hexene (0.24 mol % 1-hexene) pre-polymerized polyethylene samples. The crystallizable fractions are observed at 82.1 ℃ and 81.9 ℃, respectively. The crystallizable fraction of pure polyethylene chains is observed at *ca.* 88 °C.

The aim was to minimize the presence of copolymer sequences such as EPE for the propylene pre-polymerized PE (illustrated by an NMR peak at 33 ppm). Figure 6-5 shows that only traces of propylene units are detectable in the final polymer, indicating negligible

incorporation of propylene into the polyethylene chain. The sharp peak at 29.7 ppm represents (EEE)*n*.
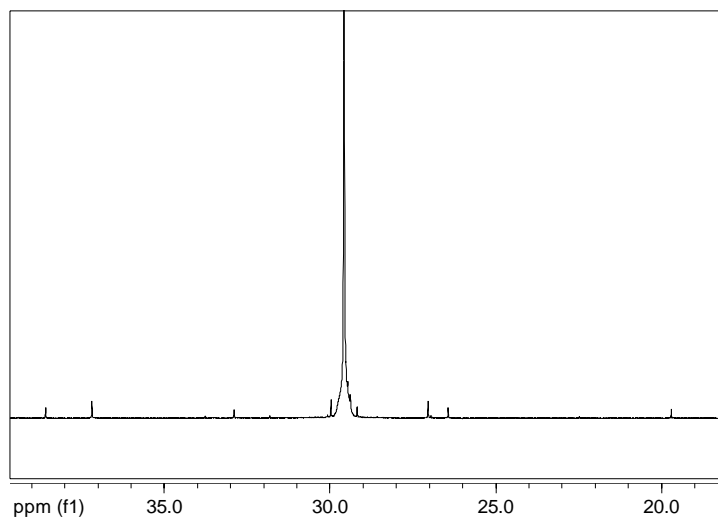

Figure 6-5 ^{13}C NMR spectra of the propylene pre-polymerized polyethylene (ppPE).

The interference of propylene monomers with the main polymerization could be restricted to a minimum and polyethylene, retaining its original properties, was achieved.

SEM imaging (Figure 6-6) reveals the effect of pre-polymerization on polymer particle morphology. These images show the sizes of the individual PE particles, as well as the cross-section morphology, indicating the effectiveness of particle fragmentation during particle growth. This can be judged to a certain extent by the presence or absence of silica cores in these images. Non-prepolymerized PE clearly shows the presence of a diffusion *limitation*, as the particle consists mainly of a silica core that is surrounded by polymer grown on the surface. (This effect was discussed Section 5.3.2.) Cross-section analysis of the pre-polymerized materials does, however, indicate the absence of a silica core and thus suggests homogeneous particle growth throughout the polymer particles. Fibrils observed in SEM imaging of polyethylene particles often indicate the stretching of the polymeric material due to ineffective fragmentation of the particle during polymerization, as a result of a *diffusion limitation*. This is still observed (as illustrated by the arrows) with the 1-hexene pre-polymerized materials (with 0.24 mol % 1-hexene). In contrast, the propylene pre-polymerized PE (with 0.35 mol % propylene) appears to be fibril-free and

full fragmentation appears to have been achieved with pre-polymerization prior to the main ethylene polymerization.
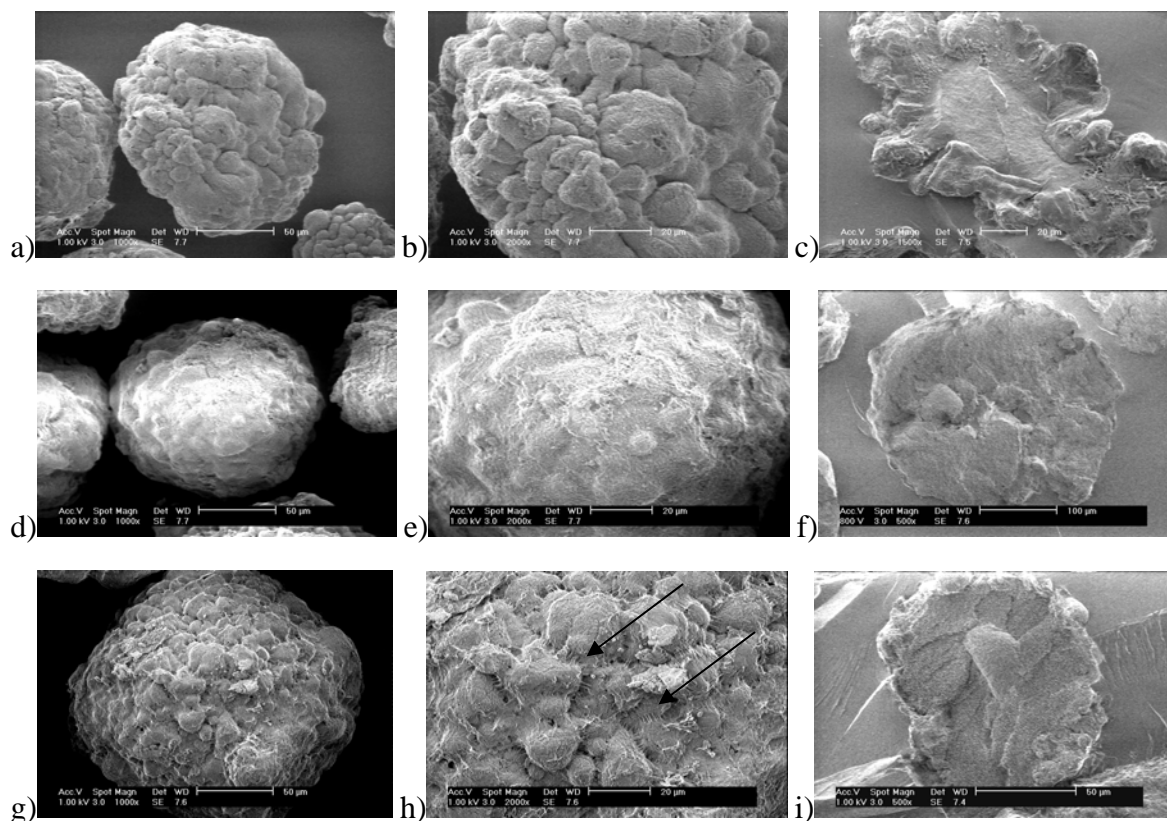

Figure 6-6   SEM images of polyethylene (a, b and c) and propylene (d, e and f) and 1-hexene (g, h and i) pre-polymerized polyethylene particles.

6.3.3.2.   Ethylene copolymer properties

In the case of ethylene copolymers, one often observes broad chemical composition distributions (CCD)[19] with heterogeneous metallocene catalyst systems. The broad CCD observed with the heterogenized systems could be explained by the presence of a variety of comonomer concentrations at the various active sites during the beginning of particle fragmentation or resulting from ineffective particle fragmentation during the polymerization period.   The idea with pre-polymerization is to enhance particle fragmentation under mild polymerization conditions in order to not only enhance catalyst activity, but also to improve particle morphology. This was achieved for polyethylene systems, as shown in Section 6.3.3.1.   The question now at hand is whether pre-polymerization does allow for an equal distribution of comonomer over the

macromolecules produced at various active polymerization sites to allow for a narrower CCD.

Two comonomers (1-hexene and 1-octene) were employed for this study for the main copolymerization with ethylene, while both pre-polymerization techniques (propylene (pp) and ethylene/1-hexene(peh)) were used. In each case, a comonomer concentration of 0.17 mmol/cm^3 was used in the main polymerization. Table 6-3 summarizes the properties of the individual copolymers.

Table 6-3   Polymer properties obtained, with and without pre-polymerization, for ethylene copolymers.

| Sample | mol % comonomer[a] | | | Activity[b] | Mw (g/mol) | Mn (g/mol) | Mw/Mn | Tm | |
	propylene	1-hexene	1-octene					Peak (°C)	Onset (°C)
PEH		5.2		600	326 600	86 500	3.8	(85.3)[c] 121.1	34.7
ppPEH	not detected	5.1		4 400	271 300	54 900	4.9	(94.3) 118.6	103.2
pehPEH		6.0		1 900	320 820	76 400	4.2	(86.0) 121.4	112.4
PEO			2.0	600	361 000	98 000	3.7	(93.1) 121.5	114.6
ppPEO	0.25		1.0	2 000	256 400	83 000	3.1	121.5	115.1
pehPEO		0.02	2.9	1 300	252 500	71 300	3.5	121.8	114.3

[a]Determined with quantitative ^{13}C NMR analysis

[b]kg Polymer/(mol catalyst.hour)

[c]Melting peak from second heating cycle in DSC analysis

[d]The DSC melting peaks listed in brackets, represent the maximum peak values determined for the shoulder peaks observed

Again an enhancement in activity is observed with pre-polymerization of catalyst particles before the main copolymerization reactions for both the 1-hexene and 1-octene systems. Also interesting to note, is that pre-polymerization with propylene results again in the biggest enhancement in catalyst activity. Pre-polymerization with propylene does thus appear to be more effective in the facilitation of controlled particle fragmentation and overcoming of the *filter effect*. A clearer view of the exact microstructure of the ethylene/1-hexene copolymers is given by the triad distributions in Table 6-4.

Table 6-4   Triad distributions calculated for the ethylene/1-hexene copolymers.

	EHE	EHH	HHH	HEH	EEH	EEE
PEH	4.7	0.5	0	0.3	11.0	83.4
ppPEH	4.8	0.3	0	0.2	8.3	86.4
pehPEH	5.7	0.3	0	0.3	11.1	82.6

It is clear that more or less the same type of microstructure is observed for the above three polymers, with pehPEH showing a higher incorporation of 1-hexene compared to the other two.

The thermal analysis data are interesting, as illustrated in Figure 6-7, which shows the second heating curves obtained in DSC analysis of the PEH samples.
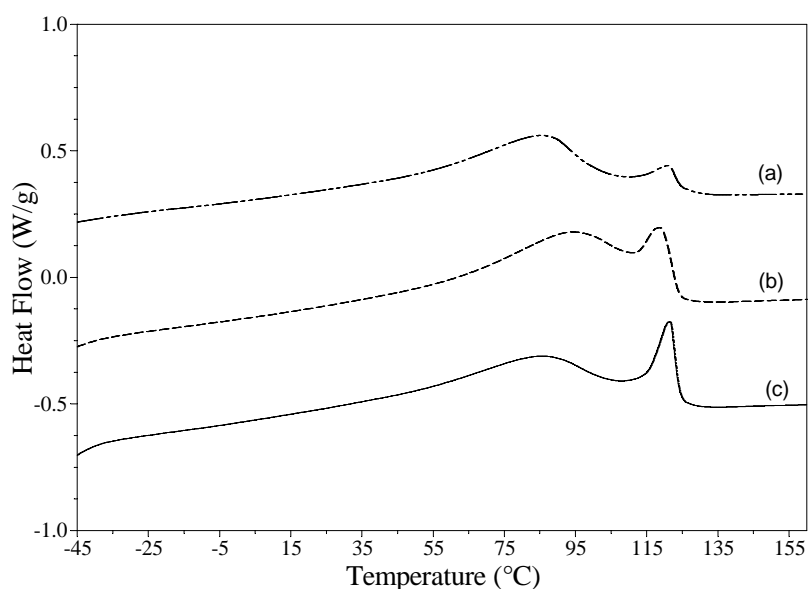

Figure 6-7   The   second   heating   curves   from   DSC   analysis   for polyethylene-co-hexene (no pre-polymerization (a), propylene (b) and 1-hexene (c) pre-polymerized (Table 6-3)).

In the non-pre-polymerized (a) copolymer curve, two distinct peaks can be observed. The peak at the highest temperature probably represents the more pure polyethylene chains, while that at the lower melting temperature is probably the result of the 1-hexene-rich copolymer chains present in the polymer sample. As discussed earlier[19], this supports the *filter effect*[21] in which case the polymer particle comprises of a copolymer

outer layer with a more polyethylene-rich core, as a result of easier diffusion of the smaller ethylene molecule compared to 1-hexene. Propylene pre-polymerization does, however, appear to reduce the effect, as the two peak maxima appear to be closer to each other, suggesting that a somewhat more uniform copolymer composition is produced. The same effect is observed (although to a lesser extent) for the pre-polymerized 1-octene copolymers. In the case of ethylene/1-octene copolymerization, the DSC data in Table 6-3 indicate a less pronounced effect of pre-polymerization.

In order to investigate the effect of pre-polymerization on copolymer chemical composition distribution, the ethylene/1-hexene and ethylene/1-octene copolymers were analyzed using CRYSTAF chromatograms and the related soluble fraction (SF) values. The results are shown in Figure 6-8.
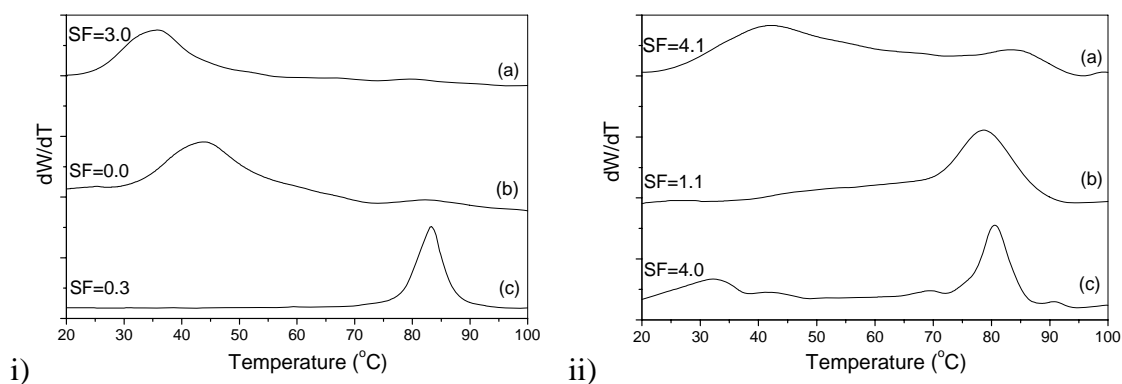

Figure 6-8   CRYSTAF data, as observed for Polyethylene-co-hexene (i) and Polyethylene-co-octene (ii) after 60 minutes of main polymerization (no pre-polymerization (a), propylene (b) and ethylene/1-hexene (c) pre-polymerized (Table 6-3)).

In all cases, a polymer fraction is observed between 70 °C and 90 °C. As illustrated in Figure 6-4, this fraction consists mainly of ethylene-rich polymer chains. A second fraction is observed at lower temperatures.

In the PEH sample without pre-polymerization, a definite crystalline fraction is observed between 20 °C and 60 °C, while the second peak, although hardly developed, appears at *ca.* 83 °C. For ppPEH, the same trend is observed, although the first peak is only observed from 28 °C to 72 °C. These data agree with the DSC data showing that the

1-hexene-rich fraction appears to be closer to the ethylene-rich fraction, suggesting a narrower CCD. (It should be noted at this point that no Tg was observed for any of the copolymers used in this study.) The advantage of CRYSTAF, as illustrated here, is that it gives a much better separation between the types of copolymer chains in a sample, as compared to DSC. The PEO without pre-polymerization, samples appear to have the same trend, as the peak (representing the 1-octene-rich and ethylene-rich fractions) observed for PEO appears from 22 °C to 96 °C, whereas the peak for ppPEO is only observed in the range 33 °C to 93 °C. The pre-polymerization of a catalyst/support material before the main ethylene copolymerization, does appear to result in materials with narrower CCDs.

In the case of the peh pre-polymerized copolymers, a distinct ethylene-rich fraction is observed at *ca.* 84 °C. The comonomer-rich fractions are not illustrated in the chromatograms, as they are observed as soluble fractions at room temperature. (Once again illustrating the better separation observed with CRYSTAF analysis compared to DSC analysis.) The lower soluble fraction values observed for the pre-polymerized PEH copolymers (of 0.0 % (ppPEH) and 0.3 % (pehPEH)) also illustrate the narrower CCD observed in comparison to PEH (3.0 %).

Soares *et al* were the first to make a direct comparison between DSC thermal fractionation (successive self-nucleating annealing (SSA)) and CRYSTAF techniques for the analysis of metallocene resins[22]. They found that that there is a very good correlation between the data obtained and that no additional calculations, regarding for instance the differences in heat of fusion as a function of comonomer concentration, are required.

In Figure 6-9, SEM images of the 1-hexene copolymers are given at 500 and 2000 magnifications. Fibrils are observed in the images taken of the non-pre-polymerized copolymer. The pre-polymerization does appear to minimize this affect and the individual fragments of the support cannot be observed at these magnifications.

Propylene pre-polymerization appears much more effective in terms of enhancement of catalyst activity and improving polymer properties. This might be due to the fact that propylene polymerization on support systems (as shown in this dissertation) easily results in fully fragmented catalyst/support particles (See Chapter 3).
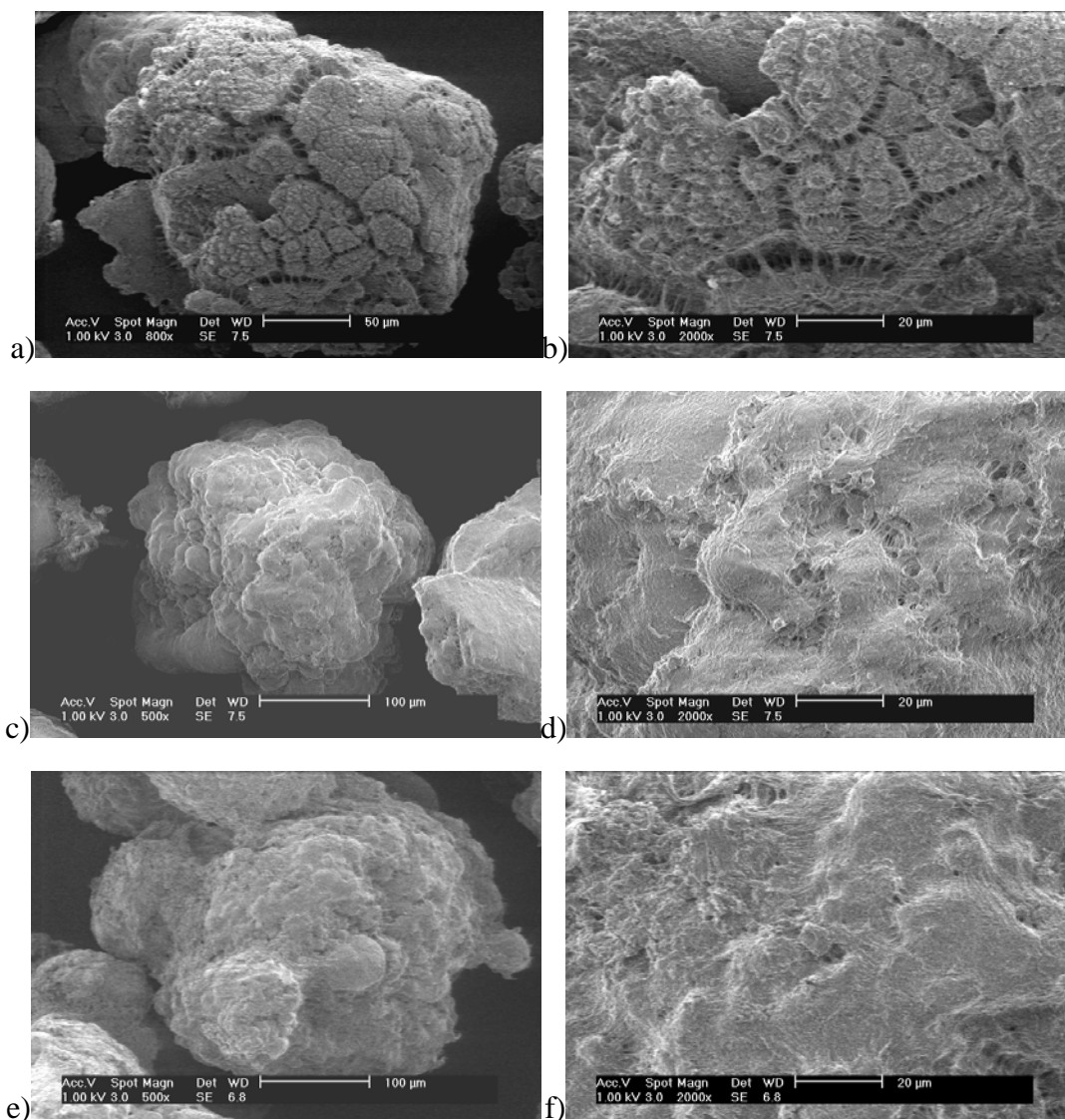
Figure 6-9   SEM images of poly(ethylene-co-hexene) (a and b) and propylene (c and d) and 1-hexene (e and f) pre-polymerized poly(ethylene-co-hexene) particles, Table 6-3.

SEM images of the 1-octene copolymers are given in Figure 6-10. Here, fibrils are observed for the pre-polymerized copolymer particles, as well as for the non-prepolymerized copolymer particles. The effect of pre-polymerization on the copolymer particle morphology is not as noticeable with the ethylene/1-octene copolymers, compared to the ethylene/1-hexene copolymers.
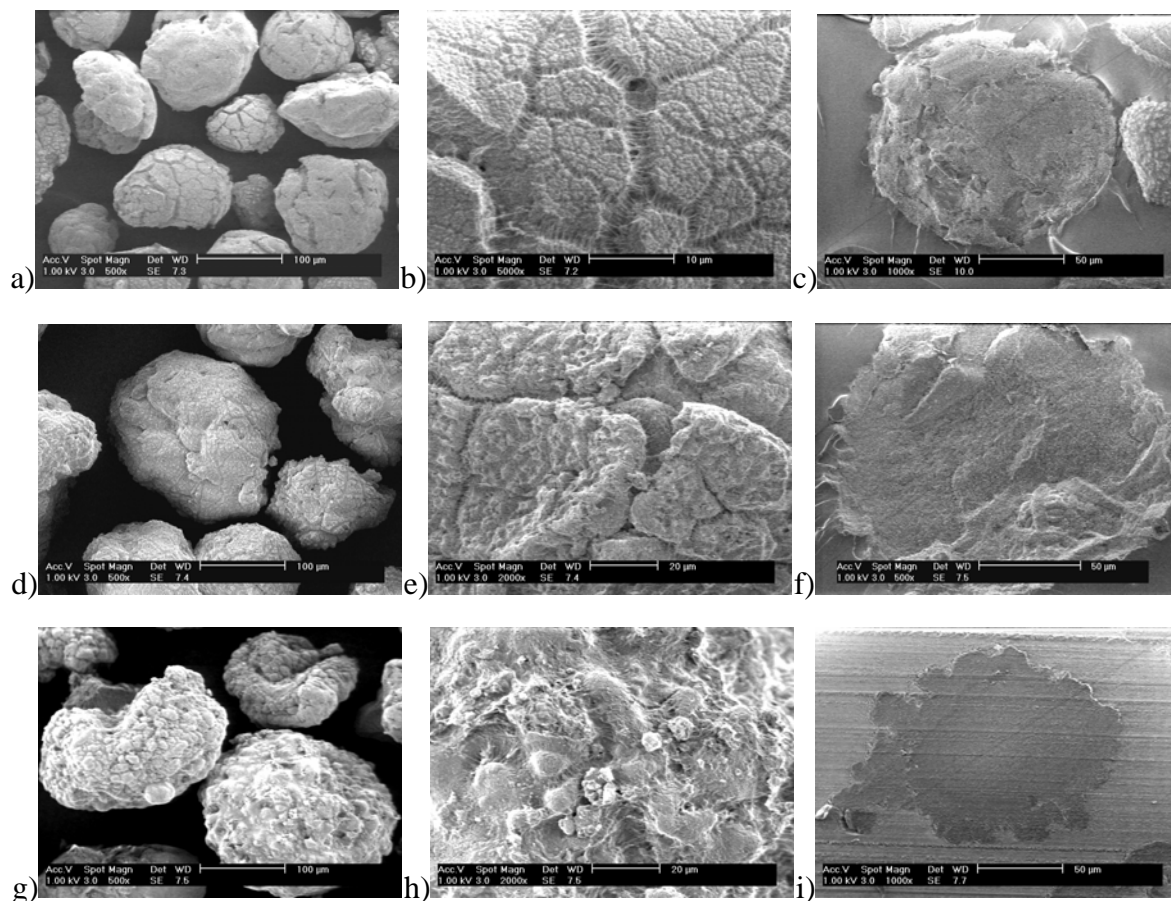
Figure 6-10   SEM images of poly(ethylene-co-octene) (a, b and c) and propylene (d, e and f) and 1-hexene (g, h and i) pre-polymerized poly(ethylene-co-octene) particles, Table 6-3.

The effect of pre-polymerization on the ethylene/1-octene based copolymers appear to be less pronounced. This could be explained by the lower incorporation (mol %) of 1-octene.

6.4 CONCLUSIONS

In this Chapter, it has been shown that a simple pre-polymerization technique could be employed to enhance both catalyst activity and improve polymer morphology, through promotion of particle fragmentation. This was true for pre-polymerization with propylene as well as ethylene/1-hexene.

The analysis of propylene pre-polymerized polymer particles showed that little of the original polyethylene characteristics were compromised. This technique, if employed in copolymerization systems, appears to narrow the CCD of 1-hexene, as well as 1-octene ethylene copolymers. Evidence was thus given to suggest that the drawbacks of the *filter effect* were overcome by pre-polymerization, in particular with propylene.

6.5 REFERENCES

1. Tait, P.J.T.; Downs, G.W.; Akimbami, A.A. In *Transition Metal Catalysed Polymerizations, Ziegler-Natta and Metathesis Polymerizations*; Quirk, R.P.; Hoff, R.E.; Klingensmith, G.B.; Tait, P.J.T.; Goodall, P.L., Eds.; Cambridge University Press: Cambridge, **1988**, p 835.

2. Tait, P.J.T.; Berry, I.G.; Soga, K.; Terano, M., Eds.; Elsevier-Kodansha: Tokyo, **1994**, p 55.

3. Tsutsui, T.; Kashiwa, N. *Polym. Commun.* **1988**, *29*, 180.

4. Uozumi, T.; Soga, K. *Makromol. Chem.* **1992**, *193*, 823.

5. Koivomäki, J.; Seppälä, J.V. *Macromolecules* **1993**, *26*, 5535.

6. Koivomäki, J.; Fink, G.; Seppälä, J.V. *Macromolecules* **1994**, *27*, 6254.

7. Karol, F.J.; Kao, S.-C.; Wasserman, E.P.; Brady, R.C. *New J. Chem.* **1997**, *21*, 797.

8. Tait, P.J.T.; Awudza, J.A.M.; Sano, T.; Uozumi, T.; Nakatani, H.; Terano, M., Eds.; Technology and Education Publishers: Tokyo, **2000**, p 214.

9. Chien, J.C.W.; Nozaki, T. *J. Polym. Sci., Polym. Chem. Ed.* **1993**, *31*, 227.

10. Zambelli, A.; Longo, P.; Ammendola, P.; Grassi, A. *Chim. Ital.* **1986**, *116*, 731.

11. Zambelli, A.; Grassi, A.; Galimberti, M.; Mazzocchi, R.; Piemontesi, F. *Macromol. Chem., Rapid Commun.* **1991**, *12*, 523.

12. Herfert, N.; Fink, G. *Prep. Mat. Sci. Eng.* **1992**, *67*, 31.

13. Rossi, A.; Zhang, J.; Odian, G. *Macromolecules* **1996**, *29*, 2331.

14. Arnold, M.; Henschke, O.; Knorr, J. *Macromol. Chem. Phys.* **1996**, *197*, 363.

15. Chien, J.C.W.; He, D. *J. Polym. Sci., Part A: Polym. Chem.* **1991**, *29*, 1585.

16. Wu, Q.; Wang, H.; Lin, S. *Makromol. Chem., Rapid Commun.* **1992**, *13*, 357.

17. Zakharov, V.A.; Bukatov, G.D.; Barabanov, A.A. *Macromol. Symp.* **2004**, *213*, 19.

18. Smit, M.; Zheng, X.; Loos, J.; Chadwick, J.C.; Koning, C.E. *J. Polym. Sci., Part A: Polym. Chem.* **2005**, *43*, 2734.

19. Smit, M.; Zheng, X.; Brüll, R.; Loos, J.; Chadwick, J.C.; Koning, C.E. *J. Polym. Sci., Part A: Polym. Chem.* **2005**, Manuscript in preparation.

20. Tait, P.J.T.; Awudza, J.A.M. *Macromol. Symp.*, 414.

21. Przybyla, C.; Tesche, B.; Fink, G. *Macromol. Rapid. Commun.* **1999**, *20*, 328.

22. Soares, J.; Shan, C. Proceedings of ANTEC, Dallas, Texas, **2001**, pp 1835.

CHAPTER 7

MAO-activated Single-center catalysts in Perspective[*]

SYNOPSIS: *This dissertation entailed an extensive study of methylaluminoxane (MAO) activated single-center catalysts immobilized on silica for olefin polymerization. The uniqueness of single-center catalyst systems and the endless possibilities surrounding them has captured the imagination of various research groups. Depending on the specialty of the various groups, new alternative cocatalysts and supports, such as clay, polymers and oxides, were developed for these catalysts. It would thus be appropriate to conclude this dissertation with a comparative study entailing an alternative support and activator.*

In this Chapter, we consider the tethering of a borate activator on triethylaluminum (TEA)-treated support materials (silica and a spherical $MgCl_2/EtOH$ adduct) for the polymerization of ethylene and propylene, respectively. Although we observed good catalyst activity with the spherical $MgCl_2/EtOH$ adduct systems, reproducibility of the catalyst immobilization appears to be a drawback.

7.1. *Introduction*

Highly active single-center catalyst systems for the polymerization of ∝-olefins are obtained through activation with either methylaluminoxane (MAO) or perfluorylborate (FAB) activators as cocatalysts[1-3]. The latter are better defined systems, compared to MAO of which, despite various efforts, the exact structure still remains a mystery after 20 years[4].

Successful activation of Group IV metal catalysts by borates was independently achieved for the first time by Marks[5,6] and Ewen[7,8] in the early 1990s. The major advantages of these systems are the fact that merely one or two equivalents of these activators are required[9] and they are not pyrophoric. Most of these materials do, however, require modification to be able to be used with heterogenized single-center catalyst systems. Chemical tethering of a cocatalyst to the surface of the desired support is a way to prevent leaching of the activated species into solution. Additionally, one can use this opportunity to introduce a spacer molecule in order to elevate the activated catalyst from the polar silica surface, preventing deactivation of the activated species. The drawback of this method is that tedious, organometallic synthesis on the support surface is often required[10] and side products produced during synthesis need to be removed in such a way as not to disturb the newly designed surface.

Pacification of the polar support surface with an alkylaluminum, before introduction of the borate anion (with a chemical handle) seems to eliminate the above-mentioned drawbacks[11]. Modification of the surface with silane groups to allow for the immobilization of OH-containing borate species has also shown to be an effective alternative[12]. Direct immobilization of the borate (such as on the support surface) often leads to low activity polymerization systems due to the presence of residual polar surface groups[13,14].

The discovery of well-defined fluoroaryl-based activators for single-center systems that could compete with industrial setups[15-18], proved to be a promising alternative for MAO. Jacobsen *et al*[11] recently reported the tethering of triethylammonium tris(pentafluorophenyl)(4-hydroxyphenyl)borate [HNEt$_3$][B(C$_6$F$_5$)$_3$(C$_6$H$_4$OH)] on various

triethylaluminum (TEA)-modified support materials. It must be noted, however, that borate activators are also expensive and result in an activated catalyst species that is very susceptible to poisoning by impurities present in the environment. Caution should thus be taken in the application of such systems.

Our group[19] recently reported on the potential of spherical supports comprising $MgCl_2/AlR_n(OEt)_{3-n}$ as a new approach to the immobilization of single-center catalysts. It was found that a range of titanium-based single-center catalysts could be easily and effectively immobilized and activated, without the use of MAO or a borate activator, but lower activities were obtained with zirconocenes. With the objective of developing a $MgCl_2$-based system for use with zirconocenes, the tethering of $[HNEt_3][B(C_6F_5)_3(C_6H_4OH)]$ on a spherical $MgCl_2/AlR_n(OEt)_{3-n}$ support was investigated in the present work and compared to results obtained using the same borate tethered to a $AlEt_3$-pretreated silica support.

7.2.   Experimental

7.2.1. Materials

All manipulations were performed under an argon atmosphere using glove box (Braun MB-150 GI or LM-130) and Schlenk techniques. Solvents were distilled from Na (toluene) or Na/benzophenone (heptane) and freeze-thaw degassed twice before use. *rac*-Ethylenebis(indenyl)zirconium dichloride $[Et(Ind)_2ZrCl_2]$ was prepared following a published procedure[20].

$AlEt_3$ (25 wt % solution in toluene) and $AliBu_3$ (1M solution in hexane) were purchased from Aldrich and Fluka, respectively. Ethylene (3.5 grade supplied by Air Liquide) and propylene (3.5 grade supplied by Hoek Loos) were purified by passing over columns of BASF RS3-11 supported Cu oxygen scavenger and 4Å molecular sieves.

7.2.2. Preparation of $[HNEt_3][B(C_6F_3)_3(C_6H_4-4-OH)]$

This compound was synthesized as suggested by literature procedures[11,21].

7.2.3. Preparation of triethylaluminum-modified MgCl$_2$ support materials

A 25 wt % solution of triethylaluminum in toluene was slowly added to 10 g of a spherical adduct of magnesium chloride and ethanol (MgCl$_2$·2.1EtOH), slurried in heptane and cooled to 0 ºC. The reaction was carried out in a standard Schlenk vessel equipped with a pressure release valve. After 2 days at ambient temperature, with occasional agitation, the solid support was isolated by filtration, washed with heptane and petroleum ether and then dried under a flow of argon and subsequently in vacuum.

7.2.4. Preparation of triethylaluminum-modified SiO$_2$ support materials

A reference AlEt$_3$-pretreated silica support was prepared by gradual addition (5-10 min.) of 6 mL of 25 wt.-% AlEt$_3$ in toluene to a slurry of 2 g Sylopol 948 silica (Grace GmbH), precalcined at 600 °C for 3 h, in 20 mL heptane cooled to 0 °C, again in a standard Schlenk vessel equipped with a pressure release valve. The slurry was agitated for a further 4 h and then filtered, washed with 4 × 10 mL heptane and dried in vacuum.

7.2.5. Preparation of [HNEt$_3$][B(C$_6$F$_3$)$_3$(C$_6$H$_4$-4-OH)]-modified support materials.

0.070 g of [HNEt$_3$][B(C$_6$F$_3$)$_3$(C$_6$H$_4$-4-OH)] was slurried in 7 mL of toluene and heated to 85 ºC to effect dissolution. 1 g of support (MgCl$_2$/AlEt$_n$OEt)$_{3-n}$ or AlEt$_3$-pretreated SiO$_2$, prepared as above, was slurried in toluene and heated to 75 ºC. The hot borate solution was then transferred to the slurry. The latter was left for 35 minutes at 75 ºC. The slurry was left to cool under argon and then placed in a shaker for 2.5 hours. A free-flowing powder was obtained after drying under 22 mbar vacuum.

7.2.6. Polymerization

Polymerizations were carried out in a 200 mL Büchi reactor equipped with a hollow-shaft turbine stirrer. 100 mg of the borate-treated support was charged to the reactor, followed by a catalyst solution containing 2.4 μmol *rac*-[Et(Ind)$_2$ZrCl$_2$] and obtained by addition of 1 mL of a 28 wt % solution of tri*iso*butylaluminum in hexane to a solution of 2 mg of *rac*-[Et(Ind)$_2$ZrCl$_2$] in 4 mL toluene and ageing for 75 min. This corresponded to a B/Zr mol ratio of 4. The support/catalyst mixture was allowed to stand for 60 min, after which 100 mL heptane, containing 1 mL of a 28 wt % solution of tri*iso*butylaluminum in

hexane, was added under an atmosphere of monomer. The reactor was heated to 50 °C and pressurized with 0.5 bar of monomer for 15 minutes before raising the pressure to 4 bar and polymerizing at a constant pressure of 4 bar for 1 h. The polymerization was terminated by degassing the reactor, followed by the addition of acidic methanol. The polymer was separated and dried at 50 ºC in a vacuum oven.

7.2.7. Characterization techniques

A Hewlett Packard (HP-5890) gas chromatograph, equipped with an AT-Wax capillary column (30 m x 0.53 m x 10 µm), was used for the determination, as ethanol, of the ethoxide content of the $MgCl_2/AlEt_nOEt)_{3-n}$ support, after dissolving the support in butanol containing a propanol as internal standard. The response factors (RF) of ethanol and propanol were determined using a separately prepared solution in butanol. The OEt content of the support is given by the following equation:

$$Alc(w\%) = \frac{RF_{alc} x A_{alc} x W_{Pr-OH} x 100}{A_{Pr-OH} x W_{carrier}}$$

Equation 1

|	
$W_{carrier}=$	Weight of support sample
$A_{Pr-OH} =$	Area under propanol peak
$W_{Pr-OH}=$	Weight of propanol in internal standard solution
$A_{alc} =$	Area under the alcohol peak
$RF_{alc} =$	Response factor

7.3.   Results and Discussion

It has been suggested[22] that the silica hydroxyl groups react in the following (Scheme 7-1) way with TEA and $[HNEt_3][B(C_6F_5)_3(C_6H_4\text{-}4\text{-}OH)]$, respectively:
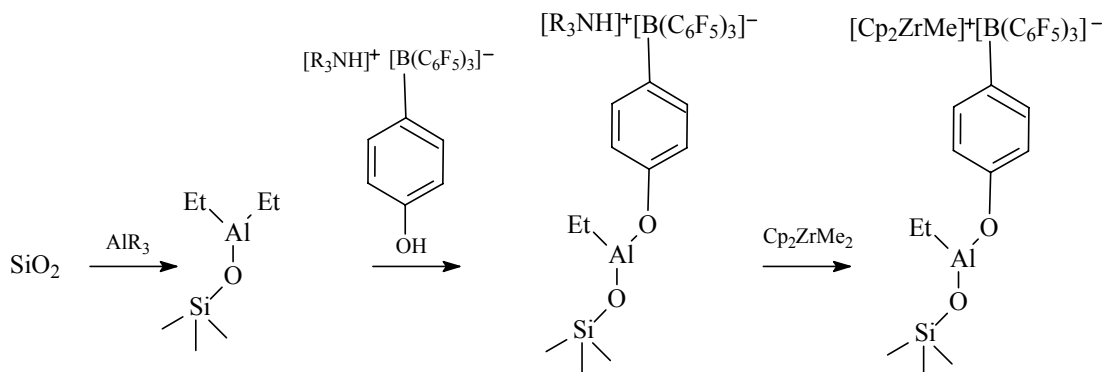
Scheme 7-1: Modification of MgCl$_2$ ethanol adduct with TEA and [HNEt$_3$][B(C$_6$F$_5$)$_3$(C$_6$H$_4$OH)].

The question does arise as to which base (the –NH species or –OH from the borate) would react in preference with the TEA-modified surface. The exact characterization of this system is currently being carried out by our colleagues at the Rijksuniversiteit Groningen (The Netherlands) under the guidance of Prof. B. Hessen. We propose a similar reaction scheme for the modification of the spherical MgCl$_2$/AlR$_n$(OEt)$_{3-n}$. (This support system has not been covered by the work of Jacobson *et al*[21].)
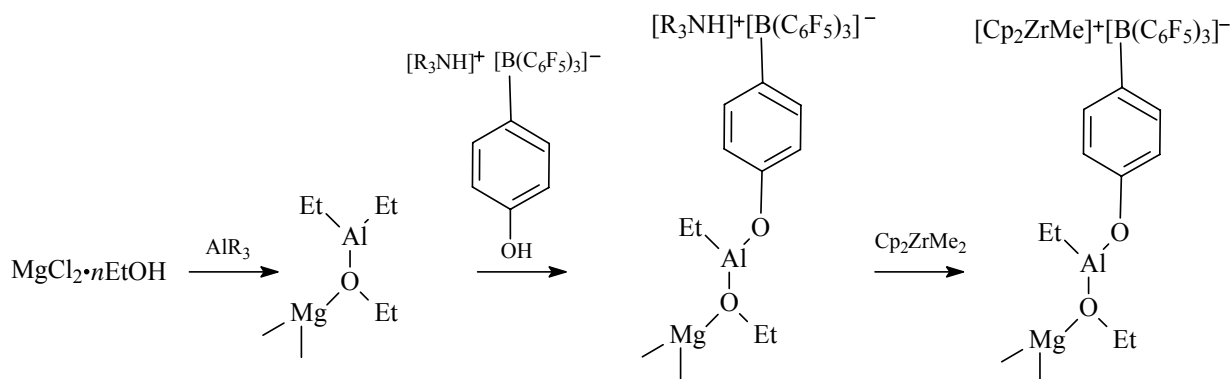
Scheme 7-2: Modification of MgCl$_2$ ethanol adduct with TEA and [HNEt$_3$][B(C$_6$F$_5$)$_3$(C$_6$H$_4$OH)].

The characteristics of the modified supports in their various stages of modification are listed in Table 7-1. It appears that the MgCl$_2$/AlR$_n$(OEt)$_{3-n}$ system has a higher surface area than the silica support; this is also supported by the greater amount of aluminum immobilized on the support.

Table 7-1:   Analysis of modified $MgCl_2$- and SiO_2 support materials.

Sample	System	Surface area[a] (m^2/g)	AES-ICP	
			Al, wt %	B, wt %
M1	$MgCl_2/Et_nAl(OEt)_{3-n}$	373	5.2	-
M2	$MgCl_2/TEA/B$	n.d.[b]	3.5	0.01
S1	SiO_2/TEA	211	3.6	-
S2	$SiO_2/TEA/B$	n.d.	2.7	0.04

[a]Determined with BET analysis
[b]not determined

The borate content on the support materials falls in the lowest detection range of the particular method for elemental analysis and should therefore not be regarded as that significant.   The residual ethoxide content on the magnesium dichloride/ethanol adduct was determined with gas chromatography and found to be 6.2 wt %. From the amount of aluminum that was immobilized and the ethoxide content of the $MgCl_2$-based support, it is possible to calculate the composition of the complex to be $MgCl_2 \cdot 0.24AlEt_{2.3}(OEt)_{0.7}$.   The surface hydroxyl content of the silica was determined via silylation (see Section 2.3.4.), followed by elemental analysis, and found to be 1.4 mmol/g of silica.

EDX images (Figure 7-1) indicate the effectiveness of the preparation method in terms of the homogeneity of the aluminum distribution throughout the support material.

a)   b)
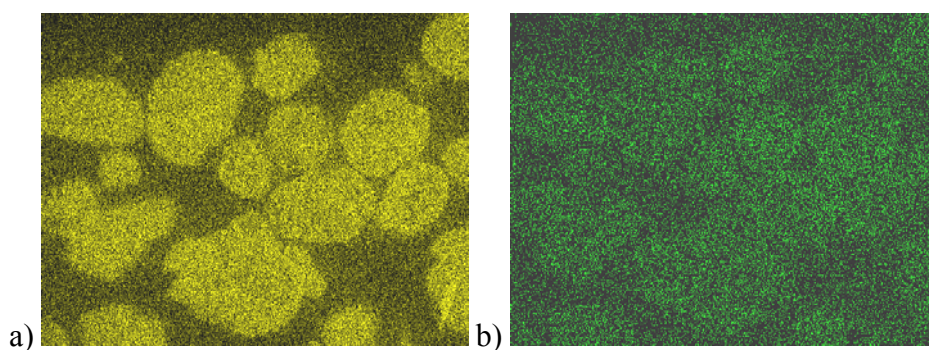
Figure 7-1:   EDX element mapping for TEA-modified silica ((a) silicon distribution and (b) aluminum distribution).

From Figure 7-1 it is apparent that homogeneous immobilization of TEA was obtained across the silica particles. It was, however, not possible to obtain EDX element mapping

for the $MgCl_2 \cdot 0.24AlEt_{2.3}(OEt)_{0.7}$ species, as they interacted with the epoxy resin used in the sample preparation for this type of analysis. Also, the detection level for borate is not so high and it is thus not possible to detect the homogeneity of the cocatalyst distribution over the support particles.

The results of ethylene and propylene polymerizations in a *n*-heptane slurry, using the borate-treated supports in combination with *rac*-[Et(Ind)$_2$ZrCl$_2$] and tri*iso*butylaluminum, are given in Table 7-2. It is apparent that, with both ethylene and propylene, significantly higher polymerization activities were obtained with the magnesium chloride-based support material compared to that of silica. This support also appears to perform better (with an activity of 3900 kg polymer/((mol cat)(hour))) in ethylene polymerization compared to the homogeneous analogue (with an activity of 1000 kg polymer/((mol cat)(hour))). For propylene polymerization, however, both support materials performed quite poorly with regard to the activity of the system when compared to the homogeneous reaction. An explanation for the higher activity observed with the magnesium chloride-based support will be proposed later on morphology analysis and consideration of the surface characteristics of the support material.

For both polyethylene and polypropylene, narrower molecular weight distributions were observed, compared to the respective homogeneous systems. Single-center behavior was retained with the PP materials. The broad molecular weight distributions observed for PE could be explained by hand of the *diffusion limitation* (as discussed in Chapter 5). Interesting to note is the fact that this phenomenon appears to have a larger influence on the silica-based materials. The melting temperatures for the polypropylenes and polyethylenes are, respectively, of the same magnitude for both support materials.

Somewhat lower molecular weights (compared to the silica systems) are apparent for the polymers obtained using the $MgCl_2/AlR_n(OEt)_{3-n}$ support. This could result from more chain transfer to aluminum in this system. As seen from the BET data, $MgCl_2 \cdot 0.24AlEt_{2.3}(OEt)_{0.7}$ seems to be more porous than the silica support material, which could result in easier diffusion of the triisobutylaluminum (used as scavenger) to the active catalyst centers in this support material.

Table 7-2: Polyolefins synthesized with $[HNEt_3][B(C_6F_5)_3(C_6H_4OH)]$ as cocatalyst.

Support	Monomer	Activity[b]	mmmm (%)	Mw (g/mol)	Mw/Mn	T_m (°C)
none	Ethylene	1 000	-	471 900	5.0	136
M2	Ethylene	3950	-	193 000	2.9	133
S2	Ethylene	220	-	277 000	3.6	133
none	Propylene	12 800	67	19 500	2.1	124
M2	Propylene	400	77	45 000	1.7	139
S2	Propylene	160	88	57 000	1.8	140

[a]Reactor/ reaction details
[b]Activity is expressed in terms of kg polymer/((mol cat)(hour))

The higher melting temperatures and isospecificity, that is also observed here for the supported catalyst systems in propylene polymerization, have been discussed in Chapter 3.

All polymers consisted of free-flowing particles and no reactor fouling was observed. SEM imaging of the polyethylenes (Figure 7-2 and 7-3), obtained with the two support systems, provides a microscopical comparison of the particle morphology. The polyethylene particles for the silica-based system, viewed in Figure 7-2, are in the range of 100-200 μm in size. Various small fragments seem to be embedded in a stretched polymer matrix, indicating the expansion and partial fragmentation of this particular support. SEM imaging of the polyethylenes produced by the $MgCl_2 \cdot 0.24AlEt_{2.3}(OEt)_{0.7}$-based system is illustrated in Figure 7-3. The polyethylene particles observed for the $MgCl_2 \cdot 0.24AlEt_{2.3}(OEt)_{0.7}$-based systems appear to be much larger in size (200-600 μm) than those observed for the silica-based system. Quite interesting particle morphology is observed at higher magnifications (1000): embedded subparticles of 5-10 μm in stretched polymer on a "torn" matrix.
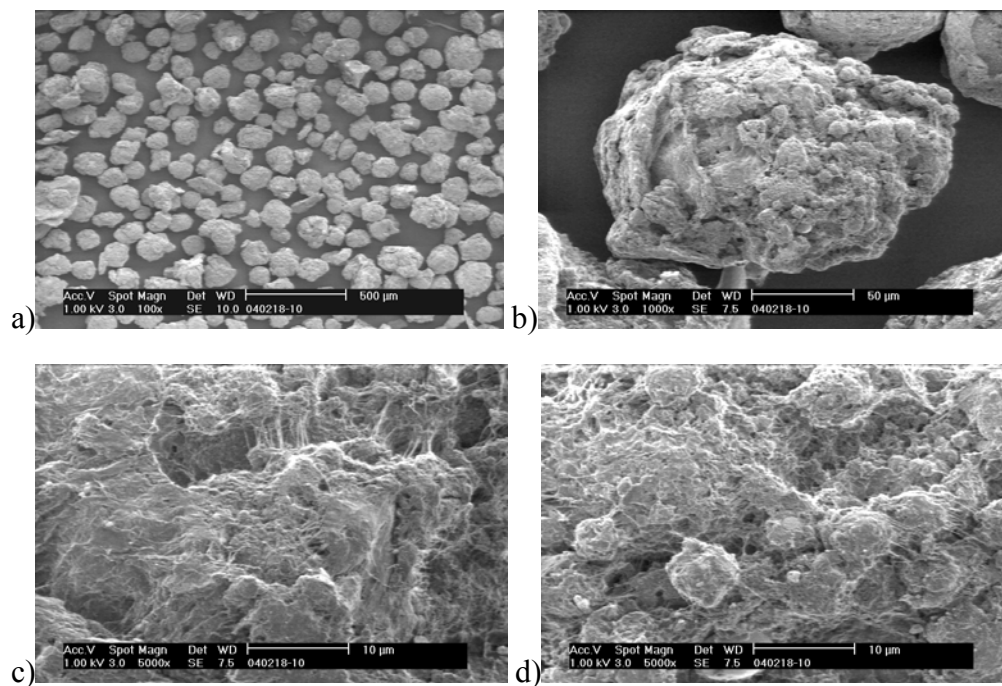
Figure 7-2:   SEM imaging of polyethylene produced by the silica-borate system (S2 in Table 7-1) at a 200 magnification (a), 1000 magnification (b) and 5000 magnification ((c) and (d)).

The influence of a diffusion limitation for the monomer through the crystalline polymer matrix, leading to fibril formation, was observed for both systems ($MgCl_2 \cdot 0.24AlEt_{2.3}(OEt)_{0.7}$ and SiO_2-based).

Further insight into the internal morphologies of the two systems is given by cross-section SEM imaging (Figure 7-4). Cross-section analysis revealed a difference in internal particle morphology between the silica and magnesium dichloride produced polyethylenes. More compact, fully fragmented polymer particles were observed in the case of the latter. The polyethylene particles produced using the silica support show incomplete fragmentation, as the silica core is easily identified in these images. The big difference in activities observed for these two systems is most probably related to the difference in morphology observed.
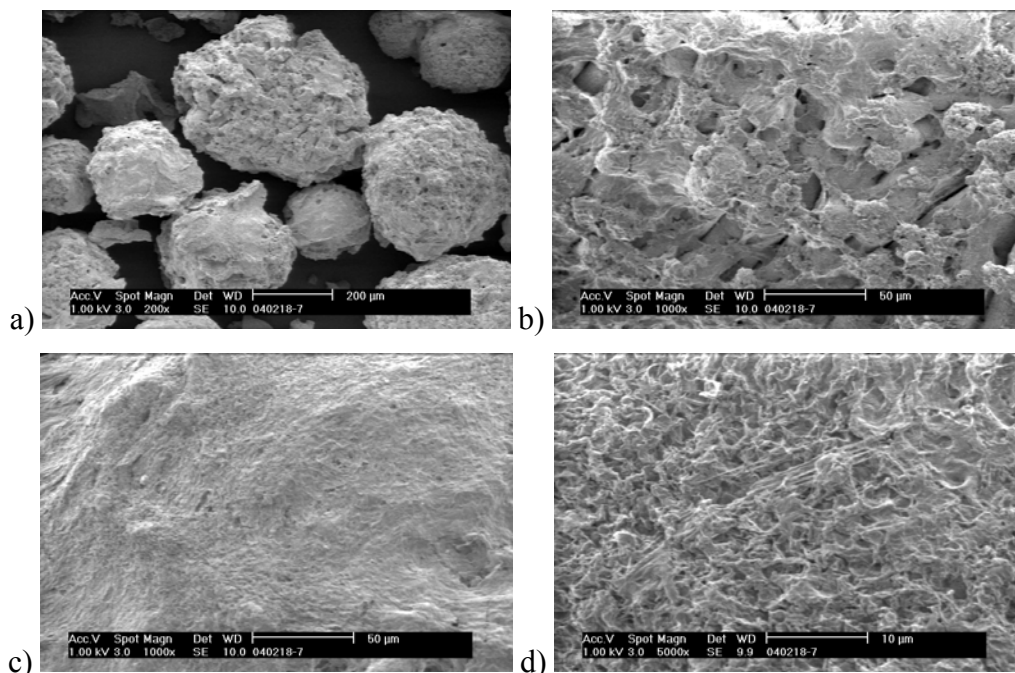
Figure 7-3:   SEM imaging of polyethylene produced by the magnesium dichloride-borate system (M2 in Table 7-1) at a 200 magnification (a), 1000 magnification ((b) and (c)) and 5000 magnification (d).
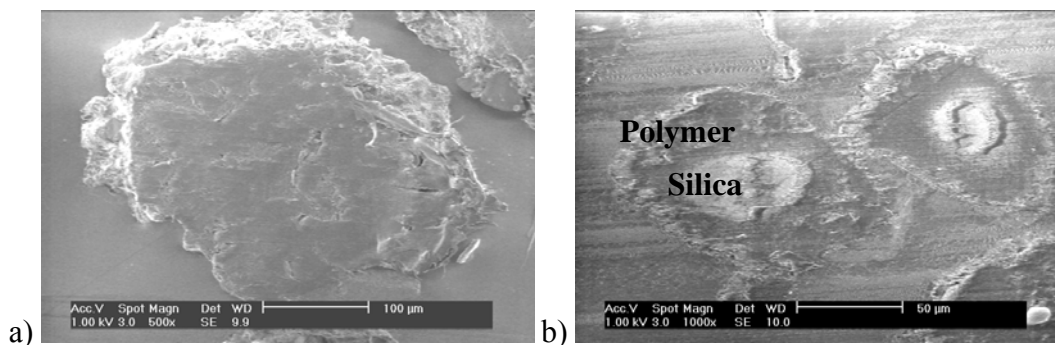

Figure 7-4:   Cross-section images of polyethylene obtained with a) the magnesium dichloride-borate system and b) the silica-borate system

In the case of polypropylene, distinct differences between the polymer particles produced by the two support materials are apparent (Figure 7-5).
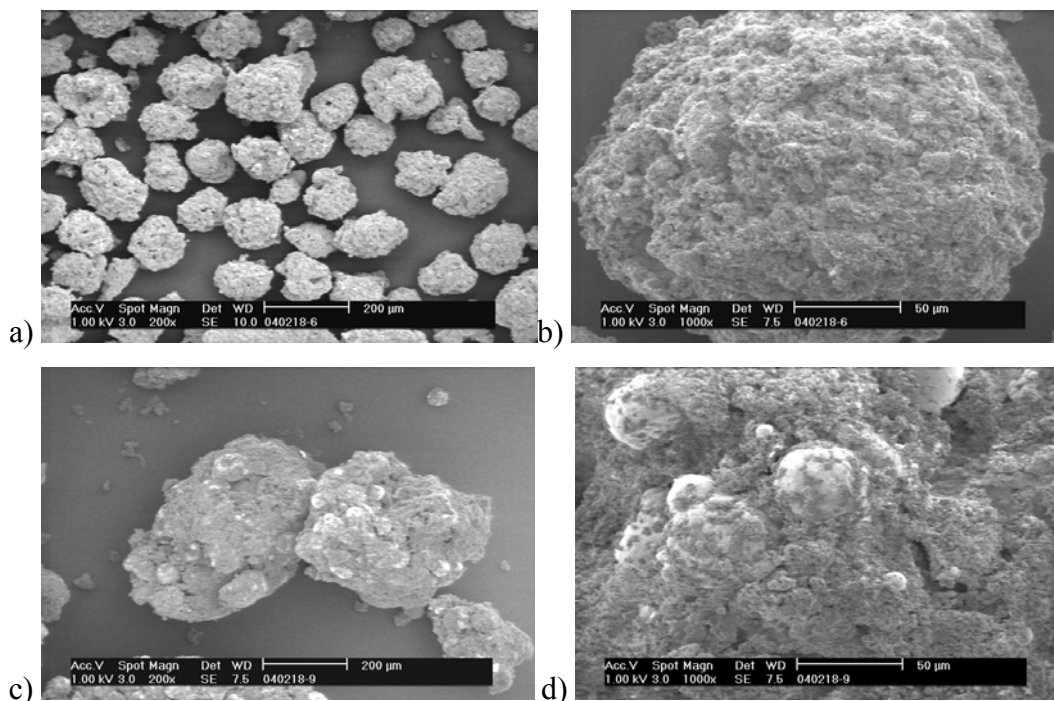
Figure 7-5   SEM imaging of polypropylene produced by the magnesium dichloride-borate system ((a) 200 magnification and (b) 1000 magnification) and silica-borate system ((c) 200 magnification and (d) 1000 magnification)

The silica system resulted in big polymer clusters (200-700 μm) with smooth particles (5-10 μm) embedded in them. Elemental EDX imaging showed that these smooth, white spheres embedded in the particle surface contained aluminum rather than carbon or silicon, indicating that they arose from hydrolysis of the Al*i*Bu$_3$ scavenger during quenching of the polymerization. In Figure 7-5 (c), some loss of morphology due to particle agglomeration is evident in the polypropylene prepared using the SiO$_2$ support. Better, although not optimal, replication of the morphology of the starting support was apparent using MgCl$_2$/AlR$_n$(OEt)$_{3-n}$, Figure 7-5 (a and b) demonstrating the formation of individual polymer particles of 100-200 μm in size. It should be mentioned that difficulties were encountered in the reproducibility of good particle morphology with the borate/metallocene systems.

7.4.   Conclusions

The tethering of $[HNEt_3][B(C_6F_5)_3(C_6H_4OH)]$ on silica and magnesium chloride support materials pretreated with aluminum alkyls seems to be quite effective with regard to the retention of single-center behavior of the catalyst species. Polymer fragmentation was observed for both support materials, although incomplete in the case of ethylene polymerization with the silica catalyst system. This work also shows that the $MgCl_2 \cdot 0.24AlEt_{2.3}(OEt)_{0.7}$ support, obtained by reaction of $AlEt_3$ with a magnesium dichloride/ethanol adduct, seems to be a much better support material (with reference to catalyst activity) than the $AlEt_3$-pretreated Sylopol 948 silica support calcined at 600 °C.

It must be noted, however, that comparable activities were obtained with the silica/MAO systems (Chapter 4) and polymer particles of better polymer morphology were shown (Chapter 6). Additionally, $[HNEt_3][B(C_6F_5)_3(C_6H_4OH)]$ is quite difficult to prepare and isolate as a dry powder. The compound is quite poorly soluble and these systems are very difficult to reproduce. Keeping this in mind, we propose that the silica/MAO systems (as introduced in this dissertation) seem to be more feasible for zirconocenes catalyzed olefin polymerization on a large scale.

7.5.   References

1. Marks, T. *Accounts Chem. Res.* **1992**, *25*, 57.
2. Kaminsky, W. *Macromol. Chem. Phys.* **1996**, *197*, 3907.
3. Chen, E. Y.-X.; Marks, T. *Chem. Rev.* **2000**, *100*, 1391.
4. Reddy, S. S.; Sivaram, S. *Program. Polym. Sci.* **1995**, *20*, 309.
5. Yang, X.; Stern, C.; Marks, T. *J. Am. Chem. Soc.* **1994**, *116*, 10015.
6. Yang, X.; Stern, C.; Marks, T. *J. Am. Chem. Soc.* **1991**, *113*, 3623.
7. Ewen, J., **1996**, p Eur. Patent Appl. 0427697.
8. Ewen, J.; Elder, M., **1996**, p U.S.5561092.
9. Hlatky, G.; Turner, H.; Eckmann, R. *J. Am. Chem. Soc.* **1989**, *111*, 2728.
10. Turner, H.; Exxon, **1995**, p U.S.5427991.
11. Jacobsen, G.; Wilkens, P.; Jastrzetsk, J.; Van Koten, G.; The Dow Chemical Company, **1998**, p US5834393.
12. Carnahan, E.; Carney, M.; Neithamer, D.; Nickias, P.; Shih, K.-Y.; Spencer, L.; WR Grace & Co, The Dow Chemical Company, **1997**, p WO9719959.

13. Walzer, J. J.; Exxon Chemicals Patent Inc: USA, p WO9604319.

14. Ward, D.; Carnahan, E.; WR Grace & Co, **1996**.

15. Turner, H. W.; Hlatky, G. G.; Eckman, R. R.: U.S. 5,198,401, **1993.**

16. Ewen, J. A.; Elder, M. J.: U.S. 5,387,568, **1995**.

17. Yang, X.; Stern, C. L.; Marks, T. J. J. Am. Chem. Soc. **1991**, *113*, 3623.

18. Ewen, J. A.; Elder, M. J.: U.S.5561092, **1996**.

19. Severn, J.; Chadwick, J. *Macromol. Rapid. Commun.* **2004**, *25*, 1024.

20. Wild, F.; Zsolnai, L.; Huttner, H.; Brintzinger, H. *J. Organometal. Chem.* **1982**, *232*, 233.

21. Jacobsen, G.; Dow Chemical Company, **2001**, p US 6271165.

22 Jacobsen, G.; Wijkens, P.; Jastrzebski, J.; Van Koten, G.; Dow Chemical Company: U.S.5834393, **1996**.

Epilogue

and

Technology Assessment

In the last decades, major advances in metallocene chemistry have been made. The development of new catalysts and heterogeneous metallocene systems for industrial application appears to be the driving force for the immense growth currently in this field.

The goals of this research have been achieved by introducing various ways of enhancing heterogeneous catalytic activity and generating further insight into these systems. The loss of catalyst activity through heterogenization of the metallocene/MAO species on a support material appears to be a major hurdle in the implementation of these systems in industry. This work not only addressed plausible reasons for this observation, but also provided 3 simple techniques to obtain high activity catalyst systems for olefin polymerization. Through successful heterogenization of the metallocene/MAO catalyst systems, the drawbacks of the homogeneous systems (i.e. large quantities expensive MAO required; reactor fouling) are overcome, while retaining high catalyst activity.

In this dissertation, we have established that a thorough analysis of the support material, the catalyst and the cocatalyst (being responsible for the activation of the catalyst precursor) is vital in order to understand and control heterogeneous metallocene catalyst systems for olefin polymerization. We have demonstrated that high activity systems can be obtained, under moderate polymerization conditions with a moderately active catalyst (rac-Et(Ind)$_2$ZrCl$_2$), through the manipulation of the method of catalyst immobilization on

the support material. Additionally, the presence of small amounts of higher α-olefins in an ethylene polymerization system, as well as the use of simple pre-polymerization techniques, could enhance catalyst activity significantly. It has been shown that propylene pre-polymerization not only greatly enhances ethylene homo- and copolymerization activities, but also increases comonomer incorporation in ethylene/1-hexene copolymerization.

The role of MAO and the presence of alkylaluminums in the heterogenized systems have also been addressed. It is proposed that the presence of alkylaluminums plays quite a significant role in the protection of the activated catalyst species against the polar silica surface, thus facilitating a maximum amount of activated catalyst species present for monomer insertion and polymerization. Additionally, less chain transfer to aluminum promotes the synthesis of high molecular weight materials. Modification of the silica surface with trace amounts of trialkylaluminum before metallocene/MAO heterogenization has proven to give much more robust systems that even show catalyst activity without the presence of an additional scavenger in the polymerization setup.

Although much has already been accomplished in this field, a great deal still remains to be done. One of the challenges is the development of simple techniques for the successful, detailed analysis of the chemistry on the silica surface and the distribution of the metal complex throughout the entire silica support particle, after heterogenization of metallocene/MAO catalyst systems. A better understanding will allow for better control, making these systems much more appealing for industrial application.

S u m m a r y

The aim of this dissertation is to broaden the current understanding of the heterogenization of methylaluminoxane (MAO)-activated metallocene catalysts for olefin polymerization.

Firstly, propylene polymerization was studied under mild conditions in order to determine the effect of silica, the amount of surface hydroxyl groups and the method of immobilization of MAO and/or the MAO-activated catalyst species on support characteristics and the resulting polymer properties. Effective, reproducible catalyst systems were obtained after contact of the MAO-activated catalyst species with silica under *wet sand* conditions. Additionally, we have learned that free $AlMe_3$ present in MAO, while undesired in homogeneous systems, appears to be essential in supported catalyst systems. It facilitates the protection of the activated catalyst species from the polar surface groups. Higher molecular weight polymers are obtained with these catalyst systems due to less chain transfer to aluminum. Furthermore, a more robust support, requiring no additional scavenger during ethylene polymerization, was obtained with MAO-activated catalyst immobilized on $AlEt_3$-impregnated silica.

Studies regarding the so-called *filter-* and *comonomer effect,* observed especially in ethylene/1-hexene copolymerizations, included SEM imaging and characterization of polymers obtained at various polymerization intervals. Novel, simple pre-polymerization techniques were developed to give further insight into particle growth during polymerization.

In this work, it was shown that thorough characterization of silica is vital in order to interpret the performance of MAO-activated metallocene species in terms of polymer

properties and catalyst activity. High activity, reproducible heterogenized catalyst species producing polymers with typical single-center characteristics (i.e. narrow molecular weight distribution) can effectively be obtained with a non-perfect support such as silica. Additional "complications" influencing the properties of polymers produced by these heterogenized active catalyst systems (ie a diffusion limitation observed in ethylene homopolymers; the filter effect observed in ethylene copolymers) can thus be minimized with the above-mentioned techniques.

The preparation and use of an immobilized borate activator for single-center catalysts, making use of both SiO_2- and $MgCl_2$-based supports, was carried out to compare our work to current innovations and alternative support materials.

Samenvatting

Het doel van deze dissertatie is om het inzicht te verbreden met betrekking tot het immobiliseren van methylaluminoxaan (MAO)-geactiveerde metalloceen katalysatoren voor olefine polymerisatie.

In eerste instantie, is de polymerisatie van propeen onder milde condities bestudeerd, met als doel de bepaling van het effect van de gebruikte silica, de hoeveelheid hydroxyl groepen aan het silica-oppervlak en de methode van immobiliseren, op samenstelling en gedrag van het verkregen systeem en op de resulterende polymeer eigenschappen. Effectieve en reproduceerbare systemen werden verkregen na contact van MAO-geactiveerde katalysator met silica onder *nat zand* condities. Het is ook gebleken dat vrij AlMe$_3$ in MAO, alhoewel niet wenselijk in homogene systemen, essentieel lijkt te zijn in gedragen systemen. Vrij AlMe$_3$ faciliteert de bescherming van de actieve katalysator tegen polaire groepen aan het oppervlak van de drager. Deze systemen geven ook polymeren met hogere moleculaire gewichten, vanwege het minder frequent optreden van ketenoverdracht naar aluminium. Bovendien werd, door middel van immobilisering van MAO-geactiveerde katalysator op een met AlEt$_3$ behandelde silica, een robuust systeem ontwikkeld dat geen verdere scavenger nodig had in etheen polymerisatie.

Studies met betrekking tot de zogenoemde *filter* en *comonomeer effecten*, vooral gezien in etheen/1-hexeen copolymerisaties, omvatten o.a. SEM imaging en karakterisering van polymeren verkregen na verschillende polymerisatie intervallen. Nieuwe en eenvoudige prepolymerisatie technieken zijn ontwikkeld om verder inzicht te geven in de groei van polymeer deeltjes tijdens polymerisatie.

Uit dit werk blijkt dat grondige karakterisering van silica essentieel is om de performance van MAO-geactiveerde metallocenen te interpreteren, in termen van polymeer eigenschappen en katalysator activiteit. Reproduceerbare geheterogeniseerde katalysatoren met een hoge activiteit, die single-site eigenschappen vertonen en die polymeren met smalle molecuulmassa verdelingen geven, kunnen verkregen worden met een minder perfecte drager zoals silica. Verdere "complicaties", die invloed hebben op de eigenschappen van polymeren die geproduceerd zijn met deze geheterogeniseerde systemen (d.w.z. diffusielimitering in etheen homopolymerisatie; het filter effect gezien in etheen copolymerisatie), kunnen dus geminimaliseerd worden met de bovengenoemde technieken.

De bereiding en het gebruik van een geïmmobiliseerde boraat activator voor single-site katalysatoren, met zowel SiO_2- als $MgCl_2$-gebaseerde dragers, werd ook bestudeerd om een vergelijking te kunnen maken van ons werk met huidige innovaties en alternatieve dragermaterialen.

Acknowledgements

I would like to start by thanking John Chadwick for offering me this PhD opportunity in his research group. John, your guidance, support and patience in the three years that I spend on this project, is highly appreciated.

My sincere gratitude also goes to Cor Koning for welcoming me into the SPC group. I found your objective opinion on my work quite valuable.

This project would not be possible without funding from the Dutch Polymer Institute (DPI) and fruitful discussions with the members from the internal reference committee, representing the various companies involved. Thank you.

The opportunity to do my PhD degree in Europe was made possible by two people: Albert van Reenen (my coach in Stellenbosch, South Africa) and Vincent Mathot (from DSM, Geleen). I will always be in your debt.

Collaborations with various people and groups were crucial in the completion of my work. I would therefore like to thank various people: Otto van Asselen (for help with the inert FTIR setup), Ton Sommon (for help on the optimization of surface measurements (BET)), Joachim Loos (for the initial SEM imaging), Robert Brüll (for CRYSTAF/ HT GPC analysis at the DKI in Darmstadt, Germany), and Andries Jekel (UG, The Netherlands) as well as Valerie Grumel (US, South Africa) for HT GPC analysis. A special thanks goes to Xuejing Zheng for all the effort that she put into SEM/EDX imaging.

Adapting in a new country and a new research setup would not have possible without the hospitable environment I found in the SPC group. Members of the Cactus lab do of

course require special mentioning. Wouter, Rachael, Joep, Kirti, Soazig, Nilesh, Rubin, Raf and of course, John Severn. It was a pleasure, thank you.

It seems there is quite a bit of South Africa in Eindhoven: Erica, Mozz, Justin, Maggie, Chris, Guido, Rachel and the rest of you that were always there, thank you. Frequent e-mails from South Africa and Canada also helped to make the cold days a bit warmer: thanks Bertus, Charl and Rainer. A very special thanks goes to Sandra, Robert, Francois and Robert Jr for letting me into their home. It was a privilege.

To my mother and father, thank you for always being there and supporting me in whatever I choose to do. That of course also includes you, Mariska.

Sven, thanks for your endless love, support and patience.

Curriculum Vitae

Madri Smit was born on the 23rd of February 1977 in Port Elizabeth, South Africa. In 1998, she completed her Bachelors Degree in Chemistry with distinction at the University of Stellenbosch, South Africa. "Polymerization of 1,5-hexadienes" was the title of her research with which she obtained her Masters Degree in Polymer Science with distinction at the University of Stellenbosch (South Africa) under the supervision of Dr Albert van Reenen.

In February 2002, she arrived in The Netherlands to start her PhD research at the Eindhoven University of Technology under the guidance of Dr John Chadwick, funded by the Dutch Polymer Institute.